INSIGHTS INTO THE MAINTENANCE AND REPAIR OF PHOTOSYSTEM II, A DYNAMIC MEMBRANE PROTEIN COMPLEX

By

APARNA NAGARAJAN

Bachelor of Science in Zoology
University of Delhi
New Delhi, India
2003

Master of Science in Biotechnology
University of Madras
Chennai, Tamil Nadu, India
2005

Submitted to the Faculty of the
Graduate College of the
Oklahoma State University
in partial fulfillment of
the requirements for
the Degree of
DOCTOR OF PHILOSOPHY
December, 2012

INSIGHTS INTO THE MAINTENANCE AND REPAIR OF PHOTOSYSTEM II, A DYNAMIC MEMBRANE PROTEIN COMPLEX

Dissertation Approved:

Robert Burnap

Dissertation Adviser

Wouter Hoff

Edward Shaw

Jeff Hadwiger

Robert Matts

ACKNOWLEDGEMENTS

PhD at Oklahoma State University has been a wonderful learning experience both for my professional and personal development. This would not have been possible without the help, guidance and support of all my colleagues, friends and family.

First and foremost, I would like to thank my advisor Dr. Robert Burnap who gladly accepted me in his lab for PhD. He has been a constant source of guidance, not just in developing ideas and providing suggestions in research, but also for helping me broaden my perspective on science beyond PhD. His persistent quest for hypotheses has taught me to focus and efficiently approach compelling research questions. His enthusiasm and encouragement have always kept me on my toes. The frequent lab presentations and writing assignments were definitely nerve-racking during the course of my post-graduate education. However, in hindsight, they have been advantageous in developing scientific writing skills and increasing the effectiveness of my presentations. Overall, I would like to thank Dr. Burnap for being my guardian in the true sense by helping me lay the foundation in research and for being the source of my inspiration.

Furthermore, I would like to thank my dissertation committee Dr. Jeff Hadwiger, Dr. Wouter Hoff, Dr. Robert Matts and Dr. Edward Shaw for their valuable suggestions and input throughout my PhD. Their ideas and insightful comments have been truly beneficial for addressing key questions in my research. And the discussions have significantly improved my work and stimulated creative ideas.

I owe my gratitude towards the faculty, staff and colleagues of the Department of Microbiology and Molecular Genetics for their constant support and creating a family atmosphere. I would also like to thank the Core facility of Oklahoma State University especially Dr. Steve Hartson and Janet Rogers for their helpful suggestions in my experiments and a scholarship that allowed me to learn high throughput mass spectrometric techniques.

The atmosphere in the Burnap lab has been very cordial and many thanks to all the members that made working in lab so enjoyable. Late night discussions, lunches, and conference-associated fun with Dr. Preston Dilbeck and Steven Holland have connected us beyond our workspaces. Working late with Juliana Artier and Dr. Han Bao on the tunes of Pandora playlists will certainly be missed. Special thanks to Dr. Shawn Daley and Dr. Hong Jin Hwang for helping me in the initial stages of my PhD with experiments and teaching me various techniques. Thanks to Dr. Anthony Kappell for listening to my ideas and providing input. I would also like to thank David Taylor for helping me setup experiments especially with the mechanics.

Lastly, this long journey would not have been possible without the support of my family and friends. I am indebted to my family for their upbringing that has allowed me to reach this stage of my academic career. Their constant encouragement and morale boosting helped me get through many difficult times. Friends have also played an important role in my life and I am truly grateful to the entire 410 Hester family and many other friends. In particular, I thank Sonal Dalvi, Jayalakshmi Nair and Rachana Rathod for bearing with my complaints and long night study sessions. I would especially like to thank Swapneel Deshpande, Dr. Shireen Hyrapiet, Muthappa Ponjanda Madappa, Akshata Ramnath Mudinoor, Raagini Subramaniam and Akhila Vasan for always being there for me.

Name: APARNA NAGARAJAN

Date of Degree: DECEMBER, 2012

Title of Study: INSIGHTS INTO THE MAINTENANCE AND REPAIR OF PHOTOSYSTEM II, A DYNAMIC PROTEIN COMPLEX

Major Field: MICROBIOLOGY AND MOLECULAR GENETICS

ABSTRACT:
Photosystem II (PSII) is recognized as the main site for high light induced damage. One of the core subunits of PSII, D1 protein encoded by the *psbA* gene, is identified as a high turnover protein that undergoes degradation and replacement as a part of the repair process in PSII. Studies on D1 repair have shown the synchronous nature of D1 degradation and synthesis. FtsH a AAA protease, is known to cause D1 degradation. Therefore, it is widely speculated that damaged D1 is replaced by newly synthesized D1. Although, there is no direct evidence suggesting the removal of damaged subunits only. Alternatively, an induction of the general increase in the turnover rate of D1 could trigger the replacement of all D1 subunits in a random fashion. In this work, I have addressed these two alternate hypotheses by developing a genetic system involving dual D1 expression. Strains were constructed with the parallel expression of a WT *psbA2* in the ectopic and a damage prone mutant *psbA2* at the native locus. Firstly, a WT ectopic strain (eWT) was constructed by transforming a *psbA* deletion strain with a WT *psbA2*, which was synthesized using synthetic biology and fusion PCR. Secondly, mutant *psbA2* was introduced into the native locus of the eWT strain. All the dual D1 strains showed high PSII activity. Higher PSII levels represent increased proportion of PSII with WT D1 incorporated, as the mutant does not correspond to high PSII levels. Immunoblot analysis of a dual strain nS345P: eWT against D1 did not show an accumulation of the S345P form, which exists as pre-D1. However, deletion of the FtsH protease in nS345P: eWT showed an accumulation of pre-D1 along with mature D1. This indicates that S345P mutant forms are targeted for repair in the dual strain. Additionally, *psbA2* gene dosage effect was also studied by expressing two WT *psbA2*. Similar levels of PSII and D1 were observed in the single and double WT strain. This suggests that level of PSII is being regulated and that D1 is not the regulating factor. Therefore, PSII homeostasis is maintained by some other protein factor.

TABLE OF CONTENTS

Chapter Page

LIST OF TABLES

Table Page

LIST OF FIGURES

Figure Page

CHAPTER I

INTRODUCTION

1.1 Overview

Photosynthesis is the process of conversion of sunlight into biologically usable chemical energy. In broad terms, there are two types of photosynthesis: anoxygenic and oxygenic. The evolutionary emergence of anoxygenic photosynthesis is thought to pre-date and form the structural basis for the emergence of the more complex oxygenic photosynthesis. Oxygenic photosynthesis represented a huge metabolic innovation that allowed expansion into new nutrient-poor ecological niches because it uses ubiquitous water as a source of electrons to build complex biomolecules and thereby avoids the scarcity of electron donors that often limits anoxygenic photosynthesis. Indeed, cyanobacteria, which perform photosynthesis using water as a substrate and releasing molecular oxygen as a product, have flourished over the course of approximately 2.7 billion years of evolution and are considered as the source of earth's oxygenic atmosphere (*1, 2*). Their descendants, contemporary cyanobacteria, algae and higher

plants retain this ability to utilize solar energy to split water as a substrate electron donor to inorganic compounds (e.g. carbon dioxide, nitrate), and thereby form organic compounds. All phototrophs have reaction centers (RCs) that convert the energy present in a photon to the energy of separating electrons from substrate electron donor. These are membrane-bound multiprotein complexes containing a variety of organic (e.g. chlorophyll) and inorganic cofactors (e.g. transition metals) that carry out electron transport for these energy conversion reactions. Reaction centers can be classified into Type I and Type II RCs according to the electron acceptors used in the electron transfer process. Iron sulfur (FeS) clusters are the terminal electron acceptors in Type I RC that mainly occur in bacteria that perform anoxygenic photosynthesis (eg. certain members of Firmicutes, Chlorobi and Acidobacteria) (*1, 3*). Photosynthetic bacteria that utilize mobile quinones as terminal electron acceptor are classified as having Type II RCs and perform aerobic or oxygenic photosynthesis, and are distributed among namely α, β, and γ proteobacteria. Cyanobacteria, the only prokaryotes capable of oxygenic photosynthesis have both Type I and Type II RCs that work together in tandem. In these organisms, water functions as the electron donor, the ultimate electron acceptor is primarily carbon dioxide, and molecular oxygen is produced as a byproduct. Similarities in the two types of RCs observed through bioinformatic and structural analyses suggest a common ancestor and demonstrate the striking patterns of evolutionary conservation of these RCs (*1, 3, 4*).

1.2 Cyanobacterium *Synechocystis* sp. *PCC 6803*

Cyanobacteria are unique prokaryotes where in addition to the periplasmic and plasma membrane, they contain the photosynthetic membranes called the thylakoids. This

highly reticulated set of membranes extends through large portions of the cytoplasm and plays an important role in light harvesting and light dependent reactions of photosynthesis. They have additional pigments apart from chlorophyll called phycobilins that function in light harvesting. *Synechocystis* sp. PCC 6803 (*Synechocystis*) belongs to the order *Chroococcales* and is a strain that was isolated from a fresh water lake and deposited in the Pasteur Culture Collection (PCC). It has the ability to undergo facile genetic transformation involving natural integration of exogenous DNA by homologous recombination into its genome. This feature of *Synechocystis* has allowed the development of effective strategies for engineering the chromosome in remarkably predictable ways by using antibiotic resistance genes to select for desired recombinants resulting from transformation using specifically designed DNA fragments containing homologous sequences. My thesis project benefits from the use of this property of *Synechocystis* as discussed in later sections. *Synechocystis* also has an advantage of growth under heterotrophic conditions in the presence of a fixed carbon source like glucose that allows the study of mutants that lack the ability to grow phototrophically. It is notably the first photosynthetic organism to have its complete genome sequenced (*5*). Therefore, information from this resource and its other advantages has made *Synechocystis* an enormously popular experimental model to study photosynthesis.

1.3 Oxygenic photosynthetic electron transport

The photosynthetic electron transport chain (PETC) principally involves three membrane protein complexes, namely photosystem II (PSII), cytochrome b_6f (Cyt b_6f), and photosystem I (PSI) that each span the thylakoid membrane, which are specialized photosynthetic membranes present in cyanobacteria and chloroplasts. The entire electron

transport chain as illustrated in Figure 1.1, functions in the transfer of electrons from water via PSII ultimately to $NADP^+$ to generate molecular oxygen, ATP and NADPH; these form the light reactions of photosynthesis. The NADPH is further utilized for the production of organic compounds through the dark reactions of photosynthesis. With the absorption of light, the electrons of P680, the so-called 'special' pair of chlorophyll in PSII, are excited and initiate the process of charge separation that results in the transfer of electrons from P680 to non-exchangeable plastoquinone called Q_A. The electron hole created by the ejection of the electrons from the PSII special pair chlorophyll is replenished by the oxidation of water that occurs at a nearby cluster of Mn and Ca ions (Mn_4CaO_5). This releases molecular oxygen and four protons into the thylakoid lumen. Cyt b_6f functions in transferring electrons from plastoquinone (PQ) to plastocyanin (PC), pumping protons in the process. Excitation of PSI by light energy allows the transfer of electrons from PC to ferredoxin. A proton gradient is generated with these electron transfer reactions in PSII that is used to produce ATP via ATP synthase and NADPH is generated by Ferredoxin $NADP^+$ reductase (FNR).

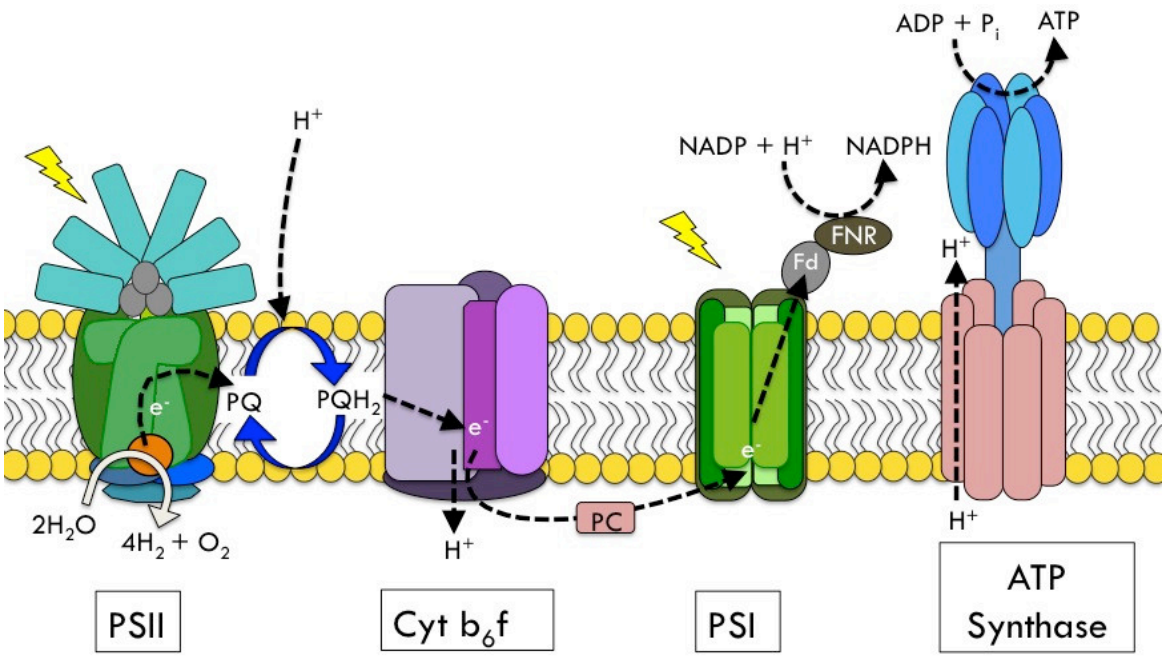

Figure 1.1. **The photosynthetic electron transport chain (PETC)** is involved in the transfer of electrons from PSII that provides the source of electrons to PSI that further excites the electrons to reduce ferredoxin and NADPH via the Cyt *b*$_6$*f*. The water oxidation process in PSII produces protons that are deposited in the thylakoid lumen and the electron transfer reactions produces an electrochemical gradient to drive the synthesis of ATP from the ATP synthase.

1.4 Photosystem II – Structure and Function

1.4.1 Structure of photosystem II

Structurally, PSII is a multi-subunit membrane protein complex that consists of 20 protein subunits comprised of both transmembrane and peripheral proteins and more than 80 different cofactors, including chlorophylls, pheophytins, β carotenes, lipids, plastoquinones, heme iron, manganese, calcium, chloride, bicarbonate, non-heme iron and more than 15 detergent molecules in each monomer (*6*). There has been considerable progress in resolving the three dimensional structure of PSII wherein several groups published crystal structure, mainly from a thermophillic cyanobacterium *Thermosynechococcus elongates (7-10)* [Protein Data Bank entries 1FE1, 1IZL, 1S5L, 3BZ1]. The most recent crystal structure was

published with a resolution at 1.9 Å (*6*) [Protein Data Bank entry 3ARC]. This structure provides the arrangements for virtually all amino acids (exceptions being the disordered N- and C-terminal regions of some polypeptides) and cofactors and reveals the arrangement of atoms in the Mn_4CaO_5 cluster.

Based on the crystal structure, PSII exists as a dimer with each monomer consisting of intrinsic core subunits D1 (PsbA), D2 (PsbD), CP43 (PsbC) and CP47 (PsbB) that are common to all PSII containing organisms and bear significant similarity amongst different genera of photosynthetic organisms (*4*). D1 and D2 exist as heterodimers and coordinate the cofactors essential for charge separation and stabilization. CP43 and CP47 coordinate majority of chlorophylls and serve as proximal antenna proteins, funneling the energy of photons to the special pair chlorophyll in the D1/D2 reaction center. Apart from these core subunits there are other intrinsic subunits, namely cytochrome b_{559} (PsbE/F), PsbH, PsbI, PsbJ, PsbK, PsbL, PsbM, PsbTc and PsbZ that are low molecular proteins but are associated with PSII. The overall structure of PSII dimer with the subunit composition is depicted in Figure 1.2.

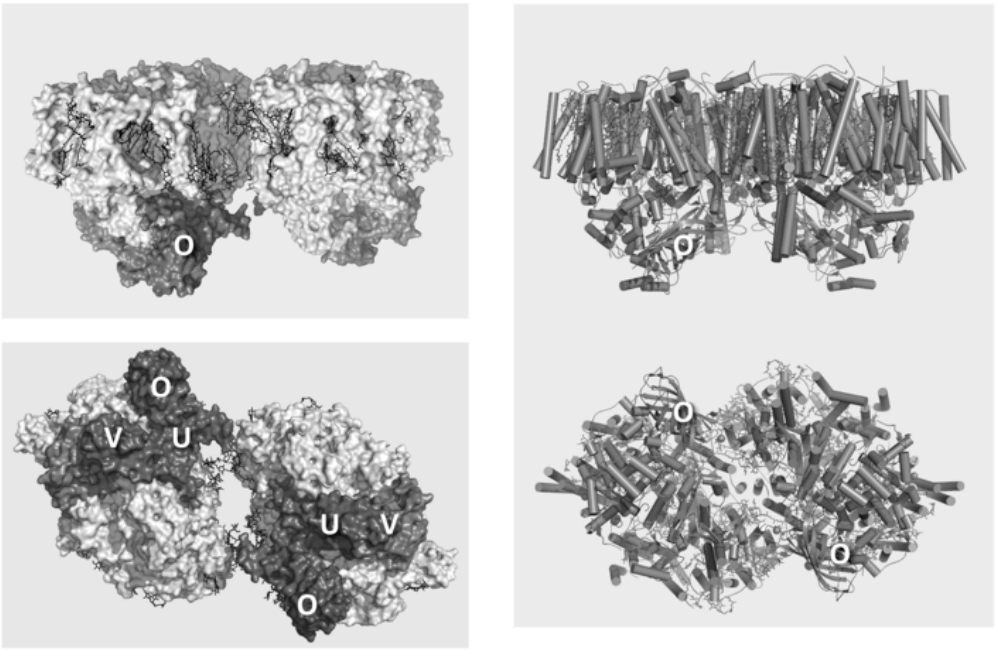

Figure 1.2. Overall structure of PSII dimer depicted as space filling (in left panels) and cartoon representations (right panels). Top panels show the side view across the plane of membrane showing the PSII dimer embedded into the thylakoid membrane and bottom panels are perpendicular to the membrane and show the luminal side of PSII with extrinsic proteins PsbO, PsbV and PsbU in dark gray and intrinsic subunits in light gray. Figures were constructed in PyMol Molecular Graphics System (Schrödinger, LLC) using structural coordinates from PDB ID 3BZ1 and 3BZ2. This figure has been published in a book chapter that contains some of my bioinformatic analysis of PSII (*4*).

Besides the intrinsic subunits there are three extrinsic subunits PsbU, PsbV and PsbO that are bound to the luminal surface of the complex surrounding the catalytic center of the Mn_4CaO_5 cluster, the catalytic heart of the domain of PSII referred to as the water oxidation complex (WOC). Of these three extrinsic subunits, PsbO (manganese stabilizing protein) is conserved across the different phyletic versions of PSII. The other extrinsic subunits are different among different phyla with PsbP and PsbQ occurring in higher plants and algae. The functions of these subunits are similar to those of cyanobacterial PsbV and PsbU for reducing the demand of Ca^{2+} and Cl^- in the Mn_4CaO_5 cluster (*11, 12*). These differences are suggested to have evolutionary significance (*4, 13*).

1.4.2. Function of photosystem II

PSII is an enzyme that functions as H_2O-plastoquinone oxidoreductase that catalyzes the light driven oxidation of H_2O and the electrons generated from this process are transferred to the plastoquinone (PQ). Figure 1.3 shows the transfer of electrons through PSII in a diagrammatic representation. The process of water splitting that occurs in the Mn_4CaO_5 cluster is very complex as the extraction of electrons from H_2O is a thermodynamically expensive process and requires a powerful oxidant. Also, for the complete oxidation of H_2O and the liberation of molecular oxygen, four electrons and four protons; the catalytic cycle of removal of electrons must be carried out four times. This is because the oxidizing power of the photochemical reaction center is univalent. Therefore, the Mn_4CaO_5 cluster, which is comprised of four Mn, one Ca ion linked by μ-oxo bridges, not only has to catalyze an energetically expensive removal of electrons from H_2O, but also needs to undergo this sequence of oxidation four times during a single catalytic cycle of H_2O-oxidation (*14*).

Each oxidation event is triggered by the absorption of a photon by P680, a chlorophyll species (*15*) and creates charge separation resulting in a reduced non exchangeable plastoquinone Q_A^- on the acceptor side and an oxidized P_{680}^+ on the donor side, forming the charge separated state $P_{680}^+Q_A^-$. The formation of the charge-separated state is preceded by the transient formation of the primary reductant, pheophytin ($Pheo^-$), which reduces Q_A in less that 500 picoseconds (Figure 1.3). P_{680}^+ provides the oxidizing power to remove the electrons from the substrate water on the donor side of PSII. This is mediated by redox active tyrosine residue (Y_z) of the reaction center D1 protein (*16-18*). The sequential

oxidation of Mn_4CaO_5 cluster cycles through a series of redox states termed as S-states (*14, 19, 20*).

On the acceptor side of PSII, transfer of electron from P680 to bound plastoquinones (Q_A and Q_B) occurs through a pheophytin molecule. Accumulation of two electrons in Q_B forms plastoquinol (PQH_2) which diffuses through the membrane to cyt *b6f* mediating the transfer of electrons to the rest of the electron transport chain. The pathway of electron transfer in PSII can be described as follows:

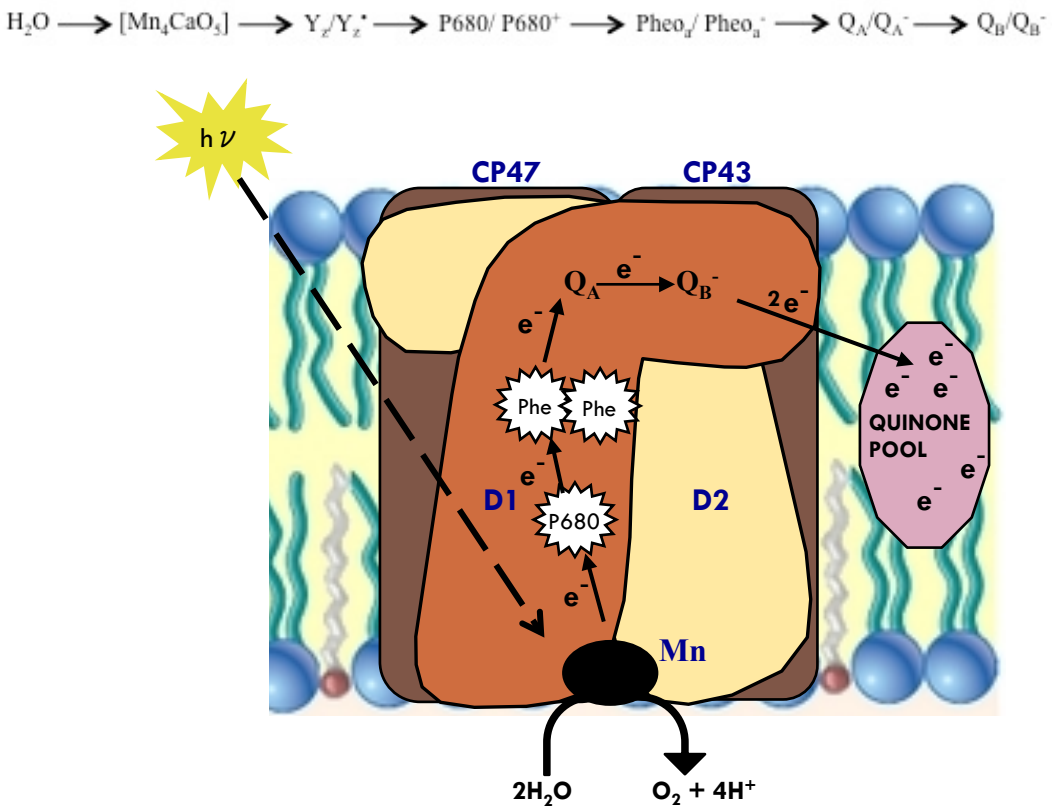

Figure 1.3. Diagrammatic representation of PSII showing charge separation and electron transfer in PSII through special pair of chlorophyll P680 and cofactors pheophytin and quinones (Q_A and Q_B). The figure shows the PSII intrinsic core subunits with D1 (orange), D2 (yellow) and CP43, CP47 (brown).

1.5 Biogenesis of PSII

The basal role of PSII in the photosynthetic mechanism combined with its high sensitivity to photodamage has invited sufficient interest in the research on the biogenesis of PSII. With a subunit composition of over 20 different protein subunits and more than 80 cofactors and several other intermediate factors (that do not form a part of complete PSII), the life cycle of PSII is very dynamic with constant flux between assembly and dis-assembly. The PSII complex is also susceptible to photodamage and it undergoes repeated cycles of subunit replacement in response to this photodamage. Therefore, the assembly process is further linked with the PSII repair process (described later). Recent structural information on PSII along with genetic, molecular and biochemical analyses have allowed an increased understanding of the process (*21*). Structure-function studies using mutants lacking specific subunits have benefitted in developing models for the stepwise assembly process involving partially assembled PSII complexes as intermediates (*22-25*) (Figure 1.4).

A scheme of the assembly process has been proposed based on the analysis of these mutants. A description of this process displaying assembly intermediates identified so far is illustrated in Figure 1.4. The incorporation of Cyt b_{559} (PsbE and PsbF) in the membrane seems to initiate the assembly process and associates with D2 to form the D2-Cytb_{559} sub complex (*22*). This is followed by the addition of preD1 (pD1) and PsbI subunit to form an RC like complex (*26*). The D1 protein is synthesized as a precursor with a C terminal extension of 16 amino acids in *Synechocystis (27)*. This extension is cleaved off with an enzyme C-terminal protease A (CtpA) to allow assembly with Mn_4CaO_5 (*28-30*), as the C terminal β-carbonyl acts as a ligand for Mn_4CaO_5. It was recently shown that pD1 is cleaved

initially to form iD1 (intermediate D1) before forming mature D1 (*31*). The process of D1 maturation from pD1 to D1 provides a selective advantage to the cells when compared to cells expressing mature D1 (*32*), however the reason for this remains unresolved. This cleavage process is essential for complete PSII assembly. Therefore, mutants expressing only the pD1 form do not have functional Mn_4CaO_5 clusters and cannot assemble functional PSII complex.

Binding of CP47 to the RC-like complex forms another assembly intermediate called the RC47 complex (*22*). Attachment of CP43 to this RC47 complex enables the formation of the monomeric core PSII complex; this being the starting point for the light driven assembly of Mn_4CaO_5 to allow water oxidation to occur. The coordination of metal ions into the apo-protein of PSII by a light driven process is called photoactivation (*33, 34*). The assembly of Mn_4CaO_5 is a complex process by itself and much research is underway to better understand this process (*35*). The association of luminally located extrinsic subunits PsbO, PsbV and PsbU along with PsbP and PsbQ stabilizes the Mn_4CaO_5 cluster to form an active PSII capable of oxygen evolution (*36*). The last step in the assembly process appears to be the dimerization of PSII. Although both PSII dimers and monomers are found to be oxygen evolving, dimers are considerably more active in biochemical preparations (*37*). Recent studies argue the formation of PSII dimers as being detergent induced artifact (*38*). However, electron micrographic analyses of intact thylakoids provide evidence of a PSII dimer being a functional unit found *in vivo* (*39, 40*). There are several other low molecular weight protein subunits like Psb27 that act as assembly factors in the assembly process and transiently associate with the PSII intermediates during biogenesis and repair (*37, 41, 42*).

Also, several single transmembrane helix protein subunits like PsbM, PsbL and PsbTc form a part of the assembly process. These subunits are mainly thought to assist PSII monomers to form dimers (*43*). Functions of several of these subunits have been described and information on these can be found in recent reviews (*21, 44*).

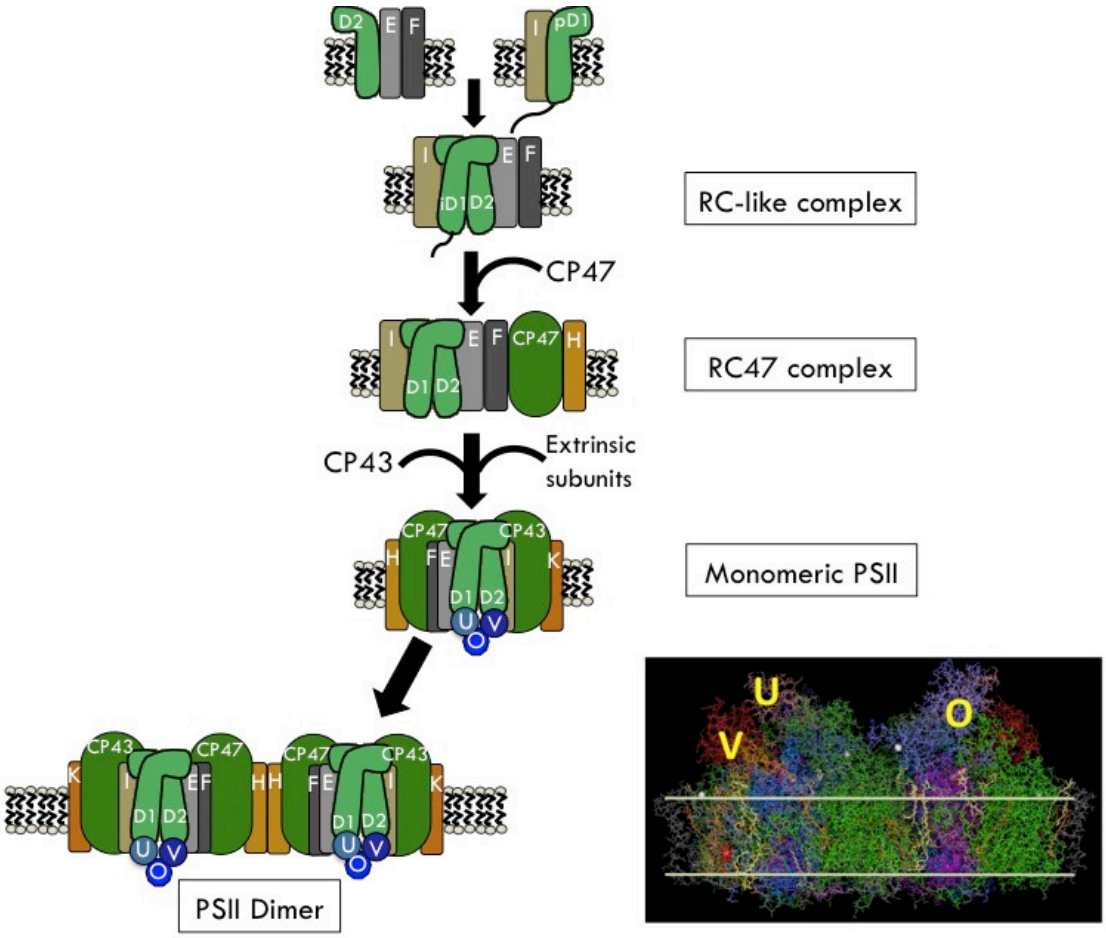

Figure 1.4. An overview of PSII assembly process involving the formation of assembly intermediates like RC-like complex, RC47 and PSII monomer. A sequential assembly of PSII subunits along with the maturation of D1 forms a PSII monomer after the association of extrinsics. The association of monomers finally forms PSII dimers with the association of certain subunits PsbL, PsbM, PsbTc (not shown in figure). On the right is the three dimensional structure of PSII as viewed across the plan of the membrane.

1.6 PSII damage and repair

1.6.1 Photodamage

Light, the driver of photosynthesis is a major stress factor causing reversible and irreversible damage to the components of the photosynthetic apparatus. A decline in the photosynthetic activity due to this light stress has been described as photoinhibition (*45-48*). PSII is most prone to photoinhibition when compared to other components of PETC as it performs water oxidation and releases oxygen that can react with redox components to form highly toxic species (*49*). Two main mechanisms of photoinhibition have been discussed in the literature based on the initial site of damage and the nature of the damaging species. These include the acceptor-side and donor-side photoinhibition. Several models for photoinhibition have been put forward in the past, many of which are based on either of these two mechanisms (*46*). In donor side photoinhibition, the disruption of Mn_4CaO_5 is the primary event. This occurs when the electron donation from Mn_4CaO_5 is unable to compete with the rate of P680 oxidation. This results in an accumulation of P_{680}^{+} and an increase in the lifetime of P_{680}^{+} and other oxidizing species in the donor side causing oxidative damage to the Mn_4CaO_5 (*47*). In acceptor side photoinhibition, the major source of photodamage is the generation of singlet oxygen ($^1O_2$) due to charge recombination in PSII. These toxic species are produced either from the spontaneous conversion of singlet state Chl to their triplet state or by the formation of $^3[P_{680}^{+}Phe^{-}]$ from charge recombination (*48, 50*).

1.6.2 Photoprotection

Photodamage to PSII can be prevented by photoprotection mechanisms that allow quenching the excitation energy and dissipation of absorbed light energy as heat. For example in cyanobacteria a conserved replacement from D1Gln130 to Glu is observed in all high light D1 forms. This variability renders the high light forms (D1Glu130) of D1 more phototolerant when compared to the wild type (D1Gln130). A change from Gln to Glu increases the redox potential of Phe therefore increasing the redox gap which has an inverse effect on the rate of direct recombination, making the D1Glu130 more phototolerant (*51*).

An interesting photoprotective mechanism with the uncoupling of phycobilisomes is observed that prevents photodamage to RCs that are still in the process of assembly of Mn_4CaO_5. Phycobilisomes are known to be mobile complexes that diffuse through the membrane. FRAP studies have shown that association of phycobilisomes to the reaction centers are very transient and unstable (*52*). The uncoupling of the phycobilisomes and PSII RCs causes an inefficient transfer of excitation energy from phycobilisome to the PSII RC. This efficient transfer of this excitation energy does not occur until the Mn_4CaO_5 is assembled (*53*).

1.6.3 PSII repair

PSII repair following photodamage can also be considered as another important photoprotective mechanism. This repair pathway is involved in the replacement of damaged components with newly synthesized protein (eg. D1). PSII, apart from undergoing maximum damage during photoinhibition is also known to exhibit a high metabolic turnover rate of

PSII proteins. The D1 protein subunit of PSII is found to have the highest turnover rate in comparison to other PSII proteins (*54*). Susceptibility of D1 to maximal damage is due the coordination of several redox active cofactors that are involved in the water oxidation process in PSII. Therefore, to cope with photodamage, the complex and efficient repair process operates to replace the irreversibly damaged D1 protein with a newly synthesized copy of the D1 protein (*21, 55*). Models for the damage-repair cycle have been developed that begin with damage to PSII, a sensing mechanism that elicits the repair process, the monomerization of the PSII dimer and dissociation or loss of certain subunits of PSII (Figure 1.5). As much of the D1 protein is buried within the dimeric PSII complex, the process would require a partial disassembly of the PSII complex in order for the proteases to access D1 degradation process to occur. Structural rearrangements in PSII are also inevitable to allow the removal of D1 and insertion of new a D1 protein into the thylakoid membrane, although, there is no direct evidence indicating the same. Reassembly of functional PSII after D1 degradation and replacement are similar to the steps involved in the *de novo* biogenesis of PSII. Figure 1.5 describes the widely accepted model for PSII repair.

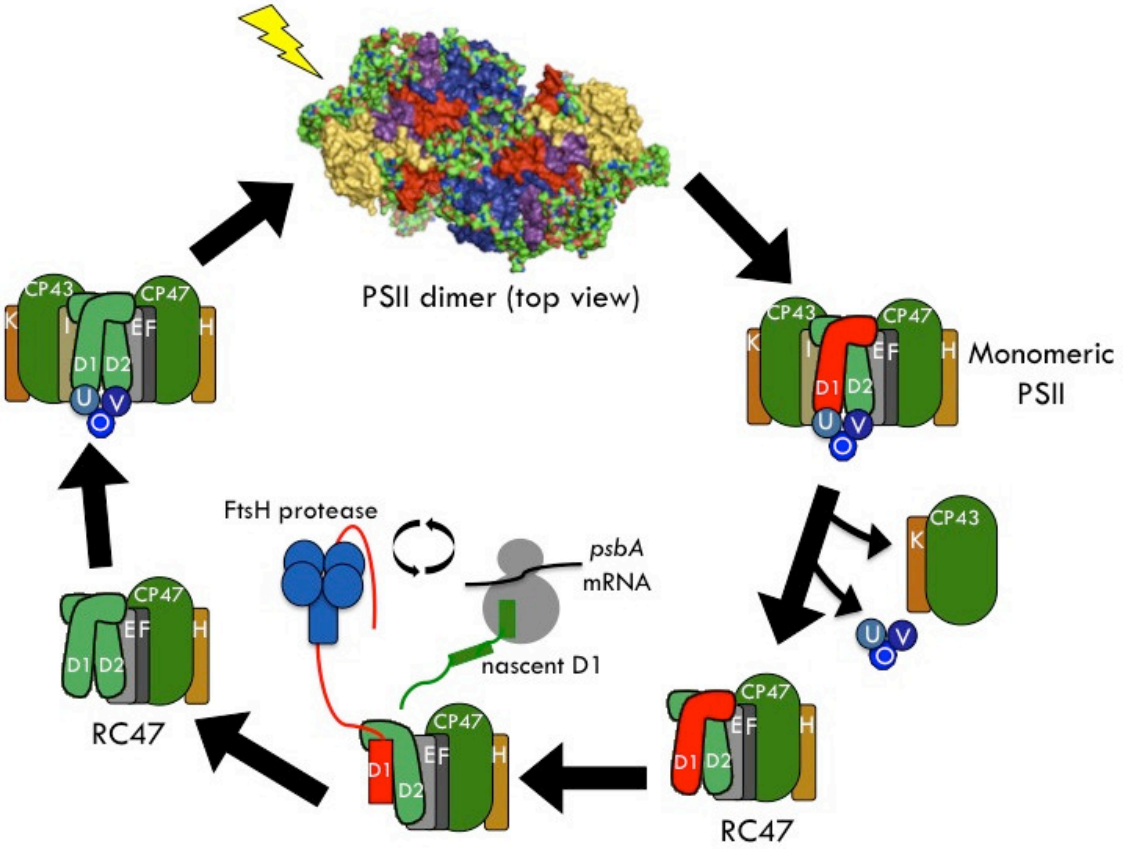

Figure 1.5. Model for PSII repair wherein the entire process appears to be triggered with photoinhibition causing damage to PSII complex. This leads to disassembly of PSII dimer (space filled representation, top view) allowing damaged D1 (red) degradation by FtsH protease (blue), replacement with newly synthesized D1 inserted in a synchronized manner. The reassembly of PSII is much like the biogenesis of PSII to form functional PSII dimer (refer to figure 1.4).

Interestingly, radioactive pulse-chase experiments *in vivo* have shown that the *de novo* synthesis of replacement D1 and degradation of D1 are coupled (*56*). Therefore, it appears that biosynthesis and repair are linked, although mechanism for this coordination for protein degradation and synthesis is not well understood. These repair mechanisms require specific proteases and assembly factors; the functions of some of these have been studied while certain others are still not clear.

Proteases in PSII repair

FtsH and Deg proteases have long been identified as important candidates for D1 degradation (*57-62*). FtsH belongs to a family of ATP dependent proteases consisting of an N-terminal transmembrane domain, a hydrophilic ATPase domain and a Zn^{2+} metalloprotease domain (*61*). There are four FtsH protease in *Synechocystis* of which FtsH2 seems to play a more direct role in D1 degradation (*63-65*). These proteases bear a moderate sequence similarity to the FtsH protease from *E.coli (61)*. The role of FtsH in the degradation of damaged D1 seems to be evolutionarily conserved from cyanobacteria through plants. FtsH has been shown to be involved during the early stages of D1 degradation and not the removal of D1 breakdown products (*65, 66*). An exposed N-terminal tail of D1 is found to be essential for its rapid degradation by FtsH (*67*). The observation that FtsH mutant strains in both *Synechocystis* and *Arabidopsis* do not completely block the D1 degradation suggests that there are additional proteases involved in this process, probably in a lower proportion (*60, 63*). FtsH is known to have a weak unfolding capacity therefore the D1 protein has to be destabilized prior to its degradation(*61*). This provides a basis for the necessity of structural rearrangements in D1 causing it to destabilize, therefore be recognized by FtsH for its degradation. Based on all the available information, it is modeled that FtsH recognizes the N-terminal of the damaged (destabilized) D1 protein subunit to engage in degradation (*67*).

The other important family namely HtrA/Deg proteases are membrane associated serine proteases present in both cyanobacteria and green plants. There are several members of Deg proteases in both *Synechocystis* (three) (*57*) and Arabidopsis (sixteen) (*58, 68*).

DegP2 from *Arabidopsis* has been shown to be required for the initial D1 cleavage event *in vitro* to produce breakdown products (*62*). In general Deg proteases in chloroplasts respond to light stress and have an indirect effect on D1 degradation. The members of Deg proteases from Synechocystis on the other hand do not seem to be involved in D1 degradation. A mutation of all three Deg proteases in *Synechocystis* did not affect the repair process (*57*). Thus, in cyanobacteria Deg proteases are not known for D1 degradation and their function is unknown. Therefore, the role of DegP protease during D1 degradation in chloroplasts might have occurred after the divergence of cyanobacteria and green algae.

1.7 Current research focus

The entire process of damage and repair in PSII could be classified into damage occurring to PSII, signaling of this damage and efficient repair of the damage thereby maintaining PSII homeostasis at any given time. Based on the studies of PSII repair (discussed in Section 1.6.2) it is evident that D1 is the primary target for photodamage and this is witnessed by the increased rate of turnover of D1 under high light intensities (*54*). D1 degradation and new D1 synthesis are found to be synchronized as the use of translation inhibitors causes D1 degradation to also cease (*56*).

These studies and others have caused some to speculate that PSII repair specifically replaces the damaged D1 subunits with newly synthesized D1; although there is no direct evidence suggesting the removal of only damaged D1 subunits. The sensing mechanism of damage is hypothesized to detect damaged PSII complexes and specifically target them for repair, however evidence for such a mechanism has yet to be obtained. An alternate

hypothesis could be the induction of increased specific D1 proteolysis and nascent D1 synthesis activity promoted by the general increase in the turnover rate of D1, to ensure the population of PSII in the thylakoids is relatively young and thus less likely to be inactivated due to photodamage.

PSII is very dynamic in nature undergoing frequent assembly and disassembly and existing in multiple forms in order to accommodate various stress conditions it is often subjected to. This dynamic nature of PSII is correlated with the localization of PSII during the biogenesis or assembly process and changes that PSII undergoes during repair (*69*). The mobility of PSII has been observed using fluorescence recovery after photobleaching (FRAP) to increase under intense red light that correlates with the redistribution of PSII to initiate repair (*70, 71*). Furthermore, the presence of biogenesis centers located in regions of connections between the plasma membrane (PM) and thylakoid membrane (TM) were recently shown to be the site of PSII assembly (*69, 72*). These regions were shown to accumulate preD1 and PratA that are important for completion of PSII assembly process. These studies could be collectively used to speculate that structural rearrangements in PSII and/or mobility of PSII proteins and thylakoid membranes into zones of repair wherein they can reassemble PSII are indeed the sensing mechanism to trigger PSII repair.

Therefore, the nature of the damaging signal could be hypothesized to either lead to a localized affect on the D1 subunit alone, allowing it to be recognized from un-damaged D1. Or on the other hand, it could traverse across the entire thylakoid membrane to affect all the PSII reaction centers. As illustrated earlier, there is indirect evidence supporting both of

these hypotheses. Hence, it is pertinent to address this question of sensing the damage that triggers the degradation process during PSII repair.

In this study, an attempt has been made to address the damage sensing mechanism that triggers the PSII repair process. The goal of this work has been to develop a parallel genetic system for the dual expression of alternate forms of D1 protein and study the effects of this parallel expression on the assembly, maintenance and activity of PSII. To develop a genetic system for parallel expression the versatility of *Synechocystis* in its natural competence for DNA uptake and its ability for alternate modes of growth was exploited. The powerful genetic system and the flexibility of multiple genetic modifications of *Synechocystis* were significant to this study.

Chapter 3 primarily describes the basis and development of the genetic expression system. In order for the parallel expression of two D1 proteins, it is necessary to be able to express D1 protein (WT *psbA2*) from a location elsewhere in the genome (non-native or ectopic). Chapter 3 discusses the novel approach of combining synthetic biology and genetic engineering to clone the full length D1 protein for the very first time into *Synechocystis*. Detailed strategy and experiments that allowed the successful expression of D1 protein at higher levels from the ectopic location of the *Synechocystis* chromosome is further discussed. This chapter has been published in the journal of Photochemistry and photobiology and is presented in this thesis with permission. As the first author of this manuscript, I performed all the experiments and scientific scholarship under the guidance of my advisor Dr. Robert Burnap who is the corresponding author. This work also involved a collaboration with Regan Winter and Julian Eaton Rye from the University of Otago, New Zealand. Their contribution

was limited to providing a strain that I used for further mutagenesis and construction of the genetic system.

Chapter 4 includes complete engineering of the dual expression strain containing two copies of D1 proteins expressing either a high turnover D1 in parallel with WT D1 or expressing two WT D1 proteins from different locations on the chromosome. The choice of high turnover mutants used in the study was based on previous literature (*63*, *73*, *74*). Characterization of the strains with a single copy of D1 (mutant or WT) and two copies of D1 (mutant or WT) were carried out to study their effects on the activity of PSII. Results from these strains provide early evidence of the PSII repair mechanism being targeted towards damage prone complexes. This chapter also introduces the concept of PSII homeostasis that could be crucial in maintaining higher levels of functional PSII complexes in a cell. This chapter is being prepared for publication. The work involved in this chapter has been primarily accomplished by me with the help an undergraduate David Taylor and under the guidance of Dr. Robert Burnap.

CHAPTER II

EXPERIMENTAL PROCEDURES

2.1 Culture and Growth Conditions

All the strains used in this study were routinely maintained on BG-11 (*75*) solid media for photoautotrophic growth and/or on BG-11 media supplemented with 5 mM glucose and 10 μM DCMU (3-(3,4-dichlorophenyl)-1,1-dimethylurea) for photoheterotrophic growth. The presence of glucose ensures growth in the absence of photosynthetic function due to mutations and the presence of DCMU blocks photosynthetic function and thereby eliminates growth advantages to potential revertants during the maintenance of strains harboring lesions in the photosynthetic mechanism. Strains were also grown on BG-11 media supplemented with appropriate concentrations of antibiotic. The final concentration for glucose, DCMU and antibiotics are listed in Table 2.1. Cultures were routinely grown in 100 ml volumes of BG-11 buffered with 10mM HEPES- NaOH (pH- 8.0) in 250 ml Erlenmeyer flasks on a rotary shaker (~150 rpm) with 20 μmol m^{-2} s^{-1} of photon flux intensity provided by Cool White fluorescent illumination. When these cultures attained log phase (OD_{750nm} ~ 0.8) they were used to inoculate 50 ml volumes of BG-11 supplemented with 20mM HEPES-NaOH (pH 8.0) in

smaller test tubes (~75 ml, 2.5 cm diameter) to an OD_{750nm} ~ 0.2. These experimental cultures were grown photoautotrophically at 30°C with constant bubbling of 3% CO_2 supplemented air (v/v). The light intensity for all the experimental cultures was maintained at 40 μmol m^{-2} s^{-1} unless otherwise stated. Specific growth conditions for strains are listed in Table 2.2 along with the list of strains used in this study. Cultures with comparable optical cell density and light conditions were used for all the experiments. This was verified by monitoring the relative cell density at 750 nm (OD_{750nm}) using the UV-Vis Scanning Spectrophotometer, Shimadzu, Japan and the light intensity was monitored using a ULM-500 (Universal Light meter & Data logger, Walz).

Antibiotic	Stock	Final
Glucose	2 M	5 mM
DCMU	10 mM	10 μM
Kanamycin	100 mg/ml	5 μg/ml – 50 μg/ml
Spectinomycin	100 mg/ml	5 μg/ml – 30 μg/ml
Ampicillin	50 mg/ml	5 μg/ml – 50 μg/ml

Table. 2.1 Antibiotic stock and final concentrations used in this study for selecting transformants and promoting growth.

2.2 Strains used in this study

The naturally transformable, glucose-utilizing strain of *Synechocystis* sp. PCC6803 (*76*) was used for the construction of all the strains described in this study. Table 2.2 lists all the strains used and constructed during this study with the antibiotic

resistance markers they possess, the physiological growth conditions and any references associated with the strains.

Strain Name	Background	Resistances	Nutrient and Light requirements
ΔA1ΔA3	Markerless deletion	None	Photoautotorphic
ΔA1ΔA3-H6	ΔA1ΔA3	Gm	Photoautotrophic
ΔA1:ΔA2Em:ΔA3 – H6	***ΔA1ΔA3-H6***	Em, Gm	Non- autotrophic
e-WT (psbA2NS)	***ΔA1:ΔA2Em:ΔA3 – H6***	Em, Gm	Photoautotrophic (40 μmol m^{-2} s^{-1})
n-WT	***ΔA1:ΔA2Em:ΔA3 – H6***	Gm, Km	Photoautotrophic (40 μmol m^{-2} s^{-1})
n-S345P	***ΔA1:ΔA2Em:ΔA3 – H6***	Gm, Km	Photoheterotrophic (10 μmol m^{-2} s^{-1})
nWT/eWT	***e-WT (psbA2NS)***	Gm, Km	Photoautotrophic (40 μmol m^{-2} s^{-1})
nS345P/eWT	***e-WT (psbA2NS)***	Gm, Km	Photoautotrophic (40 μmol m^{-2} s^{-1})
nH337Y/eWT	***e-WT (psbA2NS)***	*Gm, Km*	Photoautotrophic (40 μmol m^{-2} s^{-1})
nD170A/eWT	***e-WT (psbA2NS)***	Gm, Km	Photoautotrophic (40 μmol m^{-2} s^{-1})
ΔFtsH – ΔA	***ΔA1:ΔA2Em:ΔA3 – H6***	Gm, Em, Sp	Photoheterotrophic
ΔFtsH- psbA2NS	***e-WT (psbA2NS)***	Gm, Sp	Photoautotrophic (20 μmol m^{-2} s^{-1})
ΔFtsH- nWT/eWT	***nWT/eWT***	Gm, Km, Sp	Photoautotrophic (20 μmol m^{-2} s^{-1})
ΔFtsH- nH337Y/eWT	***nH337Y/eWT***	Gm, Km, Sp	Photoautotrophic (20 μmol m^{-2} s^{-1})

ΔFtsH-nWT	***n-WT***	Gm, Km, Sp	Photoautotrophic ($20\ \mu mol\ m^{-2}\ s^{-1}$)
ΔFtsH-nS345P/eWT	***nS345P/eWT***	Gm, Km, Sp	Photoautotrophic ($20\ \mu mol\ m^{-2}\ s^{-1}$)
ΔFtsH- S345P	***n-S345P***	Gm, Km, Sp	Photoheterotrophic ($10\ \mu mol\ m^{-2}\ s^{-1}$

Table 2.2. List of strains used and constructed during this study. Columns describe the construction background for each strain with the antibiotic resistance cassettes they harbor and the growth conditions used for these strains. The antibiotics listed were used only for the segregation process. After complete segregation strains were propagated in liquid BG-11 in presence of 5mM glucose and in solid BG-11 agar in the presence of 5mM glucose and DCMU. The last column enlists the ability of each strain to be either photoautotrophic or heterotrophic and the light conditions they were maintained routinely.

2.2.1 Construction of background strain (*ΔA1:ΔA2Em:ΔA3)*

A strain with all the three *psbA* genes deleted was used as a background strain for the introduction of mutant and WT copies of *psbA* as described in Table 2.2. The triple *psbA* deletion strain (*ΔA1:ΔA2Em:ΔA3)* was constructed by a deletion of *psbA2* from a strain ΔA1ΔA3, that has both *psbA1* and *psbA3* deleted (provided by Professor Julian Eaton Rye, University of Otago, New Zealand). The deletion of *psbA1* and *psbA3* was achieved using a marker-less deletion technique that incorporates counter-selection and homologous recombination to create knockouts. This technique extends the traditional approach of interrupting the gene with an antibiotic marker and utilizes an additional transformation step to excise the antibiotic marker thereby allowing marker recycling. The principle behind this technique is that the *sacB* gene from *Bacillus* sp. encoding for levan sucrase is lethal to *Synechocystis* in the presence of 5% sucrose (*77, 78*). The targeted gene is first replaced with an antibiotic marker and *sacB* cassette and this plasmid is transformed into wild type *Synechocystis*. This strain is then transformed with another plasmid containing homologous flanking regions alone promoting a removal of

the antibiotic marker and *sacB* fragment by homologous recombination. The transformants are then selected in the presence of 5% sucrose for the lack of *sacB* gene.

In this case, to generate a *psbA1* deletion construct, a 685 bp fragment of *psbA1* coding region from *Hpa*I site 122 bp downstream of start codon to *Ban*II site 807 bp downstream from the start codon was replaced with the 3.9 kb *Xba*I-*Xba*I fragment of pRL250 containing the kanamycin resistance cassette and the *sacB* gene that confers sensitivity to sucrose (*77*). The resultant ΔpsbA1(sacB) plasmid was used to transform *Synechocystis* wild type to create the ΔpsbA1(sacB) strain and the transformants were selected for kanamycin resistance. This strain was then transformed with a marker-less ΔpsbA1 plasmid containing the same deletion but without the kanamycin cassette and *sacB* gene. The transformants were selected for the lack of *sacB* in the presence of 5% sucrose (Figure 2.1). *PsbA3* deletion construct was also created using a similar approach wherein a 1.1 kb fragment from *Bst*EII site 55 bp upstream of start codon to *Hin*dII site 1179 bp upstream of start codon was replaced with *Xba*I-*Xba*I fragment of pRL250 (*77*) The resultant strain of *Synechocystis*, designated ΔA1ΔA3, lacks two of the three copies of *psbA* gene (*psbA1* and *psbA3*).

To delete the remaining *psbA* gene (*psbA2*) in the ΔA1ΔA3 strain, cells were transformed with the chromosomal DNA of the 4E-3 strain (*79*) that has the *psbA2* gene interrupted with an erythromycin resistance cassette. The transformants were selected for erythromycin resistance and were confirmed with the lack of the ability for photoautotrophic growth. The resultant triple deletion strain generated was designated as

ΔA1:ΔA2Em:ΔA3 and was used as a recipient strain for the introduction of mutant and WT *psbA2*.

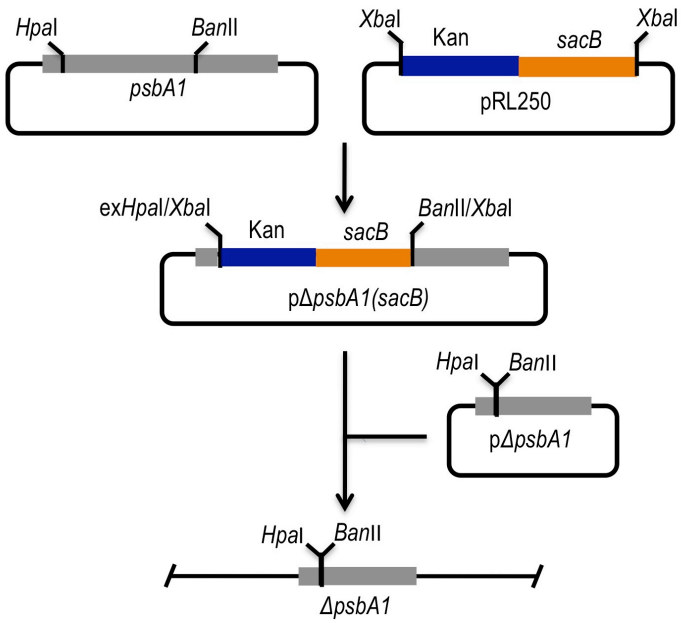

Fig.2.1. Schematic representation of construction of the markerless deletion of *psbA1* gene. The *Hpa*I-BanII fragment of psbA1 is replaced with *XbaI-Xba*I fragment of pRL250 containing the Kanamycin resistance and *sacB* gene. The resultant plasmid named p*ΔpsbA1(sacB)* is used to transform *Synechocystis* to create a *ΔpsbA1(sacB)* strain. This strain is transformed with a markerless plasmid p*ΔpsbA1* that lacks the antibiotic marker and sacB gene to generate a strain contains the markerless deletion of *psbA1* gene.

2.2.2 Synthesis of *psbA2* gene with neutral site flanking sequences

Chemical gene synthesis and fusion PCR were used to construct a gene that was directly used for transformation into *Synechocystis*. A 2671 bp gene fragment including 505 bp and 482 bp of the upstream and downstream flanking sequence respectively from the neutral site (slr0168) (*76, 80, 81*), 401 bp of *psbA2* native promoter, 1083 bp of coding sequence and 200 bp of native terminator sequence was ordered for synthesis from Blue Heron Biotechnology Inc. The coding region of *psbA2* represented the wild type version of the gene except one point mutation (T/C) at -1 location of *psbA2* to

introduce a unique restriction site (*Nde*l). The entire sequence was given for synthesis in two halves bearing a 40 bp complementary overlapping region. The two fragments designated as *psbA2*seq1 and *psbA2*seq2 were chemically synthesized and cloned into BlueHeron pUCminusMCS vectors and their sequence verified. The individual DNA fragments from the plasmids were used for one-step fusion PCR to synthesize the full-length *psbA2* gene with neutral site (NS) flanking sequences. Figure 2.2 describes a schematic representation of the design and synthesis of full-length synthesis of *psbA2*. The procedure for fusion PCR was essentially as described in (*82*) using AccuPrime *Pfx* and AccuPrime *Pfx* High fidelity DNA polymerase (Invitrogen) for standard PCR amplification and fusion PCR amplification respectively. Table. 2.3 lists the primers used for fusion PCR to obtain the full length gene with neutral site flanking sequences.

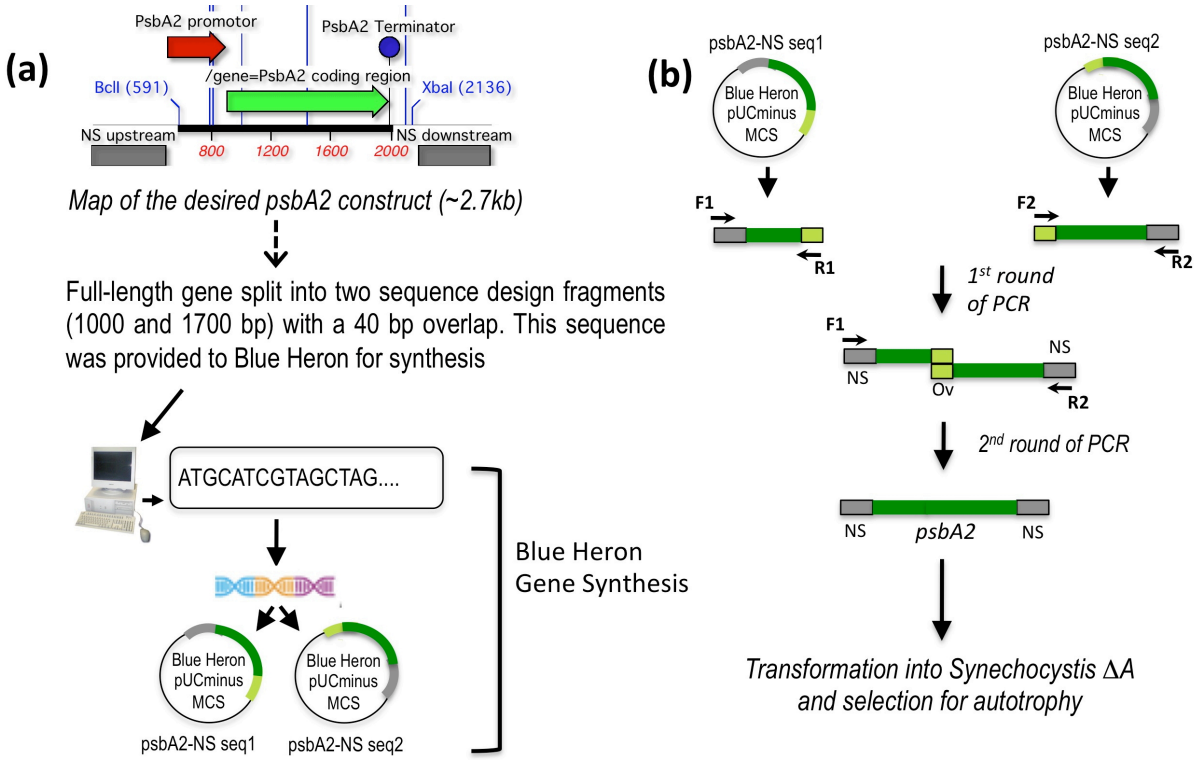

Figure 2.2. **Layout of the construction of *psbA2*NS (eWT)** (a) The process of gene synthesis starts with the construction of the gene sequence *in silico*. The full length gene included 500 bp of upstream and downstream Neutral site (NS) sequences, ~400 bp of psbA2 native promoter, ~1 kb coding region of *psbA2* gene, ~200 bp *psbA2* native terminator. The entire sequence (2.7kb) was split into two sequence fragments to enable their synthesis and cloning. A 40bp homologous region was included to the end of each fragment for easy overlap of the two sequences. These sequences were provided to Blue Heron for artificial synthesis and cloned into pUCminusMCS vector. They were designated as *psbA2*seq1 and *psbA2*seq2. (b) The two sequences from these vectors were PCR amplified with primers F1, R1 and F2, R2 respectively. NS and Ov represents the neutral site flanking region and 40bp overlap region respectively. The PCR products obtained from 1st round of PCR were used as a template for a 2nd round of PCR using external primers F1 and R2. The fusion PCR product obtained was the full length *psbA2* gene with neutral site flanking region. The PCR product was directly used for transformation into *Synechocystis*.

Primer	Sequence (5' -> 3')	Location
Neutral site (*slr0168*) upstream (F1)	GGACCATTCTCTGGATCATTGCC	Homologous to the upstream flanking region of the neutral site
psbA2 (*slr1311*) overlap region (R1)	CCGAACCAACCGACATAAATCC	Homologous to the 40 bp overlap region in fragment 1 (*psbA2-seq1*)
psbA2 (*slr1311*) overlap region (F1)	CTA CCA ACA ACC GGA TTT ATG TCG	Homologous to the 40 bp overlap region in fragment 2 (*psbA2-seq2*)
Neutral site (*slr0168*) downstream (R2)	CAGATTGCCTTTGACAACAATGTGG	Homologous to the downstream region of the neutral site
psbA2 (*slr1311*) overlap region (R1)	CCGAACCAACCGACATAAATCC	Homologous to the 40 bp overlap region in fragment 1 (*psbA2-seq1*)

Table 2.3. Primer pairs used to amplify target gene with neutral site flanking regions.

2.2.3 Construction of *psbA2* ectopic strain

The PCR product of the full-length *psbA2* gene (*psbA2* synthesis described in Chapter Three) was directly used for transformation into the *ΔA1:ΔA2Em:ΔA3* strain. This gene was introduced into an ectopic location of the *Synechocystis* chromosome. Since the recipient is not capable of autotrophic growth due to the absence of a functional *psbA* gene, transformants were selected on plates forcing autotrophic growth. The protocol for transformation was as described in (*76*) where 2-10 μg of the purified PCR product was added to 0.5 ml of cells at an OD_{750nm} of 2.5. The cells were incubated with the DNA for 6 hrs with intermittent shaking after 3 hrs. Following incubation the cells were spread plated onto autoclaved membrane filters (Immobilon transfer membranes, Millipore) laid onto BG-11. The presence of transformed colonies was observed in 7-10 days. The integration of the gene into the targeted site was confirmed by colony PCR. The primers used for the confirmation of gene integration are listed in Table 2.4.

Primer	Sequence (5' -> 3')	Location
Neutral site upstream (P1)	CCGTCCCGTAATATCTTCCGC	Homologous to the upstream neutral site flanking region
psbA2 coding region (P2)	GCACCAGAGATGATGTTGTTACCG	Homologous to the downstream *psbA2* coding region
Native site upstream (P3)	GCG TTC CAG TGG ATA TTT GCT	Homologous to the upstream region in native site of *psbA2*

Table 2.4. Primer pairs used to confirm the integration of *psbA2* at the Neutral site

2.2.4 Construction of the Dual D1 strains (2D1-strains)

A second *psbA2* gene was introduced into the native locus on the chromosome by transformation of the ectopic strain (described in Section 2.2.2 and Chapter Three) with the chromosomal DNA isolated from existing strains containing the wild-type locus or one of several mutations examined in this study. In principal, the approach that I have developed will allow the re-examination of the many mutations already produced in the D1 protein but now in the context of the parallel *psbA* expression construct. The *psbA2* gene at the native locus bears a kanamycin resistance (Km^r) gene cassette downstream of the *psbA2* locus. The location of the gene and the antibiotic cassette is described in Figure 4.2 (Chapter 4 describing the genotype of the strains). The procedure of transformation was as described in Section 2.2.2. The transformants obtained were selected for Km^r. The integration of mutant and WT *psbA2* at the native locus was confirmed by PCR. The list of PCR primers used for the confirmation of the *psbA2* gene at both the native and ectopic locus is listed in Table 2.5. The PCR products were validated for their identity by DNA sequencing. Once the desired genotypes were confirmed the transformant strains were soon stored as frozen stocks to allow repeated recovery of the original strains over the course of the described experiments in order to

avoid possible revertants. Cultures obtained from frozen stocks are referred to as stock cultures and these were maintain by growth in the presence of DCMU and glucose (photoheterotrophic growth) to neutralize the selective advantage of possible revertants. In this regard, the ability to sequence the PCR products also allowed the confirmation of the genotypes during the course of experimentation, which is important due to the possibility of recombination among the multiple copies of the *psbA* gene that could cause the reversion of the desired mutations to wild-type sequence. As noted in Chapter 4, this undesired outcome was not observed, which was likely due to vigilant maintenance of stock cultures under photoheterotrophic growth conditions.

Primer	Sequence (5' -> 3')	Location
Neutral site (*slr0168*) upstream (F1)	GGACCATTCTCTGGATCATTGCC	Homologous to the upstream flanking region of the neutral site
Neutral site (*slr0168*) downstream (R2)	CAGATTGCCTTTGACAACAATGTGG	Homologous to the downstream region of the neutral site
Native site upstream (P4)	GCGTTCCAGTGGATATTTGCTG	Homologous to the upstream region in native site of *psbA2*. Binds 73 bp upstream
Native site downstream (P5)	CAGATGTCGTTGCTGGTTACA	Homologous to the downstream region of native site. Binds 537 bp downstream

Table 2.5. Primer pairs used for the amplification of the entire ectopic site (F1 and R2) and native site (P4 and P5). These primer pairs were used for the confirmation of the gene integration at each of these two sites on the chromosome.

2.3 Extraction of genomic DNA from *Synechocystis*

Genomic DNA was isolated from a 'loop-full' of cyanobacterial culture grown on BG-11 solid media for not more than two weeks. The cells were resuspended into a 0.6 ml microfuge tube with 300 µl of TE buffer (*83*) to form a uniform suspension. 200 µl of 0.1 mm diameter glass beads was added to this cell suspension and mixed well. Cells

were broken using a Mini Bead Beater for 30 seconds. The glass beads were allowed to settle and the supernatant transferred into a 1.5 ml microfuge tube. The glass beads were washed with 200 µl TE and the supernatants from combined with the supernatant collected previously. The suspension containing the genomic DNA was centrifuged at 10,000 X g (Eppendorf 5417R, Hauppauge, NY, USA) at room temperature to remove glass beads and any unbroken cells. Equal volume of 1:1 phenol: chloroform was added to the supernatant and centrifuged at 10,000 X g for 5 minutes at room temperature. The aqueous phase was transferred to a new tube and an equal volume of chloroform was added and centrifuged again at 10,000 X g for 5 minutes. The aqueous phase was transferred again to a new tube and half volume of 7.5 M ammonium acetate (pH – 5.3) and 2.5 volumes of 100% ethanol was added and stored in -20°C for two hours. Precipitation of DNA was achieved by centrifugation at 20,000 X g for 20 minutes. The pellet was washed with 70% ethanol and dried using a Speed Vac. The dried pellet was resuspended in 20 µl of H_2O. As a note to future students in the lab: During the course of my work, another procedure for isolating chromosomal DNA was implemented in the lab and that procedure, while not used in my studies, is probably superior for chromosomal DNA isolation especially when larger (>1.5 kb) PCR fragments are to be produced.

2.4 Determination of chlorophyll concentration.

The concentration of chlorophyll in individual samples was expressed as µg of chlorophyll per ml of solution, by absorption spectroscopy measured using a UV-Vis scanning spectrophotometer (UV-2101PC, Shimadzu, Japan). The chlorophyll concentration of whole cell suspensions was determined by diluting the sample 100 fold

in liquid BG-11 growth media and measuring the absorption of the sample at 620, 678 and 750 nm in a 1 cm cuvette. The chlorophyll concentration was calculated using the following equation(*76*)

$$[Chl] = (14.96*(A_{678} - A_{750})) - 0.607*(A_{620} - A_{750}))$$

The chlorophyll concentration in thylakoid membranes was determined by dissolving a 10 µl sample in 990 µl of methanol and centrifuging the sample for 5 min at 14,000 rpm to extract chlorophylls. The absorption of the supernatant at 665 nm is measured in a 1 cm cuvette and the concentration was determined using an extinction coefficient of 12.5.

2.5 Isolation of thylakoid membranes.

A small scale thylakoid membrane isolation procedure (modified from Komenda et al., 2002 (*84*)) was used for biochemical analyses. Cultures grown to an OD_{750nm} ~ 1.2 in 100 ml volumes with continuous shaking under 20 µmol m^{-2} s^{-1} of flux intensity were chosen for harvesting and isolation of thylakoid membranes. Cells with chlorophyll concentration of at least 250 µg were harvested by centrifugation at 6,000 X g at 4°C. The pellet was washed with 25 mM Tris – HCl (pH – 7.5) and centrifuged again. The cells were resuspended to a chlorophyll concentration of 1 mg/ml in 25 mM Tris – HCl (pH – 7.5). Cells were constantly kept in the dark and on ice from this step onwards. To this cell suspension benzamidine, ε-amino-η-caproic acid and phenylmethanesufonyl fluoride (PMSF) were added at a final concentration of 1 mM. The cells were incubated

in the dark on ice for 10 minutes. Zirconium beads with a diameter of 0.1 mm (BioSpec Products, Bartlesville, OK, USA) were taken in 1.5 ml microfuge tubes and washed with 25 mM Tris – HCl (pH – 7.5). Cells of equal volume were added to the beads and mixed well to form a uniform suspension. Cells were broken in 4°C cold room using a Mini-BeadBeater (BioSpec Products, Bartlesville, OK, USA) for two cycles of 15 seconds on and 5 minutes off. The beads were allowed to settle and supernatant was collected in a new microfuge tube. The beads were washed three times with twice the volume of 25 mM Tris- HCl (pH – 7.5) and supernatant was pooled into the microfuge tube. The broken cell suspension was centrifuged at a speed of 3,500 X g for 8 minutes wherein the beads and any unbroken cells were removed. The supernatant consisting of thylakoid membranes were then centrifuged at 20,000 X g for 30 minutes at 4°C (Eppendorf 5417R, Hauppauge, NY, USA). The blue supernatant was carefully discarded and the pellet was resuspended in 25 mM MES-NaOH (pH-6.5) with 25% (v/v) glycerol, 10 mM $CaCl_2$ and 10 mM $MgCl_2$. The chlorophyll concentration of the isolated membranes was estimated with methanol as described in Section 2.4 and adjusted to a concentration of 1 mg/ml. Membrane samples with 5 μg chlorophyll were aliquoted into tubes and flash frozen in liquid nitrogen before storing at -80°C.

2.6 Fluorescence measurements

Measurements of variable fluorescence yields were performed using the double modulation kinetic chlorophyll fluorometer with a second actinic flash illumination source (PSI Instrument, Brno, Czech Republic). Cells grown to mid-logarithmic phase, diluted to a chlorophyll concentration of 5 μg/ml were used for fluorescence

measurements. The variable fluorescence was assayed as described previously (*85*). The low fluorescence (F_0) state is measured in dark adapted samples by probing fluorescence yield with four measuring pulses followed 200 μsec later by a 30 μsec saturating actinic flash, followed by a sequence of measuring pulses beginning 50 μsec after the actinic flash. PSII has a high fluorescent yield when it is in the state $P680.Q_A^-$, which is formed when a P680 absorbs a photon of light and donates an electron to Q_A. Without inhibitors, the principal component of decay of this state is due to the oxidation of Q_A^- by a plastoquinone in the Q_B site. When DCMU was used to block the electron transfer from Q_A^- to Q_B, this causes $P680.Q_A^-$ to persist until the electron recombines with oxidants on the donor side, which in the case of the intact enzyme, is principally the S_2 state of the Mn_4-Ca. Total variable fluorescence was evaluated as $F_v = (F_m-F_0)/F_0$, where F_m is maximal fluorescence and F_0 is the lowest level of fluorescence yield obtained. The maximal values of variable fluorescence obtained were normalized by using the formula $F = [(F_v-F_0)/(F_m-F_0)]$ for an appropriate comparison between the control and mutant strains.

2.7 Photoinhibition and Recovery

Experimental cultures were diluted and adjusted to an OD_{750nm} of 0.7 and returned to grow at an intensity of 40 μmol m^{-2} s^{-1} for one hour before the high light treatment to induce photoinhibition. The chlorophyll concentration of the cultures was determined to be ~ 6 μg/ml. Photoinhibition experiments were conducted in small scale using test tubes (~75 ml, 2.5 cm diameter). These culture tubes were immersed in a circulating water bath

maintaining the temperature at 30°C with constant bubbling of air enriched with 3% CO_2 throughout the experiment. Cultures were exposed to 1100 μmol m^{-2} s^{-1} incident halogen light throughout the high light treatment. Sample was withdrawn every 15 min over a period of 90 min high light treatment before returning the experimental cultures to a lower light intensity of 40 μmol $m^{-2}s^{-1}$ to monitor the recovery. Recovery was observed for 120 minutes by determining variable fluorescence at 15-minute intervals.

2.8 Analyses of thylakoid membranes using PAGE

PSII proteins were analyzed by resolving thylakoid membranes using denaturing gel electrophoresis. Proteins were typically resolved on a linear 12% - 20% denaturing gradient polyacrylamide gel containing 6M Urea (*86*). The procedure for sample preparation was modified from Komenda et al., 2002 (*84*). Fresh thylakoid membrane aliquots (without any freeze thaw cycles) of 5 μg chlorophyll were centrifuged at 20,000 X g for 20 minutes using a table top microcentrifuge (Eppendorf 5417R, Hauppauge, NY, USA). Samples were solubilized in 25 mM Tris – HCl (pH- 7.5) containing 2% sodium dodecyl sulfate (SDS), 2% dithiothreitol (DTT) and 12.5% glycerol. These samples were incubate at room temperature for 60 minutes for maximum solubilization. Samples were loaded on an equal chlorophyll basis and proteins were electrophoresed at 4°C under constant current. Proteins separated on the gel were visualized by staining with Commassie Blue R250 and/ or transferred onto PVDF membrane for western blotting (described in the next section).

For resolving the different forms of D1 protein on a polyacrylamide gel a linear 18% - 24% denaturing SDS PAGE was used which was adapted from Kashino et al., 2001 (*87*). The buffer system was maintained as described in (*87*) but preparation of protein samples were as described above.

2.9 Immunoblot analysis of PsbA

To probe accumulation of D1 protein (PsbA) in the thylakoid membrane samples, proteins resolved by PAGE were transferred onto PVDF membranes using a semidry blotting apparatus (BioRad semidry western transfer assembly). Transfer was accomplished as directed in the manual at a constant voltage of 15 V for 25 minutes. The gel was stained post transfer to detect the efficiency of transfer onto the PVDF membrane. Membranes were washed with 1 X Tris buffered saline (TBS) twice for 15 minutes with shaking and kept for blocking with 5% BioRad blocking agent or 5% BSA in TBST (TBS with 0.2% Tween 20) for 1 h with gentle agitation. The membranes were washed three times with TBST and incubated with the primary antibody rabbit anti PsbA (1:2000 dilution in TBST) for overnight at 4°C. The membranes were washed again three times for 15 minutes each with shaking before incubating them with the secondary antibody goat anti rabbit HRP (1:5000 dilution in TBST) for 2 h. Membranes were washed three times for 15 minutes each and the blot was prepared for development using SuperSignal West Pico chemiluminescence kit (Thermoscientific, Rockford, USA). The developed blots were imaged using the Alpha Innotech Chemi Imager.

CHAPTER III

Expressing high levels of D1 protein of Photosystem II from an ectopic location on the *Synechocystis* sp. PCC 6803 chromosome

This chapter has been published "Nagarajan, A., R. Winter, Eaton-Rye, J., and Burnap, R.L. (2011). A synthetic DNA and fusion PCR approach to the ectopic expression of high levels of the D1 protein of Photosystem II in *Synechocystis* sp. PCC 6803. *J Photochem Photobiol* B 104(1-2): 212-219" and is in this thesis with permission

3.1 Introduction

D1 is encoded by *psbA* gene and typically exists as a single copy in higher plants and algae while in cyanobacteria it belongs to a multigene family (*88*). In *Synechocystis* sp. PCC 6803 (*Synechocystis*) the *psbA* gene family consists of three members *psbA1*, *psbA2* and *psbA3* (*76, 88*). These genes are differentially expressed in a light dependent manner at the transcriptional level, with *psbA2* contributing to 95% of transcript levels and *psbA3* contributing to the rest (*89*). *PsbA1* has recently been shown to be up-regulated under low oxygen conditions (*90*). Both *psbA2* and *psbA3* share a 99% nucleotide identity and encode for an identical gene product whereas *psbA1* shares a 75-85% nucleotide identity at the open reading frames and thus encodes for a protein different from *psbA2* and *psbA3* (*76, 89, 91*). From the first chapter it is evident that D1 protein is the main site of light induced inactivation of PSII (photoinhibition) and there

exists a repair mechanism to facilitate the reactivation of PSII [refer Chapter 1 and reviewed in (*21*)]. The photodamage to the D1 protein appears to be irreversible and the inherent and ubiquitous mechanism of PSII reactivation involves the replacement of the damaged copy of D1 with a new copy produced by *de novo* protein synthesis. Thus, the damaged PSII complex is disassembled, and then reassembled into a complex with restored function and a mix of new D1 protein and old subunits. Consequently, D1 is recognized as a highly turned over protein in comparison with other thylakoid proteins in the presence of light. Photoinhibition is typically observed when the rate of the occurrence of photodamage exceeds the rate of PSII repair. The high light conditions associated with photoinhibition increases the rate of transcription in *psbA* (*92, 93*) and this increase in *psbA* transcripts can be correlated with the enhanced rate of D1 protein synthesis (*94*). Therefore, it is suggested that D1 degradation and *de novo* synthesis of D1 are synchronized events (*95*). It was observed that a blockage of protein synthesis using inhibitors also inhibit the degradation of D1 already present in the membrane (*96*). Hence, the rate of D1 degradation is controlled by the extent of PSII photodamage and the capacity of D1 protein synthesis for replacement of damaged D1 (*94*). Accordingly, the newly synthesized D1 protein may facilitate the displacement of damaged D1 allowing its faster recognition and degradation.

When *psbA2* gene was previously expressed from an ectopic location in the absence of other *psbA* genes, it was observed that the *psbA2* transcript levels were very low and that these low levels corresponded with slower rates of repair when compared to a natural *psbA2* expressing wild type (*97*). This observation is additional evidence that

the rate of repair is dependent upon the levels of *psbA2* transcript (*94*). The reasons for lower expression levels of *psbA2* in the ectopic strains was hypothesized to be caused by either the use of an incomplete *Synechocystis* promoter that is lacking certain crucial elements required for the light regulated expression of *psbA* or that an absence of the native terminator signals causes shortening of the transcript half life (*97*).

We have developed an improved ectopic genetic system to address the questions raised by the previous study conducted on ectopic expression of *psbA2* gene as well as use a complete replacement of the gene by heterologous versions of the gene. The described genetic approach allows mutagenesis of the full length of the *psbA* gene using a single system. The present system involves the use of fusion PCR strategy to synthesize the full-length *psbA2* gene from plasmids bearing the upstream and downstream portions of *psbA2* gene. The plasmids bear an overlapping region to allow the fusion of the two portions. This approach allows us to bypass the step of cloning the full-length gene into *Escherichia coli* (*E. coli*), which appears to be otherwise deleterious. The toxicity of full-length cyanobacterial genes in *E. coli* is attributed to the hydrophobic nature of most of the proteins that disrupts the host cell membranes and renders *E. coli* non viable (*98*). The ability of *Synechocystis* to spontaneously take up foreign DNA and integrate into their chromosome makes this fusion PCR approach very powerful and straightforward (*99*). Fusion PCR is used to construct linear DNA fragments that are transformed into *Synechocystis* without the requirement of a cloning vector (*100*). The construction of *psbA2* gene using this approach serves as a model to create other mutants with parallel mutations to study their combined effect without disrupting their native location.

3.2.Results

3.2.1. Synthesis of full-length *psbA2* gene using fusion PCR

Targeting of the *psbA2* gene locus (gene plus the flanking promoter and terminator sequences) to the neutral site was mediated by the design of chimeric sequences flanking the *psbA2* locus that were homologous to the neutral site as shown in Figure 2.2. The neutral site is defined in this case as a chromosomal location that produces no discernible phenotype when interrupted (*76*) and has been used before for other applications (*80*). In principal, other, potentially better, chromosomal locations could be utilized, but this site was chosen because previous use had demonstrated its utility. Because the full-length *psbA* gene is known to be toxic in *E. coli* (*88*), a chimeric *psbA2* gene locus was commercially synthesized and cloned in two halves. High-fidelity fusion PCR utilizing sequence overlap between the two synthetic gene halves was then used to produce a DNA fragment that was able to recombine the full-length *psbA2* gene into the *Synechocystis* chromosome at an ectopic (non-native) location using a strategy illustrated in Figure 2.2. The 1st round of PCR amplification produced the two individual DNA fragments *psbA2*seq1 and *psbA2*seq2 isolated from corresponding plasmids provided by Blue Heron using primers F1, R1 and F2, R2 respectively (Table 2.3). The 1st round was a regular PCR with standard amplification conditions using a high fidelity *Pfx* DNA polymerase (AccuPrime^{TM}, Invitrogen, USA). The PCR products were analyzed by agarose gel electrophoresis and the predicted product size from *psbA2*seq1 and *psbA2*seq2 being 1011 bp and 1701 bp respectively were observed (Figure 3.1). The

2nd round of PCR used the gel extracted products obtained from the 1st PCR as a template and the external primers F1 and R2 from Table 2.3 again using high fidelity *Pfx* DNA polymerase. The gradual increase in the extension time per PCR cycle resulted in a higher yield of the fused product. This final amplified product was also analyzed by agarose gel electrophoresis and confirmed by the expected product size of 2671 bp that represented the full-length *psbA2* gene with neutral site upstream and downstream flanking sequences (Figure 3.1B).

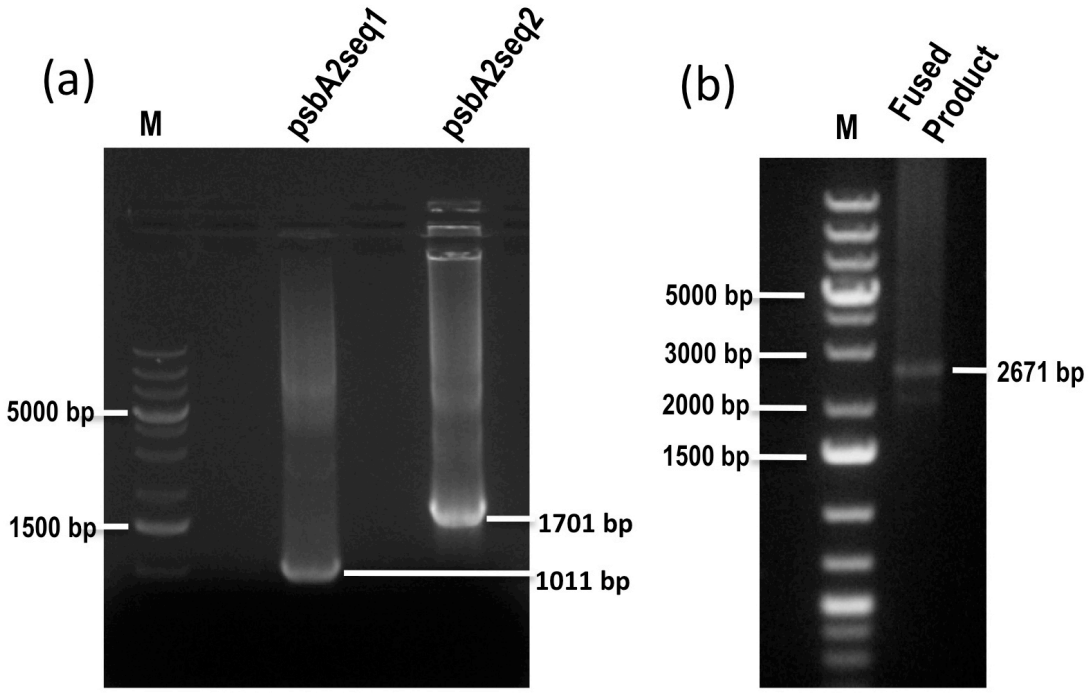

Figure 3.1. Synthesis of full-length *psbA2* gene (a) First round of PCR amplification of the two cloned gene fragments provided by Blue Heron. The size of fragments psbA2seq1 and psbA2seq2 were 1000bp and 1700bp respectively representing the split sequence of WT *psbA2*, (b) Fusion PCR of the two PCR products psbA2seq1 and psbA2seq2. The PCR amplified product was observed as a single band of size ~2700bp (entire WT *psbA2* flanked by neutral site sequences).

The combined use of artificial DNA synthesis and fusion PCR for the production of the target gene is an efficient alternative to conventional cloning or fusion PCR techniques (*100, 101*). Typically, fusion PCR technique employed in *Synechocystis* involves a three

step PCR approach that consisted of amplification of flanking sequences, production of intermediate amplified products and then the final synthesis of fused gene product (*100, 101*). The use of artificial synthesis allowed us to create a 40 bp overlapping region between the two sequence fragments thereby increasing the specificity and likeliness of a fusion event between the two sequences. This enabled us to obtain higher yields of the fused product. Using this approach we can now introduce mutations at the N-terminus that has been suggested to have structural importance in the function of PSII (*67, 102*), but using the same system as for making changes in the C-terminal region. Therefore, with this study we have established conditions that allow the synthesis of full-length target gene with one step fusion PCR approach.

3.2.2. Integration of *psbA2* at the non-native (ectopic) location

The linear DNA molecule synthesized by fusion PCR was used to transform the *ΔA1:ΔA2Em:ΔA3* (*ΔpsbA)* strain (Figure 3.2), which lacks all three copies of the *psbA* gene (construction described in Section 2.2.1. The transformants were selected onto BG-11 plates for their ability for photoautotrophic growth. The absence of any *psbA* genes in *ΔA1:ΔA2Em:ΔA3* strain allows us to exploit this property and select for photoautotrophic growth without the need for an antibiotic resistance cassette. The integration of DNA into *Synechocystis* chromosome by homologous recombination was observed by the presence of pinpoint colonies within 10 days of transformation. Transformation was performed in duplicates and the number of transformants for each was counted to be 15 and 22. Each of these colonies was re-streaked several times to obtain complete segregation and two such transformants designated as *psbA2*NS1 (primarily used in this work and described as

eWT or ectopic WT) and *psbA2*NS2 were used for confirmation of gene insertion and characterization. Verification of *psbA2* at both the neutral (ectopic) and native (original) site was achieved by colony PCR for *psbA2*NS (eWT, ectopic strain), RD1031 (control strain) and *ΔA1:ΔA2Em:ΔA3* where in the last two served as controls. A diagrammatic representation of the genotypes of all three strains is given in Figure 3.2. The primers used for this purpose listed in Table 2.4 were specific for the upstream regions of the neutral site and native site of *psbA2* and the coding region of *psbA2* to detect the presence of the gene in either of these two locations (neutral site and native site). The neutral site forward primer (P1) binds 621 bp upstream of the neutral site flanking region and the reverse primer (P2) binds 218 bp downstream of the *psbA2* translation start site. Therefore, in the event of *psbA2* insertion at the neutral site the predicted PCR product size would be ~850 bp. Similarly, the native site forward primer (P3) binds 524 bp upstream of the *psbA2* translation site and the reverse primer (P2) binds 218 bp downstream of the *psbA2* translation start site. Thus, the predicted product size for the presence of *psbA2* gene at the native site would be ~ 730 bp. All PCR amplified products were analyzed by agarose gel electrophoresis and it was observed that only *psbA2*NS gave a band of expected size (850 bp) with neutral site primers whereas RD1031 gave a band of expected size (730 bp) with native site primers (Figure 3.3). Based on the results from the colony PCR it was conceived that *psbA2* gene has been successfully integrated into *Synechocystis* chromosome at the neutral site (ectopic).

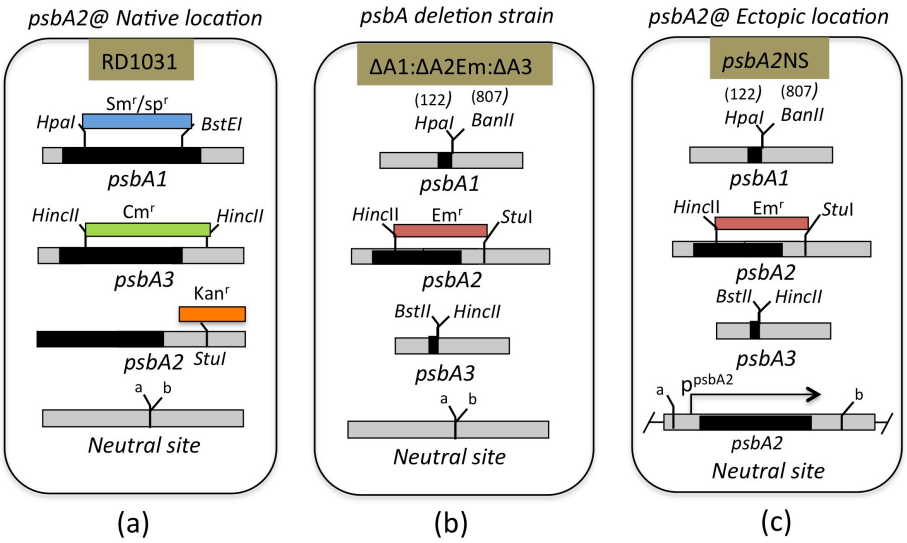

Figure 3.2. **Genotype of strains** (a) RD1031, used as a control with *psbA2* gene at the native location with a Kanamycin resistance. *PsbA1* and *psbA3* are replaced by Spectinomycin and Chloramphenicol respectively, (b) The marker-less *ΔpsbA strain* constructed by knocking out *psbA1* and *psbA3* using marker-less strategy and *psbA2* replaced with Erthromycin, (c) *psbA2*NS, mutant strain with wild type *psbA2* gene along with native promoter and terminator integrated into the neutral site of the *ΔpsbA strain*.

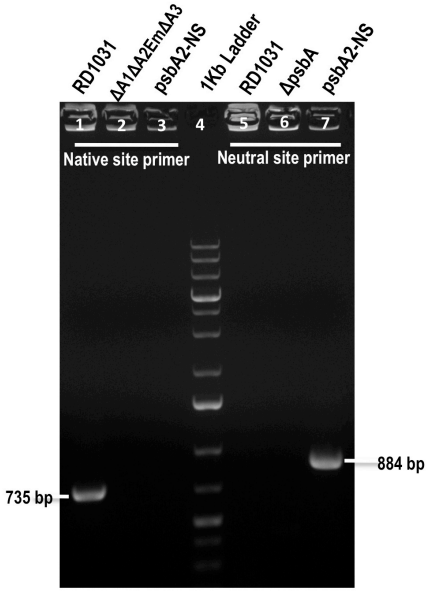

Figure 3.3. **Confirmation of the integration of psbA2 into the ectopic location**. The insertion of *psbA2* gene into the ectopic location in the *ΔpsbA* strain was confirmed using neutral and native site specific primers (PI, P2 and P3 from Table 2.4) Lanes 1-3 and lanes 5-7 represent the native site and neutral site of psbA2 respectively. The 735bp product in Lane 1 shows the presence of *psbA2* in the native locus in this control strain and its corresponding absence in lane 5. Lanes 2 and 6 show the absence of *psbA2* in the *ΔpsbA* strain. The absence of a product in lane 3 and corresponding 884bp product in lane 7 confirms the presence of the gene insertion in the mutant *psbA2*NS.

3.2.3. PSII levels in cells grown at different light intensities

A previous attempt to express the *psbA2* gene from the same ectopic location using a non-native transcriptional terminator, resulted in a strain that was sensitive to light (*97*). To determine the sensitivity of the newly constructed ectopic strain to light, PSII activity of *psbA2*NS (eWT) was compared to the control strain RD1031 by evaluating the maximal variable fluorescence. The values obtained for the maximal fluorescence levels suggest functional expression of D1 protein in the ectopic strain, *psbA2*NS (Table 3.1). Phenotypically the mutant appeared similar to the control strain and was observed to have a similar growth rate. Table 3.1 lists the maximal fluorescence levels in both the *psbA2*NS and RD1031 grown under three different light intensities. *psbA2*NS appeared to be much more tolerant to higher light intensities (~150 μmol $m^{-2}s^{-1}$) as compared to the ectopic strain (MK1) constructed in the previous attempt (*97*). The maximal fluorescence values of *psbA2*NS were almost always comparable to the control strain grown under all the three different light intensities used for evaluation, 20, 40 and 150 μmol $m^{-2}s^{-1}$. The electron transport activity of PSII as measured by the variable fluorescence in the absence and presence of the inhibitor DCMU appeared to be similar to the control suggesting that both the donor and acceptor side reactions were normal indicating the presence of normal/active PSII centers. The interesting observation of the restored PSII activity in *psbA2*NS like the control strain, which was lacking in the previously constructed ectopic strain (MK1) was due to the difference in the gene construction of *psbA2*NS. This new construction has rendered tolerance towards higher light intensity.

Strain	150 μmol $m^{-2}s^{-1}$	40 μmol $m^{-2}s^{-1}$	20 μmol $m^{-2}s^{-1}$
RD1031	0.72 ± 0.02	0.81 ± 0.04	0.52 ± 0.04
psbA2NS	0.79 ± 0.03	0.82 ± 0.05	0.51 ± 0.04

Table 3.1. Maximal variable fluorescence properties of *psbA2*NS (eWT) and RD1031 (control)

3.2.4. Photoinhibition and repair characteristics of the ectopic strain, *psbA2*NS

The light sensitivity of the previously constructed *psbA2* ectopic strain (MK1) was traced to a reduced ability to recover from photoinhibition (*97*). The ectopic strain, *psbA2*NS retained high PSII activity when grown at higher light intensities. The difference in sensitivity towards intensity of growth light from the previously constructed strain, MK1 prompted the assessment of the susceptibility of *psbA2*NS to photoinhibition. A comparison of the rates of photoinhibition of the control (RD1031) and the mutant (*psbA2*NS) strain was performed at a high light intensity (~1100 μmol $m^{-2}s^{-1}$). The rate of photoinhibition of *psbA2*NS was evaluated by the loss of variable fluorescence over time. The measurement of variable fluorescence provides an estimate of the electron transport activity of PSII. With the increased exposure to high light, PSII is subjected to donor and/or acceptor side photoinhibition thereby affecting the electron transport efficiency of PSII. Thus, a decrease in the variable fluorescence reflects a decline in the total PSII activity due to photoinhibition. The decreased PSII activity in *psbA2*NS appeared to very similar to that of RD1031 that has the *psbA2* gene in the native location on the chromosome (Figure 3.4). Similar photoinhibition kinetics indicated that the susceptibility of PSII to undergo photodamage is not altered with the ectopic expression of *psbA2*. This observation was anticipated as the MK1 ectopic strain also showed similar rates of photodamage as the control strain. Therefore, it was

established that the ectopic expression of *psbA2* gene does not affect the rate at which PSII undergoes photodamage under high light conditions.

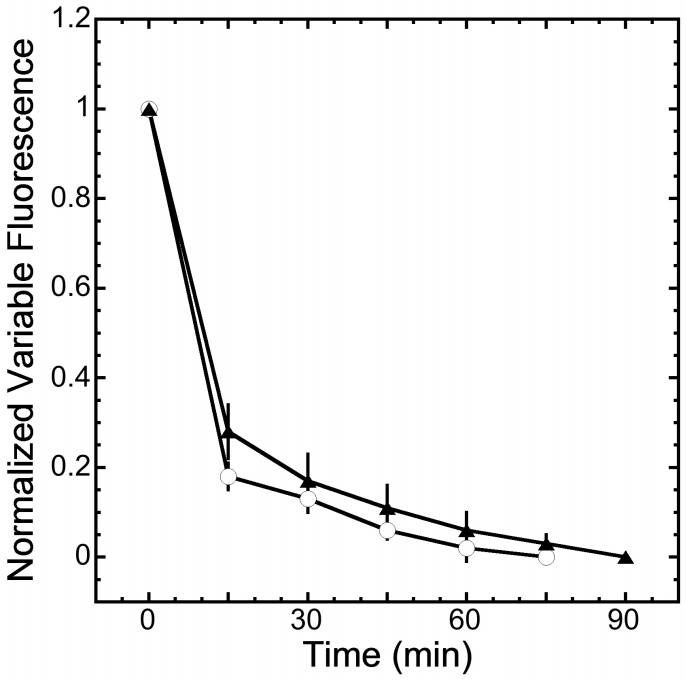

Figure 3.4 Photoinhibition characteristics of *psbA2*NS (eWT). A decrease in the variable fluorescence with time recorded when pRD1031 and psbA2NS cells were subjected to high light (1100 μmol m^{-2} s^{-1}) for 90 minutes. RD1031 and psbA2NS are represented as open circles and closed triangles respectively. The variable fluorescence values for both mutant and control were normalized to 1 for comparison. Graph represent average of three independent experiments and error bars indicate corresponding standard errors (n=3).

The net susceptibility to photoinhibition not only depends on PSII photodamage but also upon the rate of PSII repair by re-synthesis of damaged D1. Therefore a comparison of the repair characteristics of *psbA2*NS and RD1031 was conducted. Cells from these strains were subjected to photoinhibitory light conditions (~1100 μmol $m^{-2}s^{-1}$) until the PSII activity reached 10% of the initial activity as determined by variable fluorescence. These cells were then allowed to recover under lower light intensity (~ 40 μmol $m^{-2}s^{-1)}$ and the gradual increase in the total PSII activity with time was evaluated. *psbA2*NS

recovery from photoinhibition was observed to be similar to the control (RD1031) strain (Figure 3.5). This behavior was very different from the MK1 ectopic strain that showed extremely slow repair characteristics with a half time of approx. 460 min. The control (RD1031) strain showed a recovery rate with a half time of ~75 min. This rate is slightly slower than a true wild type that typically has a $t_{1/2}$ ~ 45 min. The absence of the other two *psbA* genes (*psbA1 and psbA3*) in RD1031 could be attributed to the comparatively slower rate of repair. The ectopic strain *psbA2*NS on the other hand showed improved rate of repair with a $t_{1/2}$ ~ 60 min. It is therefore perceivable that the *psbA2*NS has acquired the ability to undergo PSII repair followed by photoinhibition; a property that was lacking or inefficient in the earlier attempt. Additional genetic elements incorporated in the construction of *psbA2* gene (using a synthetic and fusion PCR approach) might be necessary for this repair capacity.

The repair rates as determined from these experiments appeared to be slightly higher for *psbA2*NS when compared to the control. The reason for this observation is not entirely clear. A plausible explanation could be the difference in the mode of construction of the two strains. The control (RD1031) strain has the genes *psbA1* and *psbA3* replaced by antibiotic cassettes whereas in *psbA2*NS there is a marker-less deletion of these two genes. This variation in the strain construction might be attributed to the lower activity of the control. Also the control (RD1031) strain has been used for many years in the lab and might not be in the perfect condition as expected. A good control to address this issue would be to construct a strain with *psbA2* gene inserted into the native location of the *ΔA1:ΔA2Em:ΔA3* background strain. This strain was constructed later on and similar

higher levels of PSII activity was observed in the both the ectopic WT strain (*psbA2*NS or eWT) and native WT strain (nWT).

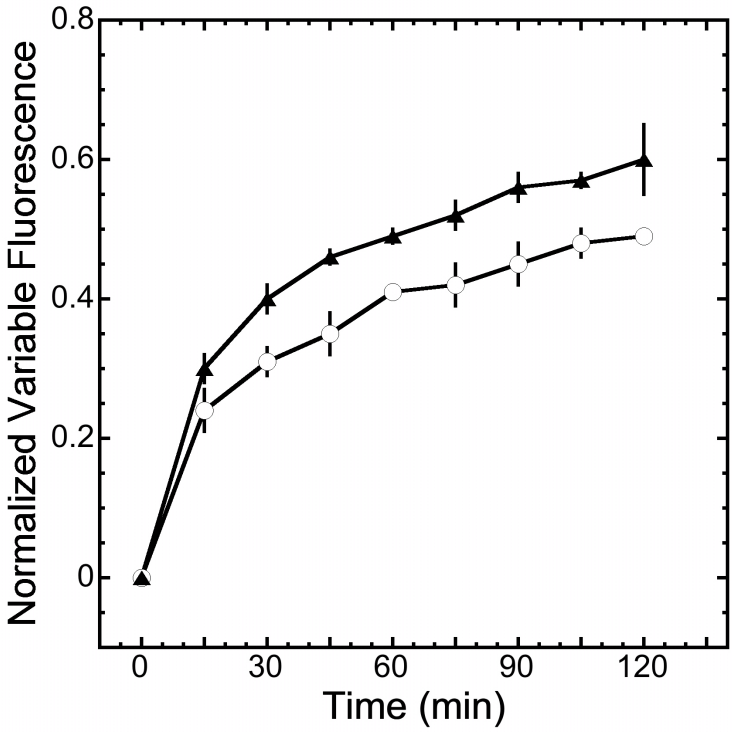

Figure 3.5. Repair characteristics of *psbA2*NS (eWT). An increase in the variable fluorescence with time determined when pRD1031 and *psbA2*NS cells were subjected to high light (1100 μmol m^{-2} s^{-1}) for 120 minutes. RD1031 and psbA2NS are represented as open circles and closed triangles respectively. The variable fluorescence values for both mutant and control were normalized to 1 for comparison. Graph represent average of three independent experiments and error bars indicate corresponding standard errors (n=3).

3.3. Discussion

The present study demonstrated a native-like expression of the D1 protein from an ectopic location on the *Synechocystis* chromosome using a synthetic and fusion PCR approach. The purpose of such an expression system is to increase the flexibility for mutagenesis of the *psbA* gene as well as to provide an model for synthetic DNA-based

gene engineering that is easy to evaluate since strains with altered expression have characteristic physiological and growth phenotypes (*94, 97*). The split gene cloning is only necessary for genes that are difficult to clone in *E. coli* due to toxicity. Full-length *psbA* has been described as being toxic in *E. coli* (*88*). This toxicity is likely due to the hydrophobic nature of the protein that disrupts the cell membrane of *E. coli* and the fact that cyanobacterial promoters function well in *E. coli* (*98*). Therefore, most of the cloning and mutagenesis systems involving *psbA* have been conducted using plasmids containing partial *psbA* gene with the desired mutation that is used to transform a recipient strain having the corresponding portion of the gene deleted. A mutated form of the gene is typically used to transform the recipient strain, thereby restoring the gene, but also carrying in a mutation in the original. These mutagenesis systems are consequently restricted to only certain portions of the gene for example most of the carboxyl terminus of *psbA* (*103, 104*) and a portion of the amino terminus (*102, 105*). Previous studies have attempted the mutagenesis of the N-terminus of *psbA2* using site-directed mutagenic primers (*67*). The present approach allows simultaneous manipulation of multiple regions of the protein and could be used to create many different kinds of engineered protein.

The method described here utilizes a synthetic construction of the *psbA2* gene in two fragments. These fragments were chemically synthesized and cloned individually into pUC vectors (Figure 2.2). The DNA synthesis process involves the synthesis and assembly of many oligonucleotides that act as 'building blocks'. Consequently, it is possible to reuse the building blocks and accordingly, the effort to produce variants of the

original construction is considerably lower. Therefore, while traditional cloning approaches or fusion PCR approaches may be more cost-effective for individual gene synthesis projects, the projects intending to explore multiple variants, multiple site-directed mutations, or targeted random mutagenesis, could benefit from this approach. Another potential drawback regards the fusion PCR part of the described approach since the PCR reaction can introduce sequence errors. However, the used of high-fidelity PCR enzymes minimizes this risk. Furthermore, popular site-directed mutagenesis techniques use *in vitro* polymerization with similar PCR enzymes and consequently, many projects routinely employ post-transformation sequence verification of the target locus to ensure that the intended sequence has indeed been introduced. Completely fusion PCR-based approaches are also an efficient approach to engineer the chromosome of *Synechocystis* (*100, 101*). The advantage in obtaining the fragments as clones is to be able to use these clones for future mutagenesis purposes, which is difficult when only PCR products are involved. More importantly, the use of artificial synthesis allows us to incorporate new restriction sites and point mutations with ease. While the changes were minimal in this present case, the procedure lends itself to many exotic types of gene engineering ideas. It has also enabled us to be able to clone the full-length *psbA2* gene that has been difficult in the past. Additionally, the use of artificial synthesis has shortened the typical three-step fusion PCR to a one-step fusion PCR. Previous studies have reported lower yields with one step fusion PCR (*100, 101*), but the addition of a 40 bp overlapping region in the two fragments seemed to increase the likelihood of fusion between the two sequence

fragments. This strategy of a combined use of artificial DNA synthesis and fusion PCR could be used for other genes and biological systems as well.

This study presents a basis for the expression of multiple forms of a gene from different locations to study their overall effect on a system. It was recently shown in *Thermosynechococcus elongatus* that the *psbA3* gene is responsible for 70% transcript levels during high light incubation (*106*). An absence of the *psbA3* gene in the strains used in this study could be a reason for the observation that strains recovered only ~ 60% of total activity in lower light. It would be interesting to study the effect of *psbA3* and *psbA2* in the same strain and their function in degradation and repair of PSII.

CHAPTER IV

Effects of the expression of alternate forms of D1 protein on the maintenance of Photosystem II

Contents from this chapter will be a part of a manuscript in preparation titled " *Effects of expression of alternate forms of D1 protein on the maintenance and repair of photosystem II*" Aparna Nagarajan, David Taylor and Robert L. Burnap.

4.1 Introduction

Susceptibility of PSII to photoinhibition depends upon the balance between photodamage and repair. Therefore, to maintain a higher PSII activity in a cell there is a continuous flux between damage and repair of PSII. This damage and repair process can be conceptually divided as the damage causing PSII to be inactivated, sensing the damage to initiate repair and the actual process of repair to form active PSII. Studies on PSII repair have shown that D1 protein is the main target for photodamage and this was noticed with the increased turnover rate of D1 in comparison to other PSII proteins during photoinhibition. *In vivo* pulse chase experiments showed the presence of a repair process wherein D1 undergoes degradation and synthesis (*54*). The synchronous nature of D1 degradation and synthesis was also demonstrated using translation inhibitors (*96*). Based

on these studies and others, it is widely assumed that PSII repair specifically replaces the damaged D1 subunits with newly synthesized D1. The damaged D1 proteins are thereby believed to undergo conformational changes causing an exposure of the N-terminus, which is relayed to FtsH as the damage signal.

Prior to addressing the question of the nature of damaging signal, it is pertinent to first address the question: Are only damaged proteins are targeted for PSII repair? Or does photoinhibition trigger the replacement of all D1 subunits by up-regulation D1 turnover rate in a generalized manner? To address this question, it is critical to visualize only that subset of PSII complexes that have incurred photodamage that exist among the entire the pool of PSII complexes present in the cell. Hence, the increased turnover rate of D1 as observed in pulse-chase protein labeling experiments do not provide an unequivocal explanation on the type of D1 subunit, damaged or both damaged and undamaged, that is being replaced. Therefore, both the alternatives of targeted and generalized PSII repair are indistinguishable considering the available indirect evidence discussed in section 1.7.

The D1 ectopic strain constructed as described in the previous chapter was utilized and further construction allowed completion of the genetic system to allow the expression of two alternate forms of D1 proteins in the same cell. The principle behind the development of this system as illustrated in Figure 4.1, was to allow parallel expression of wild type (WT) and damage prone D1 simultaneously in a cell thereby forming two populations of PSII complexes. If the damage prone D1 is specifically targeted for repair then the increased turnover rate of damaged D1 will cause the

accumulation of wild type D1 protein and assemble a higher proportion of active PSII. (Figure.4.1). On the other hand, if there were a generalized repair mechanism then both the wild type and damage prone D1 copies would have an increased rate of turnover thereby accumulating only a lower proportion of active PSII.

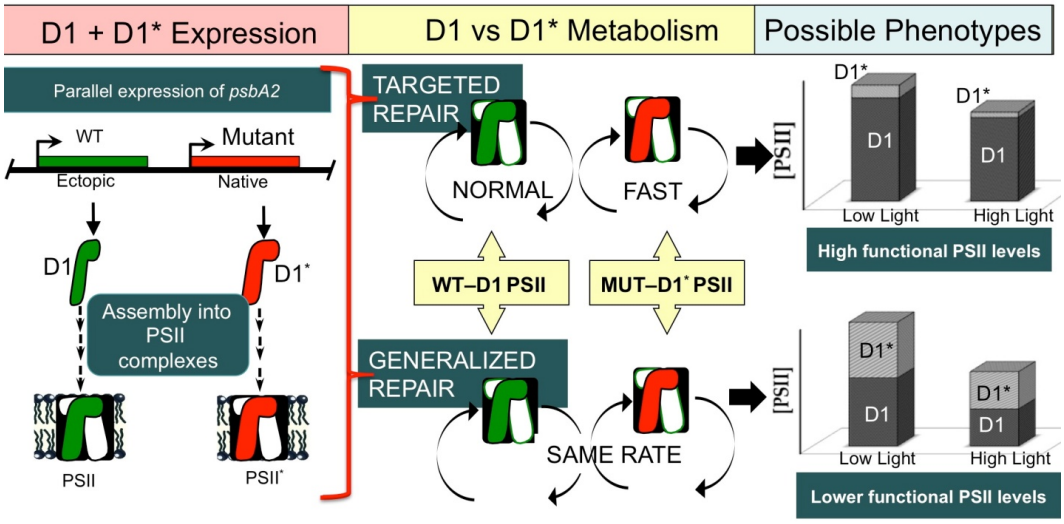

Figure 4.1. Strategy for distinguishing between targeted and generalized repair. The left most panel shows the parallel expression of wild type (green) and damage prone (red) D1 protein from different locations on the chromosome. These two proteins are expressed simultaneously and assembled into PSII complexes as shown. The middle panel depicts predicted individual turnover rates for the different variants of D1 during targeted and generalized repair and right panel shows the hypothetical levels of PSII activity that might be observed for the two plausible repair mechanisms.

4.2 Results

4.2.1. Construction of the dual expression strains

The D1 ectopic strain (*psbA2*NS) henceforth designated as eWT (ectopic WT) to distinguish between the native (n) and ectopic (e) locus on the chromosome; was used as a background for cloning the second *psbA2* gene into the native location. The construction of the dual expression strains always carried the wild type *psbA2* expressing

from the ectopic location and the mutant *psbA2* (damage prone) expressing from the native location. This was chosen to prevent the effect (if any) of gene location in the alternative the ectopic location in terms of a potentially altered phenotype of the mutant compared to the phenotype of the same mutation at the native chromosomal location. Furthermore, introducing the mutation in the native locus the likelihood of the expression of mutant *psbA2* was ensured.

Table 4.1 lists the single point mutations in D1 protein that were used in this study in terms of there previously reported characteristics. The D1-Ser345Pro mutation prevents processing of the carboxy terminus of the protein and causes an inherent instability of the protein, the D1-His337Tyr renders the PSII complex highly light sensitive, and the D1-Asp170Ala mutation prevents assembly of the manganese cluster. Each of these mutations results in lower accumulation of PSII complexes. These strains were re-evaluated for their ability to form active PSII complexes before selecting for dual expression. Along with the list of single D1 high turnover mutants a wild type *psbA2* was also re-introduced the native locus to obtain a double wild type (nWT:eWT) dual strain intended to be used as a control but as discussed in later sections gene dosage effects were studied from the double WT strain.

Strain	Mutant properties from literature
D1 – nS345P	C-terminal extension mutant, PSII content 25% WT, increased D1 turnover rate (*27, 63, 107*)
D1 – nH337Y	Light sensitive, PSII content 42%WT (*108*)
D1 – nD170A	Incorrect Mn_4CaO_5 assembly, PSII content 70%WT, increased D1 turnover rate (*107*)

Table 4.1. List of single D1 point mutations with their properties as described in previous literature

The eWT strain was transformed with the genomic DNA isolated from all the single D1 mutants and WT as described in chapter two. As depicted in Figure 4.2 the *psbA2* gene introduced at the native locus had a kanamycin resistance cassette downstream of the *psbA2* coding region and therefore transformants obtained from the dual expression strain were selected for kanamycin resistance. The introduction of two copies of *psbA2* genes did not seem to alter the transformation efficiency and more than 30 -50 transformants were obtained for each dual strain.

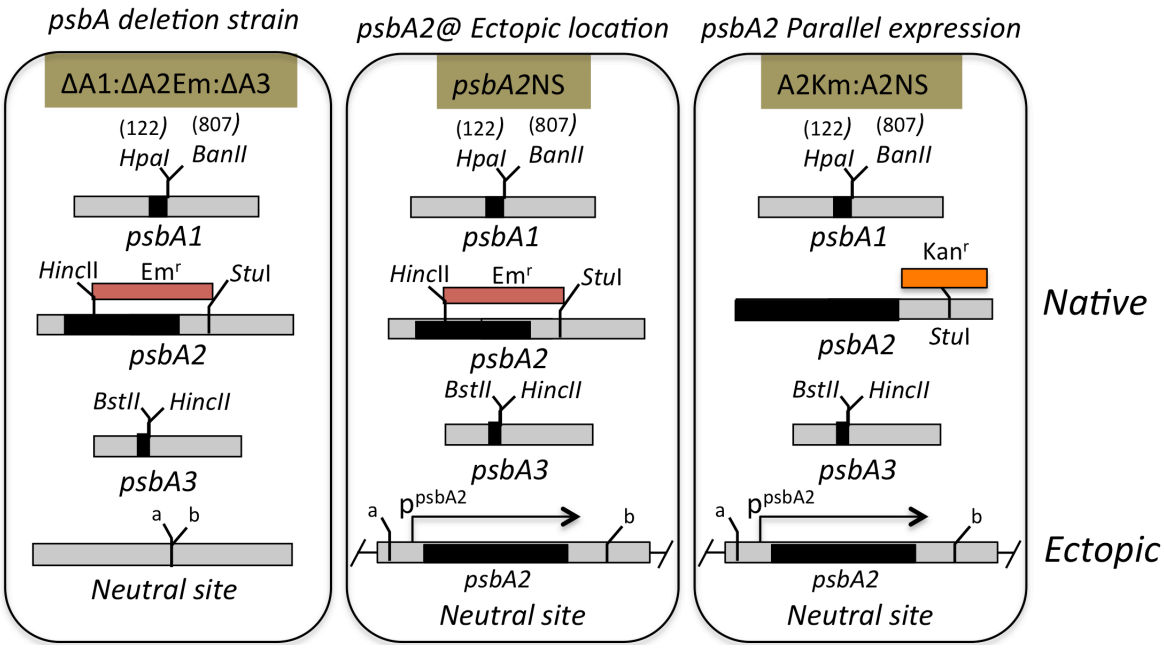

Figure 4.2. Genotype of all the strains used in the construction of dual expression strain. Left panel representing the genotype of the triple psbA deletion strain (described in chapter 2), center panel shows the eWT strain with the *psbA2* gene at the ectopic location (described in chapter three) and right panel shows the genotype of the dual expression strain with a psbA2 at the native locus with Kanamycin resistance and WT *psbA2* expressed from the ectopic (neutral) site.

4.2.2. Confirmation of dual integration of psbA2

The integration of *psbA2* genes both at the native and ectopic locus of the chromosome was confirmed using PCR amplification of the native and ectopic sites using primers listed in Table 2.4. Figure 4.3 shows the amplification of DNA fragments encompassing the full-length native and neutral sites. Band corresponding to 3,500 bp observed in last four lanes of Figure 4.3a represent the *psbA2* gene harboring the kanamycin resistance cassette. Lanes 1 and 2 represent the empty native locus from triple *psbA* deletion strain and eWT (*psbA2*NS) strain wherein the *psbA2* gene has been replaced with erythromycin resistance cassette.

The neutral site amplification in Figure 4.3b shows the full-length *psbA2* gene (2,700 bp) in the last three lanes corresponding to three dual expression strains. The empty neutral site of 1,000 bp was observed in the triple *psbA* deletion strain and the nWT strain. The amplification products from native and neutral site of each of these strains were also sequenced to confirm the introduction of point mutation at the native site and the WT sequence at the ectopic location.

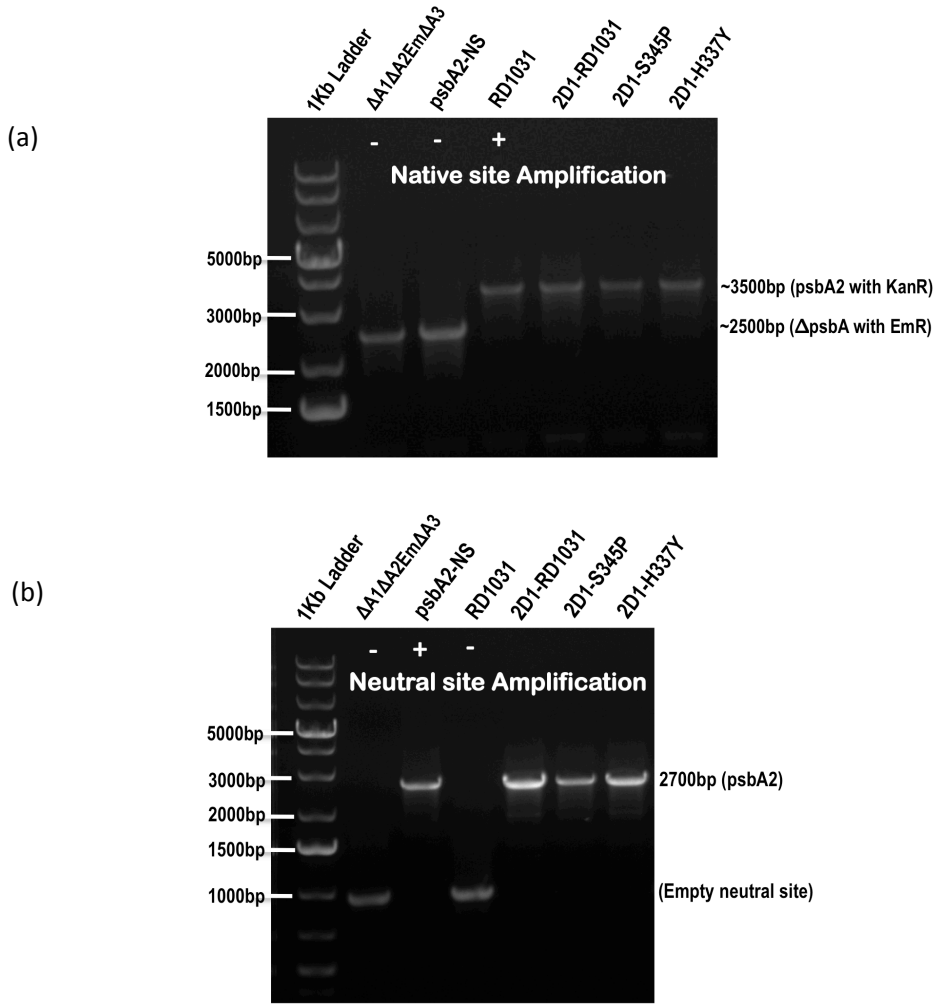

Figure 4.3. Confirmation of dual integration of *psbA2* in 2D1 strain. (a) Native site amplification of the 2D1 strain Ln 2 and 3(2500 bp) are negative controls showing absence of *psbA2* (EmR), Ln 4 (3500 bp) is positive control with *psbA2* and upstream kanamycin resistance cassette. Ln 5-7 (3500 bp) show integration of *psbA2* at native site. (b) Shows *psbA2* at the ectopic locus. Ln 2 and 4 (1000 bp) are negative controls showing empty neutral site, Ln 3 (2700 bp) positive control, Ln 5-7 (2700 bp) shows *psbA2* at the ectopic locus.

4.2.3. Estimation of relative PSII activity in single and dual D1 strains

Relative PSII activity was estimated in all the strains based on variable fluorescence measured using a dual modulation kinetic fluorometer. This assay provides an estimate of the relative concentration of PSII complexes that are assembled and

capable of light-induced charge separation. Specifically, the changes in the chlorophyll fluorescence induced by a single saturating flash in the presence of DCMU provides an estimate of the percentage of PSII centers that can undergo charge separation to form $P680Q_A^-$ state. This represents a high fluorescence state as compared to the $P680Q_A$ ground state of these photochemical reactants. Additionally, the rate of decay of the high fluorescence state reflects the assembly status of the donor site (Mn_4CaO_5). Because the assembled (Mn_4CaO_5) can be oxidized by the primary donor $P680^+$ via Yz, the high fluorescence charge separated state is relatively more stable than in its absence and the lifetime of the high fluorescence state is, accordingly, approximately one second. The absence of a fully assembled functional Mn_4CaO_5, the decay of the high fluorescence state is expected to be much faster resulting from the charge recombination between Q_A^- and oxidant localized in the P680/Yz ensemble. This charge recombination and concomitant decay of the high fluorescence state occurs in about ten milliseconds. This is due to the inability of the Mn_4CaO_5 in providing an electron to the P680/Yz thereby creating an electron hole in P680/Yz causing the Q_A^- to rapidly recombine with P680/Yz. Comparison with wild type yields the percentage of functional PSII centers for each strain. Table 4.2 lists the strains with their variable fluorescence and percentage of active PSII centers relative to wild type.

D1-Ser345Pro (*S345P*) and *nS345P: eWT*

The D1–S345P mutation was re-created by transformation of the triple *psbA* deletion strain with plasmid DNA of pRD1031 bearing the point mutation S345P with a kanamycin resistance cassette downstream of the gene. After complete segregation of the

strain, this mutant was assayed for the ability to sustain photoautotrophic growth, undergo charge separation and accumulate PSII. *S345P* was observed to have a light-sensitive phenotype and was unable to grow photoautotrophically and therefore cultures were maintained in the presence of 5 mM glucose. This observation was consistent with previous characterizations of this mutation reported in the literature (*63, 73*). The mutation Ser345Pro disrupts the cleavage site for the C-terminal protease A (CtpA) and it is unable to cleave the C-terminal extension required for the assembly of Mn_4CaO_5 (*27*). Therefore, the strain is expected to synthesize only the pre-D1 form bearing the C-terminal extension of 16 amino acids (*63*).

The relative PSII activity in *S345P* measured as maximal variable fluorescence was observed to be only 5% of WT (Table 4.2). This value is much lower than what was observed by Chu et al., 1995 where it was shown to accumulate 25% of wild type PSII centers (*73, 108*), but similar to Nixon et al (*63*). This difference could be attributed either to the growth conditions or the new background strain (marker-less triple *psbA* deletion strain). For all our measurements *S345P* was maintained in the presence of 5mM glucose at a light intensity of 10 -15 μmol m^{-2} s^{-1}. Alternatively, the difference may reflect the type of fluorometer used and it is possible that the higher estimates observed by Chu et al were due to the weak but significant actinic affect of the PAM-type (pulse-amplitude modulated) fluorometer that may promote transient binding and photoxidation of Mn ions, thereby contributing to a longer lifetime of the charge-separated state and consequently, a correspondingly higher estimate of charge separating centers (*73*).

Strain	Fv	Relative PSII Activity (% WT)
n-WT (native WT)	0.81 ± 0.07	100
e-WT (ectopic WT)	0.81 ± 0.07	100
D1 – nS345P	0.04 ± 0.01	5
D1 – nH337Y	0.04 ± 0.01	5
D1 – nD170A	0.21	26
n-S345P: e-WT	0.78 ± 0.05	97
n-H337Y: e-WT	0.71 ± 0.11	89
n-D170A: e-WT	0.67 ± 0.08	83
n-WT: e-WT	0.80 ± 0.04	100

Table 4.2. Characterization of PSII activity in all the single and dual D1 expression strains. Columns represent *Fv* (variable fluorescence) and relative PSII activity. *Fv* was evaluated based on the maximal variable chlorophyll *a* fluorescence (calculated as $(F_{max} - F_0)/F_0$) for each strain measured in the presence of 10 μM DCMU where F_0 is the basal fluorescence yield for a sample before exposure to actinic light and F_m is the maximal fluorescence yield that each sample reaches after the actinic light is turned on. The relative PSII activity for each strain was calculated as percent (%) WT. Values represented are an average of five independent experiments.

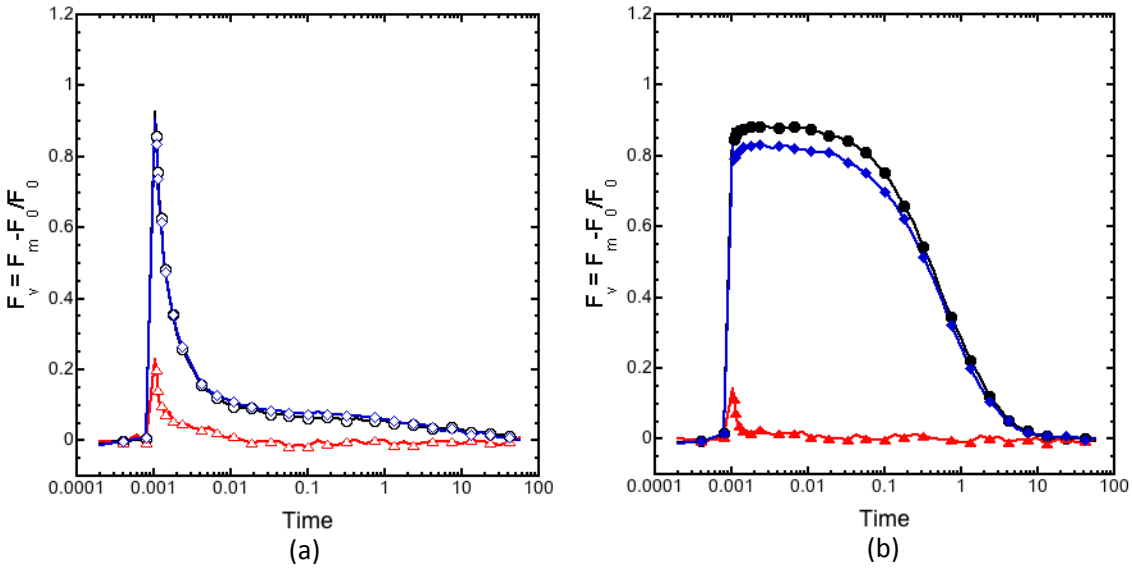

Figure 4.4. Q_A reoxidation kinetics of WT (black), S345P (red) and nS345P: eWT (blue). Left (a) and right panel (b) indicate the decay kinetics of variable chlorophyll *a* fluorescence in the absence of DCMU (open symbols) and presence of 10 μM DCMU (closed symbols) respectively. Values plotted are calculated as $(Ft-F_0)/F_0$ wherein F_0 corresponds to the average fluorescence yield of first four weak measuring flashes given to each sample before exposure to actinic flash.

The decay kinetics in *S345P* strain was very different from the wild type and the dual D1 strain *nS345P: eWT* (Figure 4.4, red). The amplitude of variable fluorescence for the *S345P* was very low suggesting that there is only a very small fraction of PSII centers capable of charge separation. Due to lower amplitudes, the decay components could not be analyzed for this study. But from previous characterization elsewhere it is known that that the mutant undergoes incorrect assembly of Mn_4CaO_5 (*27, 73*). This has been shown by the presence of 25% PSII centers compared to control but lack of any oxygen evolution (*27, 73*). The charge separated state $P_{680}^{+}Q_A^{-}$ corresponding to high fluorescence is much lower in the mutant even in the presence of reduced Q_A^{-}; this is due to a rapid quenching from P_{680}^{+}. An increased chlorophyll fluorescence quenching is indicative of incomplete reduction by the Mn_4CaO_5 due to a disruption of the donor side of PSII. The mutant strain has been shown to contain photooxidizable Mn that causes the reduction of Y_z^{+} (*73*).

In the dual D1 strain *nS345P: eWT*, when the wild type was added to the ectopic location of the S345P strain there was a dramatic increase in the fraction of PSII centers that could successfully undergo charge separation (Figure 4.4, blue). The amplitudes of variable fluorescence are comparable to the single wild type (eWT) strain and accumulate 97% PSII centers when compared to wild type (Table 4.2). The fluorescence decay kinetics both in the presence and absence of DCMU suggest the presence of a fully functional Mn_4CaO_5 and resembles wild type (eWT) strain indicating that the dual D1 strain nS345P: eWT accumulates primarily the wild type PSII centers and the fraction of

PSII complexes with either negligible amounts (with no apparent kinetic differences) or absence of mutant S345P D1 form.

D1 – Asp170Ala (*D170A*) and *nD170A- eWT*

D1- D170A is a mutation at the donor side of PSII that affects the early stages in the assembly of Mn_4CaO_5 (*109*). The mutant has been shown to accumulate 70% of PSII centers in comparison with wild type. In our characterization of this mutant, the PSII activity was observed to be 25% of that of wild type (Table 4.2). This mutant was non-photoautotrophic and they were maintained in the presence of 5 mM glucose in 10-15 μmol m^{-2} s^{-1} of flux intensity.

The kinetics of Q_A reoxidation was measured in *D170A* both in the presence and absence of DCMU (Figure 4.5 (a) and (b)). In the absence of DCMU, the decay in fluorescence reflects the transfer of electrons from Q_A^- to Q_B site in the plastoquinone and the much slower recombination of the Q_A^- with the Mn_4CaO_5. In the presence of DCMU, the decay of high fluorescence yield after the first saturating flash reflects primarily the charge recombination between the Q_A^- and the Mn_4CaO_5 as the flow of electrons to Q_B site is blocked. In D170A, the faster decay in fluorescence as observed in Figure 4.5 (b) in the presence of DCMU is due to charge recombination between Q_A^- and Y_z^+. This is in accordance with is in accordance with previous observations. This decay is due to lack of photooxidizable Mn ions for the reduction of Y_z^+. Earlier observations also show an increased quenching of fluorescence due to a slow reduction of Y_z^+ from an alternate

electron donor (P_{680}^{+}). The decay observed in Figure 4.5 (a) could be attributed to this quenching of fluorescence.

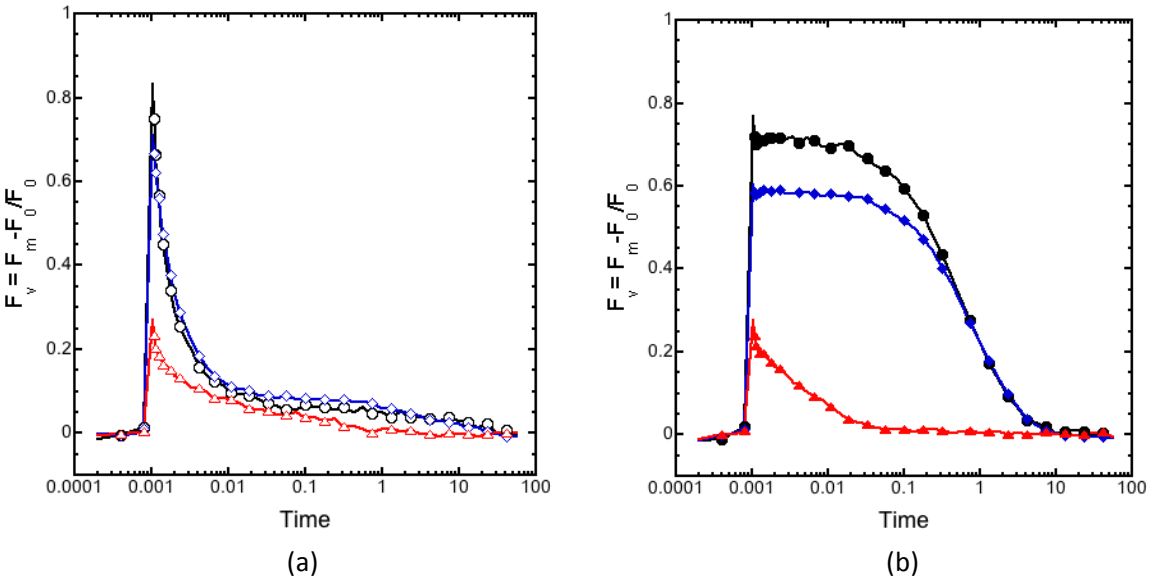

Figure 4.5. Q_A reoxidation kinetics of WT (black), *D170A* (red) and *nD170A: eWT* (blue). Left (a) and right panel (b) indicate the decay kinetics of variable chlorophyll *a* fluorescence in the absence of DCMU (open symbols) and presence of 10 μM DCMU (closed symbols) respectively. Values plotted are calculated as $(Ft-F_0)/F_0$ wherein F_0 corresponds to the average fluorescence yield of first four weak measuring flashes given to each sample before exposure to actinic flash.

When D1- WT was expressed in parallel from the ectopic site with D1- D170A at the native site (*nD170A: eWT*) the amplitudes of total variable fluorescence obtained were much higher (Figure 4.5 (a) and (b), blue) showing a 70% increase in the proportion of PSII centers capable of undergoing charge separation when compared to the mutant *D170A* alone (Table 4.2). The decay of fluorescence in the presence and absence of DCMU essentially resemble the *e-WT* strain (in black) suggesting an accumulation of wild type D1 PSII centers in the dual strain *nD170A: eWT*.

D1–His337Tyr (*H337Y*) and *nH337Y: eWT*

D1-H337Y was chosen for its light sensitive non-photoautotrophic phenotype(*108*). This mutant has been previously shown to accumulate 42% PSII relative to WT. This mutant was initially chosen for the previously published evidence of higher PSII content. However, during our analyses of this mutant the relative PSII activity was observed to be only 5% of WT levels. This observation could be due to the differences in the light and growth conditions of the strain. The mutant has been shown to undergo partial quenching of fluorescence by donor side and much slower rate of electron transfer from Q_A^- to Q_B. In the presence of DCMU, H337Y undergoes charge recombination between Q_A^- and Y_z^+. This mutant has been suggested to generate reactive oxygen species due to its photoinhibitory phenotype. The amplitudes of variable fluorescence were extremely low for the mutant (Figure A.1) and could not be analyzed into different decay components. Although, when D1-WT was expressed in parallel with H337Y, there was an increase in the amplitude of the total variable fluorescence (Figure A.1 (b)) representing the proportion of PSII centers with WT D1 incorporated.

4.2.4. Fluorescence Decay Kinetics

The high fluorescence state reached after a single saturating flash followed by series of weak measuring flashes denotes the fraction of PSII centers at $P680Q_A^-$. The kinetics of fluorescence relaxation in the presence of DCMU allows us to monitor the charge recombination with the donor side (Mn_4CaO_5). Since, the mutants used in this study are essentially affecting the donor side of PSII, the decay of this high fluorescence

yield in the presence of DCMU was further analyzed by normalizing the amplitudes of variable fluorescence for each of these strains. In the presence of an intact Mn_4CaO_5 when the forward electron flow to Q_B is (by DCMU), the only option for the electron from Q_A^- is to find its way back to Mn_4CaO_5 and this is a much slower process (Figure 4.6, black). In the absence of an intact functional Mn_4CaO_5 there is a much more rapid recombination between the Q_A^- and Y_z^+ as the Mn_4CaO_5 is not available for the reduction of Y_z^+ (Figure 4.6, blue).

In the dual D1 strains expressing both mutant D1 (from native) and WT D1 (from ectopic) we expected heterogeneity in PSII centers. To evaluate the presence of heterogeneous PSII population (if any) in the dual D1 strain, the decay kinetics were normalized and compared with the mutant and wild type separately. In the dual strain nD170A: eWT there a proportion of PSII centers were observed to undergo a slightly faster decay when compared to the *eWT* strain (Figure 4.6, red). This observation was consistent for more than one occasion and seemed to vary with growth conditions. This faster decay component could be attributed to the PSII centers with D1-D170A incorporated. The variations in the decay observed in different growth conditions suggest that by changing the light conditions we could alter (increase or decrease) the accumulation D1- D170A in the cell.

Similarly, the decay kinetics were analyzed for the other two dual D1 strains (nS345P: eWT and nH337Y: eWT) depicted in Figures A.2 (a) and (b). No such differences in the rate of fluorescence decay were observed. This could be due to a lower accumulation of S345P and H337Y observed in our growth conditions (Table 4.2). An

attempt to increase in PSII content by changing the light and growth conditions might allow us to accumulate fraction of PSII centers with mutant D1 (S345P and H337Y) incorporated.

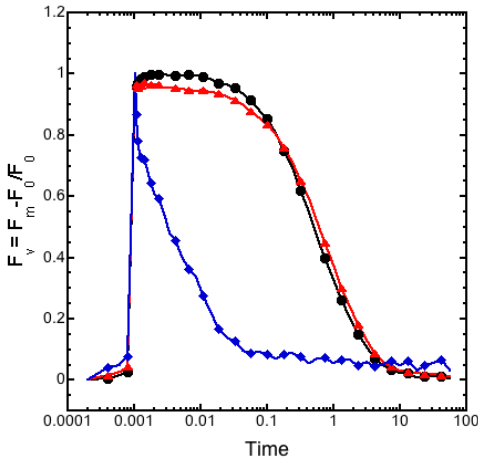

Figure 4.6. Relaxation Kinetics of chlorophyll *a* fluorescence in WT (black), D170A (blue) and nD170A: eWT (red). Decay of fluorescence during QA reoxidation was measured in the presence of DCMU for each sample. The values of variable fluorescence were normalized to 1 and plotted as F_t-F_0/ F_m-F_0 wherein F_0 and F_m are basal and maximal fluorescence before and after exposure of the sample to actinic light respectively. Data points represent an average of three different samples.

4.2.5. Expression of pD1 and D1 in dual expression strains

As noted, the S345P mutant cannot process of C- terminal extension of the nascent D1 apo-protein due and consequently the 16 amino acid C- terminal extension remains intact in the mutant as a pre-D1 (pD1) form. Due to the inability to form mature D1 protein, S345P has been shown to undergo incomplete PSII assembly process and these partially assembled complexes with pD1 have been shown to have a higher D1 turnover rate (~15 minutes) than wild type (*63*). The pD1 forms being longer than the

mature D1 form runs slower and can be resolved using SDS-Urea polyacrylamide gel electrophoresis.

The parallel expression of S345P and WT D1 in *nS345P: eWT* strain was evaluated for the co-expression of pD1 and D1 form. The thylakoid membranes isolated from *nS345P: eWT* was compared with *e-WT* and *S345P* strains on a 12% - 20% SDS 6M Urea denaturing gel electrophoresis. Samples were loaded on an equal chlorophyll basis of 0.5μg and the D1 and pD1 forms were probed with antisera PsbA. Figure 4.7 shows the D1 and pD1 accumulation in the thylakoid membranes of these strains. The observation of less accumulation of pD1 form in the mutant *S345P* is consistent with lower PSII content as observed in variable fluorescence measurements (Table 4.2). This is also in accordance with previous biochemical analysis of *S345P* (*63*). The accumulation of D1 in the dual strain *nS345P: eWT* was very similar to that of the *e-WT* strain. Additionally, there was no detection of the pD1 protein in this strain. This would suggest that PSII complexes in the dual strain are primarily consisting of D1- WT and there are only fewer PSII complexes with D1- S345P (pD1) incorporated, which is beyond the limit of detection by immunoblotting. Therefore, it could be concluded that D1-S345P molecules are not being synthesized at all or they are being synthesized but due to a higher rate of D1 turnover they are degraded rapidly due to the presence of the wild-type version.

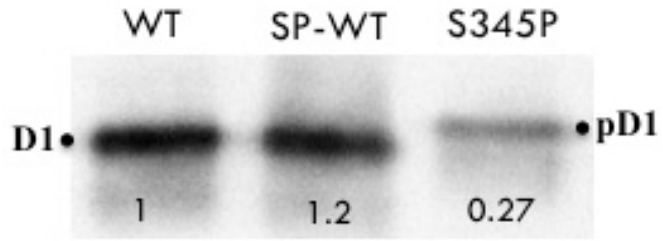

Figure 4.7. Accumulation of D1 and pD1 using immunoblot analysis against PsbA (D1) Thylakoid membranes isolated from WT, SP-WT (*nS345P: eWT*) and *S345P* were resolved on a 12% - 20% SDS 6M Urea denaturing PAGE and probed using antisera against PsbA (D1). Lanes were loaded on an equal chlorophyll basis with 0.5µg chlorophyll. The blot obtained was analyzed using Image J analysis software and the relative density for each band listed on the blot was calculated using WT as a reference.

4.2.6. Effect of FtsH2 deletion on accumulation of pD1

FtsH a member of ATP dependent AAA family of proteases has four homologues in *Synechocystis*. FtsH2 (*slr* 0228) has been shown to be involved in early stages of PSII repair by proteolytically removing D1 subunits (*65*). It has been observed that FtsH recognizes the N-terminus of D1 protein to initiate the D1 degradation process (*67*). When FtsH2 was knocked out from these dual D1 strains, the PSII activity in all these strains were 20% less than their non-knockout variants (Table A.1). This was expected because with the inability to undergo PSII repair these strains were accumulating damage.

To examine the effect of FtsH deletion on the expression of D1 and pD1, thylakoid membrane samples from *eWT*, *S345P*, *nS345P: eWT* (SP-WT) and ΔFtsH- SP-WT were resolved on a 12% - 20% SDS 6M Urea denaturing gel (Figure 4.8). The accumulation of D1 and pD1 were observed using antisera against D1. The relative intensity of the D1 protein band indicates similar levels of accumulation across different samples whereas pD1 was accumulated to only ~25% of mature D1 levels. This was

consistent with previous observation in Figure 4.7. An accumulation of pD1 and D1 was observed in ΔFtsH- SP-WT indicating co-expression of both mutant (S345P) and wild type (WT) D1 proteins in the dual D1 strain (Figure 4.8). Additionally, absence of the pD1 band in the nS345P:eWT strain suggests that S345P mutant form are being synthesized but they have a higher rate of turnover therefore do not accumulate to higher levels for visualization on an immunoblot.

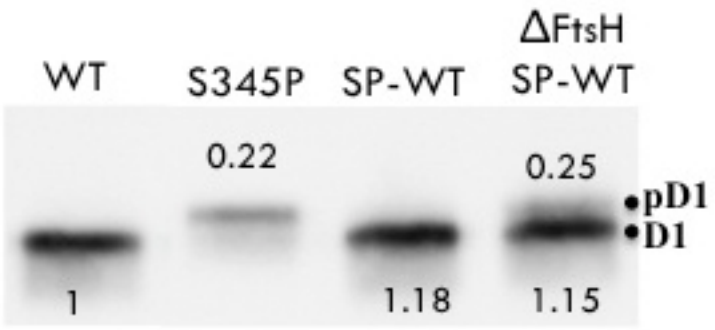

Figure 4.8. Effect of FtsH protease deletion on the accumulation of D1 and pD1. Thylakoid membranes from WT (*eWT*), *S345P*, SP-WT (*nS345P: eWT*) and ΔFtsH- SP-WT were resolved on a 12% - 20% SDS denaturing PAGE and probed using antisera against PsbA (D1). Lanes were loaded on an equal chlorophyll basis with 0.5µg chlorophyll. Bands were analyzed using Image J analysis software and the relative density for each as listed on the blot was calculated using WT as a reference.

4.2.7. Gene dosage effect of PSII activity – nWT: eWT

Expression of two WT *psbA2* genes was accomplished to study the effects of gene dosage on the PSII activity. The total variable fluorescence for the double WT (nWT: eWT) was very similar to single WT strains (Table 4.1) showing 100% PSII centers relative to WT. This suggests that the proportion of charge separating centers in the double WT strain similar to single WT strain. The fluorescence decay kinetics during QA reoxidation (Figure 4.9 (a) and (b)) was compared with the wild type at the native site

(red) and at the ectopic site (black). The decay in the presence and absence of DCMU were identical for the most part. Overall, kinetics of PSII activity from variable fluorescence shows that the proportion of PSII centers in the three strains double WT (nWT:eWT), eWT and nWT are all similar.

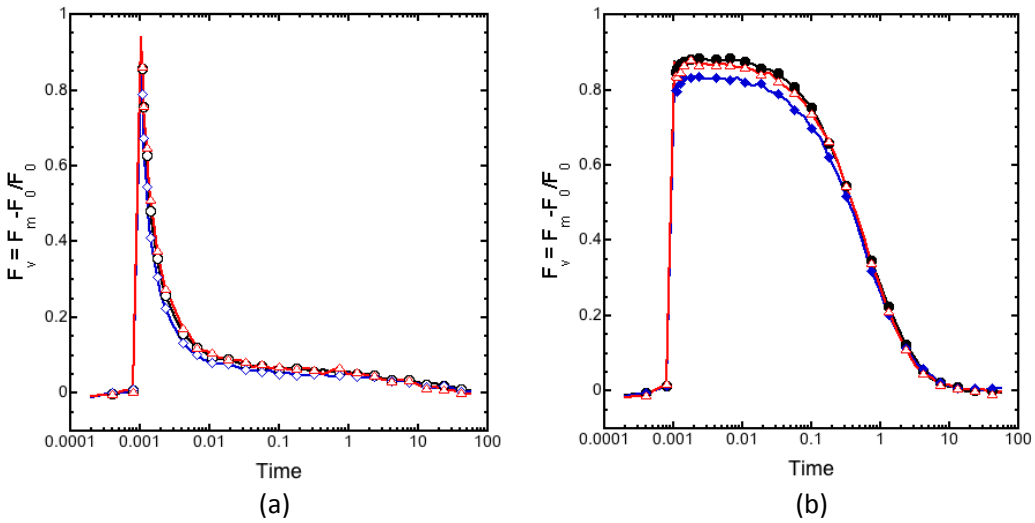

Figure 4.9. QA reoxidation kinetics in *eWT* (black), *nWT* (red) and *nWT: eWT* (blue). Panel (a) and (b) indicate the decay kinetics of variable chlorophyll *a* fluorescence in the absence (open symbols) and presence of 10 μM DCMU (closed symbols) respectively. Values plotted are calculated as $(Ft-F_0)/F_0$ wherein F_0 corresponds to the average fluorescence yield of first four weak measuring flashes given to each sample before exposure to actinic flash.

4.2.8. Expression of D1 protein in Double WT (nWT:eWT)

The accumulation of D1 protein was observed in the double WT strain and compared to the single WT strain to evaluate if the presence of two copies of wild type D1 causes an accumulation of D1. Thylakoid membrane samples from nWT: eWT and eWT were resolved and probed using antisera against PsbA (Figure 4.10). The relative intensities estimated using Image J analyzer shows similar levels of D1 accumulation in both the strains. It can be concluded that assuming there are twice the number of wild

type *psbA2* transcripts yet only a certain proportion of the transcripts are translated into D1 and this corresponds with the concentration of PSII in the cell.

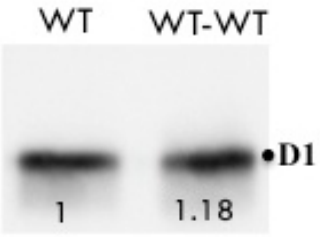

Figure 4.10 Accumulation of D1 in nWT: eWT. Thylakoid membranes from WT (*eWT*) and *nWT: eWT* were resolved on a 12% - 20% SDS denaturing PAGE and probed using antisera against PsbA (D1). Samples were loaded on an equal chlorophyll basis with 0.5µg chlorophyll. The intensity of bands was calculated in terms of relative density using Image J analysis software using WT as a reference and the values in the blot represent relative density.

4.3. Discussion

The development of parallel genetic system described in this chapter utilizes the ectopic WT strain that has been constructed as described in Chapter three. This enabled the co-expression of alternative forms of the D1 protein from identical promoters allowing tests on the possible alternative cellular fates of the co-expressed alleles. Thus, the overall purpose of this dual D1 expression system was to address the underlying question of whether PSII complexes that are damaged during photoinhibition are targeted for PSII repair as opposed to the alternative hypothesis that photodamaging conditions elicit a general up-regulation in the rate of the D1 replacement process such that damaged and undamaged subunits both have increased turnover probabilities.

The principle for this parallel expression approach of expressing a damage prone mutant with a faster rate of D1 turnover and a wild type with normal D1 turnover as

described in Figure 4.1 was to accumulate heterogeneous populations of PSII consisting of either a mutant or wild type D1. By introducing heterogeneity in a single strain, we can monitor if the cell specifically targets mutant PSII complexes for repair or if both the mutant and WT complexes undergo an increase in turnover and get replaced in a random manner. If there were a targeted repair mechanism, the mutant PSII complexes would be targeted for repair while the PSII complexes with WT would accumulate. Therefore, by evaluation of the overall PSII activity in these dual strains we can address these two alternate hypotheses. A high PSII activity would indicate a higher proportion of wild type PSII RCs and this could be due to the faster rate of turnover in mutant PSII RCs that do not form a part of functional PSII. A lower PSII activity would suggest towards an existence of equal proportion of wild type and mutant PSII RCs.

For the successful construction of dual D1 strains, damage prone D1 mutants were cloned into the native locus and the WT was cloned into the ectopic locus of the chromosome. By using this approach we ensured the expression of mutant *psbA2* normal levels, as it was being cloned into the original site in the chromosome. Cloning the wild type *psbA2* instead of a mutant into the ectopic site prevented any untoward alteration in the phenotype of the mutant that would otherwise be attributed to differences in the gene location. Both the genes (mutant and wild type) were under the control native *psbA2* promoter and shared the same 5' and 3' UTR (untranslated region). This increased the likelihood that both the genes are being regulated similarly and any difference in the expression of one gene would be carried over to the other gene as well. Thus, both the

genes were constructed with an intention to maintain similar gene regulation including transcription and translation.

Damage prone D1 mutants for dual D1 constructions were chosen (Table 4.1) primarily based on their sensitivity to photoinhibition, which would imply an increased rate of D1 turnover and their ability to accumulate non-functional PSII to a moderate level. Three such D1 mutants S345P, D170A and H337Y essentially affecting the donor side of PSII were used for the dual D1 strain construction with an introduction of WT in the ectopic location of each of these mutants. D1- Ser345Pro, C-terminal extension mutant that does not undergo D1 C- terminal processing and has a 16 amino acid extension causing the Mn_4CaO_5 to not assemble correctly thereby has an increased D1 turnover rate (*27*). This mutant has been shown previously to accumulate 25% PSII centers compared to wild type (*27, 73*). Similarly, D1-Asp170Ala is also a mutant affecting the donor side of PSII. This mutant is known to not assemble Mn_4CaO_5 cluster, accumulates 75% of PSII centers relative to WT and has been shown to have a D1 turnover rate of 15 minutes (*73, 94, 109*). Additionally, D1- His337Tyr is also a mutation causing the incorrect assembly of Mn_4CaO_5. This mutant has been suspected to create reactive oxygen species making this mutant extremely light sensitive. It has been shown to accumulate 45% PSII relative to WT (*108*).

Towards targeted repair mechanism

All the three dual D1 *strains nS345P: eWT*, *nD170A: eWT* and *nH337Y: eWT* restored the mutant phenotype of low PSII activity (Figure 4.3, 4.4 and A.1). When the

mutants were expressed from the native site alone their PSII activity was very low (Table 4.2). The values of relative PSII activity observed were much lower than those previously reported. This could be due to the differences in the strain background (marker-less triple psbA deletion, discussed in chapter two) and light and growth conditions. The relative PSII activity of the dual D1 strains corresponded well with the strain expressing single WT *psbA* gene. Based on the total variable chlorophyll *a* fluorescence as a measure of relative PSII activity, there appears to be an increased proportion of PSII RCs with WT D1 protein assembled. Also, the kinetics of the decay of high fluorescence state in the presence and absence of DCMU suggest a large population of PSII centers undergoing charge recombination between the Q_A^- and Mn_4CaO_5 (in the presence of DCMU, Figure 4.4 (b) and 4.5 (b)) and a large proportion of RCs undergo Q_A^- to Q_B transfer (in the absence of DCMU, Figure 4.4 (a) and 4.5 (a)). The kinetics of Q_A reoxidation was similar to a large extent in all the dual D1 strains suggesting a predominant accumulation of PSII center with WT D1 protein implying that there either no accumulation or very less accumulation of mutant PSII centers. Consequently, the question to be asked would be why are the mutant PSII RCs not being accumulated?

As reasoned earlier, a high PSII activity in dual D1 strains could be indicative of a targeted repair mechanism of the damage prone PSII complexes. This can explain the absence or lower amounts of mutant PSII complexes (non functional PSII). Another less plausible alternative could be that introduction of two copies of a gene has some regulatory affect on the mutant *psbA2* causing the gene to be silenced. This seems highly unlikely as the mutant *psbA2* are being expressed from the native locus and we would be

expecting an affect (if any) on the WT expressing from the non-native (ectopic) location. This suggests preliminary evidence towards a targeted repair mechanism.

However, choosing a mutant that would accumulate an increased proportion of non-functional RCs would benefit in addressing this hypothesis. D170A by far was able to accumulate maximum PSII under the conditions this study was performed and we were able to accumulate 25% of WT PSII centers. The dual strain nD170A: eWT also accumulated 85% PSII centers relative to WT. When the decay kinetics of fluorescence was analyzed by normalizing the amplitudes of all the strains it was observed that a smaller fraction of PSII centers undergo a slightly faster decay. This faster decay component was consistently observed and can be attributed to the faster decay in the mutant D1- D170A (Figure 4.6). This observation could be indicative of a co-expression of both the mutant and wild type copies of D1 protein. We believe that if these strains are grown at the different light conditions we might be able to increase PSII accumulation.

Analysis of D1 and pD1 accumulation in the thylakoid membranes isolated from *S345P* and *nS345P: eWT* did not show an accumulation of the pD1 form in the dual strain *nS345P: eWT* (Figure 4.7). The amount of pD1 accumulated in S345P was approximately 30% of that of the D1 protein observed in WT. A lower accumulation of pD1 has been reported previously (*63*). However, there was no pD1 observed in the dual again. Again, suggesting that PSII complexes are predominantly incorporated with WT PSII complexes.

From the fluorescence decay kinetics in nD170A: eWT we observe a small fraction of PSII centers that might have D1-D170A assembled into PSII RCs suggesting that both the native and ectopic sites are viable and are expressing the respective *psbA2* genes. Taken together the observations from decay kinetics and the absence of a pD1 form in dual strain *S345P: eWT*, it could be inferred that both the mutant and wild type psbA2 genes are being expressed and mutant D1- S345P gets targeted for repair and therefore does not accumulate in the dual strain (nS345P: eWT) to be visualized by immunoblotting.

When thylakoid membranes from FtsH knockout version of nS345P: eWT were compared with S345P: eWT, an accumulation of the pD1 form was observed in immunoblots corresponding to the fraction of PSII RCs with mutant S345P incorporated (Figure 4.8). A deletion of FtsH protease causes the repair process to terminate leading to an accumulation of the damaged D1 and pD1 that is unable to undergo PSII repair. Therefore, by using the FtsH knockout strain it is evident that both are genes (mutant and wild type) are being co-expressed and the increased PSII levels observed in dual D1 strains (Table 4.2) and the absence of pD1 (D1-S345P) form in the dual strain S345P: eWT are due to specific targeting of PSII complexes with D1-S345P incorporated. This mutant form cannot complete the assembly process beyond pD1 and therefore gets turned over rapidly whereas the PSII complexes with WT incorporated are much more stable and complete the PSII assembly process.

Homeostatic control of PSII

Cloning two wild type *psbA2* genes in a single strain (nWT: eWT) to study gene dosage effects have shown similar PSII activity to that of the single WT strain, evaluated based on variable chlorophyll *a* fluorescence. The percentage of RCs capable of charge separation was same as that of a single WT strain (eWT and nWT separately) (Table 4.2). The QA reoxidation kinetics also suggests similar decay of the high fluorescence state both in the presence and absence of DCMU as the single WT strain (Figure 4.9). The presence of two copies of wild type D1 proteins does not seem to increase the levels of PSII in the cell. From previous discussion on the co-expression of mutant and wild type D1 it is known that both the native and ectopic locations are viable. Hence, it is conceivable that both the wild copies are being expressed, however only a certain maximum number of PSII are being assembled in a cell which is corresponding to the proportion in a single WT strain. Accumulation of D1 was observed in the double wild type (nWT: eWT) and compared with a single WT (eWT) strain on an immunoblot (Figure 4.10). The level of D1 protein accumulated is similar to that of a single WT strain. The accumulation of D1 reflects the total D1 protein in thylakoid membranes and correlates with the amount of PSII in the thylakoids. The presence of a finite number of PSII complexes and corresponding levels of D1 protein, even though there is presumably twice the number of wild type transcripts (this needs to be checked in future studies), indicate a regulatory mechanism maintaining this PSII homeostasis. What controls this PSII homeostasis?

A transcriptional regulation of D1 controlling the PSII homeostasis is not very likely as both the genes at the native and ectopic site are under the control of identical native *psbA2* promoter and 5' and 3' UTRs. Therefore, controlling the abundance of transcripts would also influence both the native and ectopic sites and this in turn would have an affect in the strains expressing a mutant and wild type in parallel limiting the number of transcripts of both mutant and WT observed as a lower proportion of active PSII.

It is known that translation of D1 is regulated in a manner that D1 degradation and synthesis are coupled (*54*). This could explain the similar levels of D1 protein observed to be accumulated in western blots in the double WT. But, if this translational regulation were controlling PSII homeostasis, then the transcripts of mutant and WT in the dual mutant strains would have to be screened and removed early on before translation elongation. Although, this possibility cannot be dismissed with absolute certainty, the likeliness of the regulation of PSII homeostasis by some other protein (factor) appears more plausible.

A factor X is probably a part of the PSII assembly process and the association of this factor (X) early on stabilizes the complex for complete PSII assembly. The stoichiometry of this factor X determines the finite number of PSII in a cell. Candidates for this factor could be any PSII protein from the complex, although the core subunits CP47, CP43, D1 and D2 might not be the most favorable candidates for regulating PSII homeostasis. Deletion of the FtsH protease has been shown to influence the accumulation of CP47, D2 and CP43 in some mutants (*63*). It has been suggested that during the

insertion new subunits in PSII assembly process there is accumulation of unassembled CP47 and D2, while D1 and CP43 are almost immediately inserted into PSII. CP47 and D2 are early members of the PSII assembly process and D1 and CP43 only get associated afterwards. Therefore, the factor X could be a protein subunit that plays a role prior to the association of D2 and CP47, for example Cyt b_{559}. And this could explain the increased pool of CP47 and D2 waiting for the factor X stabilized PSII complex for assembly.

CHAPTER V

CONCLUSIONS AND FUTURE DIRECTIONS

5.1. Summary

This work describes the development of a novel genetic system involving the parallel expression of two alternate forms of *psbA2* genes encoding for D1 protein. More importantly, it describes the application of this system to evaluate the hypothesis that the PSII repair mechanism results in the replacement of photodamaged D1 subunits by specifically targeting the damaged subunits for replacement. With these results, all evidence points now towards the existence of a targeted repair mechanism, as opposed to the generalized mechanism as outlined in the beginning of Chapter 4. Although a targeted D1 replacement mechanism has been widely assumed, this is the first direct evidence for its existence.

PSII repair process as described in Chapter 1, copes with damage during photoinhibition by increasing the turnover rate of D1 protein causing the replacement of D1 protein subunits i.e. the removal of D1 subunits in the PSII complex with newly synthesized D1 protein. This process requires a partial dis-assembly and assembly of the PSII complex because the D1 protein is buried into the PSII dimer (illustrated in Figure

1.5). The increased turnover of D1 was observed by isotopic pulse-chase labeling of cells subjected to high light. This increase in D1 turnover rate was viewed by the disappearance of the D1 protein band after during chase on an autoradiogram at a rate higher than other PSII proteins. The increased turnover rate suggests that the rate of D1 removal and new D1 synthesis is elevated and consequently it is known that degradation and synthesis is coupled. A metalloprotease FtsH belonging to the family of AAA-ATP dependent proteases are known to involve in the D1 degradation. The mechanism/s by which FtsH recognizes D1 and initiates the process of degradation in currently not clear. However, it was shown that presence of the N-terminus of D1 protein was crucial for the FtsH mediated degradation to occur. Due to this coupled degradation and synthesis it is widely speculated that during PSII repair damaged D1 subunits are replaced with newly synthesized D1.

With isotopic pulse-chase labeling, we cannot distinguish between a damaged and an un-damaged D1 subunit, therefore, is it critical to determine if the FtsH mediated degradation process can distinguish between damaged versus undamaged D1. There is preliminary evidence that suggests the other alternative of a general increase in the turnover of all D1 proteins replacing the D1 subunits in random to replace the entire population of D1 in the cell. PSII complexes have been shown to undergo increase in mobility throughout the membrane when subjected to high light. Also, it has been suggested that during repair FtsH localizes to “zones of repair” that are regions where the cytoplasmic membrane and thylakoid membranes connect. It would be speculated that the

increased mobility of PSII is indicative of their movement towards these "zones of repair" to initiate repair.

The genetic system developed in this work, expressing alternate forms of D1 proteins in one cell allowed us to address this question of targeted versus generalized PSII repair process. This system utilized the expression of a WT and a high D1 turnover mutant in parallel to emulate the high light conditions in a cell. It is known that high light triggers photoinhibition causing damage to PSII complexes. And being very dynamic in nature undergoes frequent damage, dis-assembly and assembly. Therefore, under high light we expect a mixed population of PSII complexes including damaged and undamaged PSII. The strains expressing dual D1 proteins were constructed with the idea of mixed PSII populations consisting of damaged (in this case high D1 turnover mutant) and undamaged (wild type D1) complexes.

The genetic system was developed in two steps, first step involving the expression of the normally high levels of wild type *psbA2* gene, but from an ectopic location on the chromosome. This part of the system is described in Chapter 2. A novel approach of a combination of synthetic biology and fusion PCR was utilized to construct a full-length *psbA2* gene. The gene fragment used for cloning at the ectopic site was designed such that it consisted of native *psbA2* promoter, terminator; native 5' UTR, 3' UTR; wild type *psbA2* coding region and the upstream, downstream ectopic site flanking sequences. This entire gene fragment (approximately 2.7 kb) was split cloned into two pUC vectors (ordered for synthesis from Blue Heron Bio). A full-length *psbA2* gene is known to be toxic to E.*coli.* This is because the gene can be expressed in E. *coli* and being very

hydrophobic in nature it can span the E.*coli* membrane and causing its disruption. Split gene cloning as used in this work, bypasses the full-toxicity of the gene and the PCR amplified products from these plasmids are joined to generate the full-length *psbA2* gene by fusion PCR. The PCR product was directly used for transformation into the ectopic location of a triple *psbA* deletion strain (*ΔA1ΔA2:EmΔA3*). The WT ectopic strain thereby constructed (eWT) restored PSII activity as measured by variable chlorophyll fluorescence, as well as maintained the photoinhibition and recovery rates similar to the native expression of *psbA2* gene (RD1031).

The eWT strain was used as a background for cloning the alternate *psbA2* gene in parallel at the native locus of the chromosome. Chapter 4 describes the complete developed of the parallel genetic system wherein three high D1 turnover mutants (listed in Table 4.1) were used for the introduction into the native site of the eWT strain. These mutants D1-S345P, D1-H337Y and D1-D170A are well-characterized mutants that undergo faster rate of D1 turnover due to either structural perturbations, increased susceptibility to photoinhibition or defect in Mn_4CaO_5 assembly. These single D1 mutants have a low PSII activity whereas when these mutant were expressed in parallel with the wild type D1 they restored this mutant phenotype and maintained higher levels of PSII activity. High PSII activity suggests an increased population of PSII complexes with wild type D1 incorporated indicating that either the high turnover D1 mutants are not expressed or they are targeted for repair and therefore do not accumulate.

D1-S345P is a mutant that unable to process the C-terminal D1 extension and causes the D1 to exist only as a premature form (pD1). The mature D1 and pre-D1 (pD1) protein has a difference of 16 amino acids that can be resolved by electrophoresis. unoblot analyses of the nS345P: eWT strain does not show an accumulation of pD1 form. However, an immuoblot analysis of the FtsH deficient nS345P:eWT strain indicates the presence of both pD1 and D1. This suggests co-expression of both wild type and high turnover mutant forms of D1 protein. Biophysical characterization using variable chlorophyll fluorescence of the dual D1 strain nD170A: eWT also showed the co-expression of mutant and wild type D1 subunits. Single D1 mutant D170A has been characterized to have a faster decay in chlorophyll fluorescence indicative of the charge recombination between the Q_A^- and Y_z^+ due to an inactive Mn_4CaO_5. A small component of faster decay in fluorescence was observed in the dual D1 strain nD170A: eWT representing the fraction of reaction centers with mutant D1-D170A forms incorporated.

The accumulation of pD1 in FtsH deficient nS345P: eWT shows that pD1 gets targeted for repair. A knockout of the FtsH protease blocks the D1 degradation process causing the accumulation of pD1. Additionally, the presence of wild type D1 somehow appears to increase the rate of degradation of pD1 in the dual D1 strain nS345P: eWT. This is based on the observation that when the mutant S345P is present alone it is able to accumulate the pD1 whereas there is absence of an accumulation of pD1 when the wild type D1 is expressed in parallel with mutant S345P.

To study the *psbA2* gene dosage effect on PSII activity, two wild type *psbA2* genes were cloned such that each is expressed from a native and an ectopic site of the chromosome. The PSII activity in this double WT strain was almost identical to the activity of a single WT strain (being expressed from either native or ectopic). This suggests that the fraction of active reaction centers in the double and single WT strains are similar and that the amount of PSII is constant. The accumulation of D1 protein in both the single and double WT strain also indicate similar amounts. Therefore, it appears that amount of PSII in a cell is regulated and this is not controlled by D1 protein because the presence of two copies of wild type *psbA2* gene accumulates the same amount of D1 as single *psbA2* copy.

5.2. Implications of this work

5.2.1 Selective and Targeted D1 degradation

The degradation process during PSII repair has been known to be selective for D1 protein. This has been established by the increased D1 turnover rate when compared to other PSII proteins during high light. This work provides evidence that FtsH protease specifically targets the damaged PSII complexes for repair. Therefore, when cells are subjected to photoinhibition the increase in the D1 turnover rate that is observed represents the fraction of reaction centers that are targeted for repair while the PSII complexes that are not yet subject to photodamage continue to be functional. This finding provides basis for the existence of a mechanism by which FtsH distinguishes between damaged D1 and un-damaged D1.

5.2.2 PSII Homeostasis: Maintaining Active PSII

PSII is very dynamic in nature undergoing continuous damage and repair cycle and yet maintaining higher levels of active PSII in the cell. Collectively from the observations made during this work it can be concluded that a "factor" controls PSII homeostasis by allowing the assembly of only a finite number of PSII per cell. Only the precomplexes that have this factor X attached to them are stable to go further in the PSII assembly process (as depicted in Figure 5.1). Those complexes that are not stabilized by assembly factors are triggered for degradation via a non-FtsH mediated degradation. In the strains expressing both mutant and wild type D1 protein there is an equal probability of either mutant or WT to be assembled into PSII. An insertion of a damage prone mutant gets triggered for repair due to the targeted repair mechanism thereby freeing a PSII that again as a equal probability to assemble either mutant or WT. During each turnover event, if a WT D1 is inserted into PSII, the complex is stable for ~45 minutes whereas if a mutant D1 is inserted the complex is unstable and is replaced in ~ 15 minutes. Therefore, over a period of several D1 turnover events the proportion of WT- PSII complexes would be higher as the likelihood of a WT to be assembled increases with every turnover event.

Thus, there seems to be an internal competition between the most competent and incompetent D1 proteins. The most competent (represented by WT) allowing the PSII to be fairly stable while the incompetent (represented by mutant) is unstable and undergoes targeted repair. With this interplay between PSII homeostasis and repair controlling the number and the stability of PSII respectively ensures higher levels of active PSII in a cell.

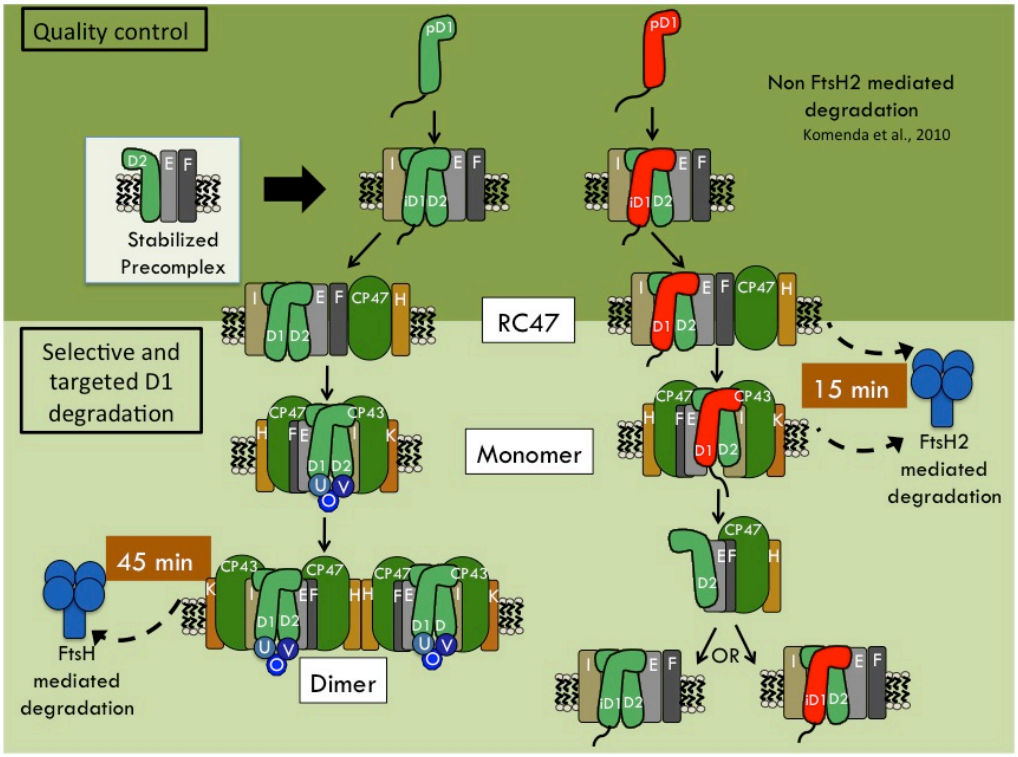

Figure 5.1. A proposed model for PSII Homeostasis suggesting a quality control of PSII complexes at various stages during the assembly and repair processes. The first stage of control occurs at the very early stage of PSII assembly with the formation of a stabilized precomplex (highlighted in white box), removal of subunits that do not enter the assembly process by non-FtsH mediated pathways acts as the second checkpoint and finally those PSII complexes that do go further in PSII assembly processes to form monomers and dimers get targeted by FtsH based on the individual D1 protein turnover rates. FtsH mediated degradation recognizes the damage prone complexes and targets them for repair.

5.2.3 Applications of the genetic system

The genetic system developed in this study shows the first report of the cloning of a full-length *psbA2* gene. This can enable mutagenesis studies involving the N-terminus of D1 which has not been possible with the previous mutagenesis systems. The structure-function studies in relation with the N-terminus of D1 might be important as it was shown that an exposed N-terminus was required for the degradation of D1. The dual

expression system that was developed in this study can be beneficial for study other gene dosage effects of other genes as well. Overexpression mutants of cyanobacterial membrane proteins are difficult due to the expression of these genes in E.*coli*. Dual expression systems can serve as a biotechnological tool for the double expression of genes either under the control of native promoters or other strong promoters. Overall, having an alternate location on the genome open for mutagenesis could be used to study effects of multiple genes in parallel and monitor any pleiotropic phenotype the cell might display.

5.3. Future Directions

The findings from this work have lead to key questions that can be followed for an improved understanding of this concept of PSII homeostasis. Firstly, it was observed that PSII complexes exist in a finite number and this is regulated by a "factor X". We believe this "factor X" might be one of other PSII subunits that get associated at very early stages of PSII assembly. An identification of this "factor X" might be important for studying PSII homeostasis. Based on the model for PSII assembly process, a few probable candidates could be Cyt b_{559} and CP47. Cyt b_{559} is known to be associated with D2 at the very beginning of the PSII assembly process and CP47 associates with smaller single transmembrane subunits before being entering the assembly process (*110*). With the knowledge of factor X we can alter the levels of PSII in a cell that could be utilized for biotechnological applications.

This work contributed to the finding that FtsH2 protease can distinguish between damaged and undamaged D1 proteins. This leads us to the interesting question of what is

the damage signal? It is known that an exposed N-terminus of D1 protein is essential for degradation to occur. It would be interesting to know the changes in D1 protein during damage that causes the N-terminus to be exposed. These changes might be speculated involve structures changes in PSII associated with D1 protein. With the use of these dual D1 strains one can address this question by mutagenesis of the N-terminus.

FtsH belongs to the member of AAA proteases that are conserved ATP-dependent proteases. Apart from being present in chloroplast these proteases are also present in bacteria and mitochondria and function in membrane integrated quality control. Mitochondria are known to have m-AAA protease that function in the posttranslational assembly of the respiratory chain (*111*). The mechanism by which these proteases recognize their targets for degradation is not well understood. Using photosystem II as a model, the mechanism of degradation by AAA proteases can be studied.

REFERENCES

1. Hohmann-Marriott, M. F., and Blankenship, R. E. (2011) Evolution of Photosynthesis, *Annual Review of Plant Biology 62*, 515-548.

2. Allen, J. P., and Williams, J. C. (2010) The evolutionary pathway from anoxygenic to oxygenic photosynthesis examined by comparison of the properties of photosystem II and bacterial reaction centers, *Photosynth Res (in press)*.

3. Bryant, D. A., and Frigaard, N. U. (2006) Prokaryotic photosynthesis and phototrophy illuminated, *Trends in Microbiology 14*, 488-496.

4. Nagarajan, A., and Burnap, R. L. (2012) Patterns of Conservation and Divergence of the Photosystem II Complex, In *Functional Genomics and Evolution of Photosynthetic Systems* (Burnap, R., and Vermaas, W., Eds.), pp 317-344, Springer Netherlands.

5. Kaneko, T., Sato, S., Kotani, H., Tanaka, A., Asamizu, E., Nakmura, Y., Miyajima, N., Hirosawa, M., Sugiura, M., Sasamoto, S., Kimura, T., Hosouchi, T., Matsuno, A., Muraki, A., Nakzaki, N., Naruo, K., Okumura, S., Shimpo, S., Takeuchi, C., Wada, T., Watanabe, A., Yamada, M., Yasuda, M., and Tabata, S. (1996) Sequence analysis of the genome of the unicellular cyanobacterium Synechocystis sp. strain 6803. II. Sequence determination of the entire genome and assignment of potential protein-coding regions., *DNA Research 3*, 109-136.

6. Umena, Y., Kawakami, K., Shen, J. R., and Kamiya, N. (2011) Crystal structure of oxygen-evolving photosystem II at a resolution of 1.9 Ångstrom, *Nature 473*, 55-U65.

7. Zouni, A., Witt, H. T., Kern, J., Fromme, P., Krauss, N., Saenger, W., and Orth, P. (2001) Crystal structure of photosystem II from *Synechococcus elongatus* at 3.8 Å resolution, *Nature 409*, 739-743.

8. Kamiya, N., and Shen, J. R. (2003) Crystal structure of oxygen-evolving photosystem II from Thermosynechococcus vulcanus at 3.7-Å resolution, *Proc Natl Acad Sci U S A 100*, 98-103.

9. Ferreira, K. N., Iverson, T. M., Maghlaoui, K., Barber, J., and Iwata, S. (2004) Architecture of the photosynthetic oxygen-evolving center, *Science 303*, 1831-1838.

10. Guskov, A., Kern, J., Gabdulkhakov, A., Broser, M., Zouni, A., and Saenger, W. (2009) Cyanobacterial photosystem II at 2.9-Ångstrom resolution and the role of quinones, lipids, channels and chloride, *Nature Structural & Molecular Biology 16*, 334-342.

11. Kashino, Y., Inoue-Kashino, N., Roose, J. L., and Pakrasi, H. B. (2006) Absence of the PsbQ protein results in destabilization of the PsbV protein and decreased oxygen evolution activity in cyanobacterial photosystem II, *J Biol Chem 281*, 20834-20841.

12. Thornton, L. E., Ohkawa, H., Roose, J. L., Kashino, Y., Keren, N., and Pakrasi, H. B. (2004) Homologs of plant PsbP and PsbQ proteins are necessary for regulation of photosystem II activity in the cyanobacterium *Synechocystis* 6803, *Plant Cell 16*, 2164-2175.

13. Sato, N. (2010) Phylogenomic and structural modeling analyses of the PsbP superfamily reveal multiple small segment additions in the evolution of photosystem II-associated PsbP protein in green plants, *Mol Phylogenet Evol 56*, 176-186.

14. Kok, B., Forbush, B., and McGloin, M. (1970) Cooperation of charges in photosynthetic oxygen evolution: I. A linear four step mechanism., *Photochem Photobiol 11*, 457-475.

15. Holzwarth, A. R., Muller, M. G., Niklas, J., and Lubitz, W. (2006) Ultrafast Transient Absorption Studies on Photosystem I Reaction Centers from Chlamydomonas reinhardtii. 2: Mutations near the P700 Reaction Center Chlorophylls Provide New Insight into the Nature of the Primary Electron Donor, *Biophys J 90*, 552-565.

16. Barry, B., and Babcock, G. (1987) Tyrosine radicals are involved in the photosynthetic oxygen-evolving system, *Proc Natl Acad Sci USA 84*, 7099-7103.

17. Debus, R. J., Barry, B. S., Sithole, I., Babcock, G. T., and McIntosh, L. (1988) Directed mutagenesis indicates that the donor to $P680^+$ in photosystem II is Tyr-161 of the D1 polypeptide., *Biochemistry 27*, 9071-9074.

18. Noren, G. H., and Barry, B. A. (1992) The YF161D1 mutant of *Synechocystis* 6803 exhibits an EPR signal from a light-induced photosystem II radical., *Biochemistry 31*, 3335-3342.

19. Joliot, P., Barbieri, G., and Chabaud, R. (1969) Un nouveau modele des centres photochimique du systeme II., *Photochem Photobiol 10*, 309-329.

20. Forbush, B., Kok, B., and McGloin, M. P. (1971) Cooperation of charges in photosynthetic O_2 evolution: II Damping of flash yield oscillation, deactivation., *Photochem Photobiol 14*, 307-321.

21. Nixon, P. J., Michoux, F., Yu, J., Boehm, M., and Komenda, J. (2010) Recent advances in understanding the assembly and repair of photosystem II, *Ann Bot 106*, 1-16.

22. Komenda, J., Reisinger, V., Muller, B. C., Dobakova, M., Granvogl, B., and Eichacker, L. A. (2004) Accumulation of the D2 protein is a key regulatory step for assembly of the photosystem II reaction center complex in *Synechocystis* PCC 6803, *J Biol Chem 279*, 48620-48629.

23. Komenda, J., Tichy, M., and Eichacker, L. A. (2005) The PsbH protein is associated with the inner antenna CP47 and facilitates D1 processing and incorporation into PSII in the cyanobacterium *Synechocystis* PCC 6803, *Plant Cell Physiol 46*, 1477-1483.

24. Sobotka, R., Komenda, J., Bumba, L., and Tichy, M. (2005) Photosystem II assembly in CP47 mutant of *Synechocystis* sp. PCC 6803 is dependent on the level of chlorophyll precursors regulated by ferrochelatase, *J Biol Chem 280*, 31595-31602.

25. Boehm, M., Romero, E., Reisinger, V., Yu, J., Komenda, J., Eichacker, L. A., Dekker, J. P., and Nixon, P. J. (2011) Investigating the early stages of photosystem II assembly in

Synechocystis sp. PCC 6803: isolation of CP47 and CP43 complexes, *J Biol Chem 286*, 14812-14819.

26. Komenda, J., Nickelsen, J., Tichy, M., Prasil, O., Eichacker, L. A., and Nixon, P. J. (2008) The cyanobacterial homologue of HCF136/YCF48 is a component of an early photosystem II assembly complex and is important for both the efficient assembly and repair of photosystem II in Synechocystis sp. PCC 6803, *J Biol Chem 283*, 22390-22399.

27. Nixon, P. J., Trost, J. T., and Diner, B. A. (1992) Role of the carboxy terminus of polypeptide D1 in the assembly of a functional water oxidizing manganese cluster in photosystem II of the cyanobacterium *Synechocystis* sp. PCC 6803: assembly requires a free carboxyl group at C terminal position 344, *Biochemistry 31*, 10859-10871.

28. Inagaki, N., Maitra, R., Satoh, K., and Pakrasi, H. B. (2001) Amino acid residues that are critical for in vivo catalytic activity of CtpA, the carboxyl-terminal processing protease for the D1 protein of photosystem II, *J Biol Chem 276*, 30099-30105.

29. Anbudurai, P. R., Mor, T. S., Ohad, I., Shestakov, S. V., and Pakrasi, H. B. (1994) The ctpA gene encodes the C-terminal processing protease for the D1 protein of the photosystem II reaction center complex, *Proc Natl Acad Sci U S A 91*, 8082-8086.

30. Liao, D. I., Qian, J., Chisholm, D. A., Jordan, D. B., and Diner, B. A. (2000) Crystal structures of the photosystem II D1 C-terminal processing protease, *Nat Struct Biol 7*, 749-753.

31. Komenda, J., Kuvikova, S., Granvogl, B., Eichacker, L. A., Diner, B. A., and Nixon, P. J. (2007) Cleavage after residue Ala352 in the C-terminal extension is an early step in the maturation of the D1 subunit of Photosystem II in Synechocystis PCC 6803, *Biochim Biophys Acta 1767*, 829-837.

32. Ivleva, N. B., Shestakov, S. V., and Pakrasi, H. B. (2000) The carboxyl-terminal extension of the precursor D1 protein of photosystem II is required for optimal photosynthetic performance of the cyanobacterium *Synechocystis* sp. PCC 6803, *Plant Physiol 124*, 1403-1412.

33. Burnap, R. L. (2004) D1 protein processing and Mn cluster assembly in light of the emerging photosystem II structure, *Phys Chem Chem Phys 6*, 4803-4809.

34. Ono, T. (2001) Metallo-radical hypothesis for photoassembly of (Mn)4-cluster of photosynthetic oxygen evolving complex, *Biochim Biophys Acta 1503*, 40-51.

35. Becker, K., Cormann, K. U., and Nowaczyk, M. M. (2011) Assembly of the water-oxidizing complex in photosystem II, *Journal of Photochemistry and Photobiology B: Biology 104*, 204-211.

36. Jackson, S. A., Fagerlund, R. D., Wilbanks, S. M., and Eaton-Rye, J. J. (2010) Crystal structure of PsbQ from Synechocystis sp. PCC 6803 at 1.8 A: implications for binding and function in cyanobacterial photosystem II, *Biochemistry 49*, 2765-2767.

37. Nowaczyk, M. M., Hebeler, R., Schlodder, E., Meyer, H. E., Warscheid, B., and Rogner, M. (2006) Psb27, a cyanobacterial lipoprotein, is involved in the repair cycle of photosystem II, *Plant Cell 18*, 3121-3131.

38. Takahashi, T., Inoue-Kashino, N., Ozawa, S., Takahashi, Y., Kashino, Y., and Satoh, K. (2009) Photosystem II complex in vivo is a monomer, *J Biol Chem 284*, 15598-15606.

39. Seibert, M., Dewit, M., and Staehelin, L. A. (1987) Structural Localization of the O-2-Evolving Apparatus to Multimeric (Tetrameric) Particles on the Lumenal Surface of Freeze-Etched Photosynthetic Membranes, *J Cell Biol 105*, 2257-2265.

40. Bumba, L., and Vacha, F. (2003) Electron microscopy in structural studies of Photosystem II, *Photosyn Res 77*, 1-19.

41. Roose, J. L., and Pakrasi, H. B. (2008) The Psb27 protein facilitates manganese cluster assembly in photosystem II, *J Biol Chem 283*, 4044-4050.

42. Mamedov, F., Nowaczyk, M. M., Thapper, A., Rogner, M., and Styring, S. (2007) Functional characterization of monomeric photosystem II core preparations from *Thermosynechococcus elongatus* with or without the Psb27 protein, *Biochemistry 46*, 5542-5551.

43. Bentley, F. K., Luo, H., Dilbeck, P., Burnap, R. L., and Eaton-Rye, J. J. (2008) Effects of inactivating *psbM* and *psbT* on photodamage and assembly of photosystem II in *Synechocystis* sp. PCC 6803, *Biochemistry 47*, 11637-11646.

44. Roose, J. L., Wegener, K. M., and Pakrasi, H. B. (2007) The extrinsic proteins of Photosystem II, *Photosynth Res 92*, 369-387.

45. Aro, E. M., McCaffery, S., and Anderson, J. M. (1993) Photoinhibition and D1 Protein Degradation in Peas Acclimated to Different Growth Irradiances, *Plant Physiol 103*, 835-843.

46. Adir, N., Zer, H., Shochat, S., and Ohad, I. (2003) Photoinhibition - A historical perspective, *Photosyn Res 76*, 343-370.

47. Murata, N., Takahashi, S., Nishiyama, Y., and Allakhverdiev, S. I. (2007) Photoinhibition of photosystem II under environmental stress, *Biochim Biophys Acta 1767*, 414-421.

48. Vass, I., and Cser, K. (2009) Janus-faced charge recombinations in photosystem II photoinhibition, *Trends Plant Sci 14*, 200-205.

49. Lupinkova, L., and Komenda, J. (2004) Oxidative modifications of the Photosystem II D1 protein by reactive oxygen species: from isolated protein to cyanobacterial cells, *Photochem Photobiol 79*, 152-162.

50. Keren, N., Berg, A., van Kan, P. J., Levanon, H., and Ohad, I. I. (1997) Mechanism of photosystem II photoinactivation and D1 protein degradation at low light: The role of back electron flow, *Proc Natl Acad Sci U S A 94*, 1579-1584.

51. Giorgi, L. B., Nixon, P. J., Merry, S. A., Joseph, D. M., Durrant, J. R., De Las Rivas, J., Barber, J., Porter, G., and Klug, D. R. (1996) Comparison of primary charge separation in the photosystem II reaction center complex isolated from wild type and D1 130 mutants of the cyanobacterium Synechocystis PCC 6803, *J. Biol. Chem. 271*, 2093 2101.

52. Joshua, S., and Mullineaux, C. W. (2004) Phycobilisome diffusion is required for light-state transitions in cyanobacteria, *Plant Physiol 135*, 2112-2119.

53. Hwang, H. J., Nagarajan, A., McLain, A., and Burnap, R. L. (2008) Assembly and disassembly of the photosystem II manganese cluster reversibly alters the coupling of the reaction center with the light-harvesting phycobilisome, *Biochemistry 47*, 9747-9755.

54. Ohad, I., Kyle, D. J., and Arntzen, C. J. (1984) Membrane protein damage and repair: removal and replacement of inactivated 32-kilodalton polypeptides in chloroplast membranes, *J Cell Biol 99*, 481-485.

55. Nixon, P. J., Barker, M., Boehm, M., de Vries, R., and Komenda, J. (2005) FtsH-mediated repair of the photosystem II complex in response to light stress, *J Exp Bot 56*, 357-363.

56. Komenda, J., and Masojídek, J. (1995) Functional and structural changes of the photosystem II complex induced by high irradiance in cyanobacterial cells, *European Journal of Biochemistry 233*, 677-682.

57. Barker, M., de Vries, R., Nield, J., Komenda, J., and Nixon, P. J. (2006) The Deg proteases protect Synechocystis sp PCC 6803 during heat and light stresses but are not essential for removal of damaged D1 protein during the photosystem two repair cycle, *J Biol Chem 281*, 30347-30355.

58. Huesgen, P. F., Schuhmann, H., and Adamska, I. (2009) Deg/HtrA proteases as components of a network for photosystem II quality control in chloroplasts and cyanobacteria, *Res Microbiol 160*, 726-732.

59. Huesgen, P. F., Schuhmann, H., and Adamska, I. (2006) Photodamaged D1 protein is degraded in Arabidopsis mutants lacking the Deg2 protease, *Febs Letters 580*, 6929-6932.

60. Adam, Z., Rudella, A., and van Wijk, K. J. (2006) Recent advances in the study of Clp, FtsH and other proteases located in chloroplasts, *Curr Opin Plant Biol 9*, 234-240.

61. Ito, K., and Akiyama, Y. (2005) Cellular functions, mechanism of action, and regulation of the FtsH protease, *Ann Rev Microbiol 59*, 211-231.

62. Hauszuhl, K., Andersson, B., and Adamska, I. (2001) A chloroplast DegP2 protease

performs the primary cleavage of the photodamaged D1 protein in plant photosystem II, *EMBO J 20*, 713-722.

63. Komenda, J., Knoppova, J., Krynicka, V., Nixon, P. J., and Tichy, M. (2010) Role of FtsH2 in the repair of Photosystem II in mutants of the cyanobacterium *Synechocystis* PCC 6803 with impaired assembly or stability of the $CaMn_4$ cluster, *Biochim Biophys Acta 1797*, 566-575.

64. Komenda, J., Barker, M., Kuvikova, S., de Vries, R., Mullineaux, C. W., Tichy, M., and Nixon, P. J. (2006) The FtsH protease slr0228 is important for quality Control of photosystem II in the thylakoid membrane of *Synechocystis* sp. PCC 6803, *J Biol Chem 281*, 1145-1151.

65. Silva, P., Thompson, E., Bailey, S., Kruse, O., Mullineaux, C. W., Robinson, C., Mann, N. H., and Nixon, P. J. (2003) FtsH is involved in the early stages of repair of photosystem II in *Synechocystis* sp PCC 6803, *Plant Cell 15*, 2152-2164.

66. Bailey, S., Thompson, E., Nixon, P. J., Horton, P., Mullineaux, C. W., Robinson, C., and Mann, N. H. (2002) A critical role for the Var2 FtsH homologue of Arabidopsis thaliana in the photosystem II repair cycle in vivo, *J Biol Chem 277*, 2006-2011.

67. Komenda, J., Tichy, M., Prasil, O., Knoppova, J., Kuvikova, S., de Vries, R., and Nixon, P. J. (2007) The exposed N-terminal tail of the D1 subunit is required for rapid D1 degradation during photosystem II repair in *Synechocystis* sp PCC 6803, *Plant Cell 19*, 2839-2854.

68. Schuhmann, H., Huesgen, P. F., and Adamska, I. (2012) The family of Deg/HtrA proteases in plants, *BMC plant biology 12*, 52.

69. Nickelsen, J., Rengstl, B., Stengel, A., Schottkowski, M., Soll, J., and Ankele, E. (2011) Biogenesis of the cyanobacterial thylakoid membrane system--an update, *FEMS Microbiol Lett 315*, 1-5.

70. Sarcina, M., Bouzovitis, N., and Mullineaux, C. W. (2006) Mobilization of photosystem II induced by intense red light in the cyanobacterium Synechococcus sp PCC7942, *Plant*

Cell 18, 457-464.

71. Mullineaux, C. W. (2008) Factors Controlling the Mobility of Photosynthetic Proteins†, *Photochem Photobiol 84*, 1310-1316.

72. Stengel, A., Gugel, I. L., Hilger, D., Rengstl, B., Jung, H., and Nickelsen, J. (2012) Initial steps of photosystem II de novo assembly and preloading with manganese take place in biogenesis centers in Synechocystis, *Plant Cell 24*, 660-675.

73. Chu, H.-A., Nguyen, A. P., and Debus, R. A. (1994) Site-directed mutagenesis of photosynthetic oxygen evolution: Increased binding or photooxidation of manganese in the absence of the extrinsic 33-kDa polypeptide in vivo., *Biochemistry 33*, 6150-6157.

74. Diner, B. A., and Nixon, P. J. (1992) The rate of reduction of oxidized redox-active tyrosine, Z^{+}, by exogenous Mn^{2+} Is slowed in a site-directed mutant, at aspartate 170 of polypeptide D1 of photosystem II, inactive for photosynthetic oxygen evolution, *Biochim Biophys Acta 1101*, 134-138.

75. Allen, M. M. (1968) Simple conditions for growth of unicellular blue-green algae on plates, *J Phycol 4*, 1-&.

76. Williams, J. G. K. (1988) Construction of specific mutations in Photosystem II photosynthetic reaction center by genetic engineering methods in *Synechocystis* 6803., *Methods in Enzymology 167*, 766-778.

77. Cai, Y. P., and Wolk, C. P. (1990) Use of a conditionally lethal gene in *Anabaena* sp. strain PCC 7120 to select for double recombinants and to entrap insertion sequences, *J Bacteriol 172*, 3138-3145.

78. Ermakova-Gerdes, S., and Vermaas, W. (1999) Development of a *psbA*-less/*psbD*-less strain of *Synechocystis* sp. PCC 6803 for simultaneous mutagenesis of the D1 and D2 proteins of photosystem II, In *The Phototrophic Prokaryotes* (Peschek, G. A., and Loffelhardt, W., Eds.), pp 51-60, Dordrecht.

79. Debus, R. A., Nguyen, A. P., and Conway, A. B. (1990) Identification of ligands to manganese and calcium in photosystem II by site-directed mutagensis., In *Current*

Research in Photosynthesis (Baltscheffsky, M., Ed.), pp 829-832, Kluwer, The Netherlands.

80. Kunert, A., Hagemann, M., and Erdmann, N. (2000) Construction of promoter probe vectors for *Synechocystis* sp. PCC 6803 using the light-emitting reporter systems Gfp and LuxAB, *J Microbiol Methods 41*, 185-194.

81. Lagarde, D., Beuf, L., and Vermaas, W. (2000) Increased production of zeaxanthin and other pigments by application of genetic engineering techniques to Synechocystis sp. strain PCC 6803, *Appl Environ Microbiol 66*, 64-72.

82. Szewczyk, E., Nayak, T., Oakley, C. E., Edgerton, H., Xiong, Y., Taheri-Talesh, N., Osmani, S. A., and Oakley, B. R. (2007) Fusion PCR and gene targeting in Aspergillus nidulans, *Nat. Protocols 1*, 3111-3120.

83. Sambrook, J., Fritsch, E. F., and Maniatis, T. (1989) *Molecular cloning: A laboratory manual*, 2 ed., Cold Spring Harbor Laboratory, Cold Spring Harbor, New York.

84. Komenda, J., Lupinkova, L., and Kopecky, J. (2002) Absence of the psbH gene product destabilizes photosystem II complex and bicarbonate binding on its acceptor side in *Synechocystis* PCC 6803, *Eur J Biochem 269*, 610-619.

85. Allahverdiyeva, Y., Deak, Z., Szilard, A., Diner, B. A., Nixon, P. J., and Vass, I. (2004) The function of D1-H332 in Photosystem II electron transport studied by thermoluminescence and chlorophyll fluorescence in site-directed mutants of Synechocystis 6803, *Eur J Biochem 271*, 3523-3532.

86. Laemmli, U. K. (1970) Cleavage of Structural Proteins during the Assembly of the Head of Bacteriophage T4, *Nature 227*, 680-685.

87. Kashino, Y., Koike, H., and Satoh, K. (2001) An improved sodium dodecyl sulfate-polyacrylamide gel electrophoresis system for the analysis of membrane protein complexes, *Electrophoresis 22*, 1004-1007.

88. Jansson, C., Debus, R. J., Osiewacz, H. D., Gurevitz, M., and Mcintosh, L. (1987) Construction of an obligate photoheterotrophic mutant of the cyanobacterium

Synechocystis 6803 inactivation of the *psbA* gene family, *Plant Physiol (Bethesda) 85*, 1021-1025.

89. Mohamed, A., Eriksson, J., Osiewacz, H. D., and Jansson, C. (1993) Differential expression of the *psbA* genes in the cyanobacterium *Synechocystis* 6803, *Mol Gen Genet 238*, 161-168.

90. Summerfield, T. C., Toepel, J., and Sherman, L. A. (2008) Low-Oxygen Induction of Normally Cryptic psbA Genes in Cyanobacteria,Ä†, *Biochemistry 47*, 12939-12941.

91. Mohamed, A., and Jansson, C. (1989) Influence of light on accumulation of photosynthesis specific transcripts in the cyanobacterium *Synechocystis* 6803, *Plant Molec Biol 13*, 693-700.

92. Kulkarni, R. D., Schaefer, M. R., and Golden, S. S. (1992) Transcriptional and posttranscriptional components of *psbA* response to high light intensity in *Synechococcus* sp. strain PCC 7942, *J Bacteriol 174*, 3775-3781.

93. Bustos, S. A., Schaefer, M. R., and Golden, S. S. (1990) Different and rapid responses of four cyanobacterial psbA transcripts to changes in light intensity, *J Bacteriol 172*, 1998-2004.

94. Komenda, J., Hassan, H. A. G., Diner, B. A., Debus, R. J., Barber, J., and Nixon, P. J. (2000) Degradation of the photosystem II D1 and D2 proteins in different strains of the cyanobacterium *Synechocystis* PCC 6803 varying with respect to the type and level of *psbA* transcript, *Plant Molec Biol 42*, 635-645.

95. Komenda, J., Koblizek, M., and Masojidek, J. (1999) The regulatory role of photosystem II photoinactivation and de novo protein synthesis in the degradation and exchange of two forms of the D1 protein in the cyanobacterium *Synechococcus* PCC 7942, *J Photochem Photobiol B 48*, 114-119.

96. Komenda, J., and Barber, J. (1995) Comparison of *psbO* and *psbH* deletion mutants of *Synechocystis* PCC 6803 indicates that degradation of D1 protein is regulated by the QB site and dependent on protein synthesis, *Biochemistry 34*, 9625 9631.

97. Kommalapati, M., Hwang, H. J., Wang, H. L., and Burnap, R. L. (2007) Engineered ectopic expression of the psbA gene encoding the photosystem II D1 protein in *Synechocystis* sp. PCC680*P*3, *hotosyn Res*, 315-325.

98. Chisholm, D., and Williams, J. G. K. (1988) Nucleotide sequence of *psbC*, the gene encoding the CP-43 chlorophyll a-binding protein of Photosystem II, in the cyanobacterium *Synechocystis* 6803, *Plant Molec Biol 10*, 293-301.

99. Vermaas, W. F. (1998) Gene modifications and mutation mapping to study the function of photosystem II, *Methods Enzymol 297*, 293-310.

100. Wang, H. L., Postier, B. L., and Burnap, R. L. (2002) Optimization of fusion PCR for in vitro construction of gene knockout fragments, *Biotechniques 33*, 26-30.

101. Wang, H. L., Postier, B. L., and Burnap, R. L. (2002) Polymerase chain reaction-based mutageneses identify key transporters belonging to multigene families involved in Na+ and pH homeostasis of Synechocystis sp. PCC 6803, *Mol Microbiol 44*, 1493-1506.

102. Funk, C., Schroder, W. P., Salih, G., Wiklund, R., and Jansson, C. (1998) Engineering of N-terminal threonines in the D1 protein impairs photosystem II energy transfer in Synechocystis 6803, *FEBS Lett 436*, 434-438.

103. Boerner, R. J., Nguyen, A. P., Barry, B. A., and Debus, R. J. (1992) Evidence from directed mutagenesis that aspartate 170 of the D1 polypeptide influences the assembly and-or stability of the manganese cluster in the photosynthetic water-splitting complex, *Biochemistry 31*, 6660-6672.

104. Metz, J. G., Nixon, P. J., Rogner, M., Brudvig, G. W., and Diner, B. A. (1989) Directed alteration of the D1 polypeptide of photosystem II: Evidence that tyrosine-161 is the redox component, Z, connecting the oxygen-evolving complex to the primary electron donor, P680., *Biochemistry 289*, 6960-6969.

105. Eriksson, J., Salih, G. F., Ghebramedhin, H., and Jansson, C. (2000) Deletion mutagenesis of the 5' psbA2 region in Synechocystis 6803: identification of a putative cis element involved in photoregulation, *Mol Cell Biol Res Commun 3*, 292-298.

106. Sander, J., Nowaczyk, M., Buchta, J., Dau, H., Vass, I., De√°k, Z., Dorogi, M. r., Iwai, M., and R√∂gner, M. Functional Characterization and Quantification of the Alternative PsbA Copies in Thermosynechococcus elongatus and Their Role in Photoprotection, *Journal of Biological Chemistry 285*, 29851-29856.

107. Chu, H.-A., Nguyen, A. P., and Debus, R. A. (1994) Site-directed mutagenesis of photosynthetic oxygen evolution: Instability or inefficient assembly of the manganese cluster in vivo., *Biochemistry 33*, 6137-6149.

108. Chu, H. A., Nguyen, A. P., and Debus, R. J. (1995) Amino acid residues that influence the binding of manganese or calcium to photosystem II. 2. The carboxy terminal domain of the D1 polypeptide, *Biochemistry 3496*, 5859-5882.

109. Nixon, P. J., and Diner, B. A. (1992) Aspartate 170 of the photosystem II reaction center polypeptide D1 is involved in the assembly of the oxygen evolving manganese cluster, *Biochemistry 31*, 942 948.

110. Komenda, J., Sobotka, R., and Nixon, P. J. (2012) Assembling and maintaining the Photosystem II complex in chloroplasts and cyanobacteria, *Curr Opin Plant Biol*.

111. Langer, T. (2000) AAA proteases: cellular machines for degrading membrane proteins, *Trends in Biochemical Sciences 25*, 247-251.

112. Herranen, M., Battchikova, N., Zhang, P., Graf, A., Sirpiö, S., Paakkarinen, V., and Aro, E.-M. (2004) Towards Functional Proteomics of Membrane Protein Complexes in Synechocystis sp. PCC 6803, *Plant Physiology 134*, 470-481.

113. Klinkert, B., Ossenbuhl, F., Sikorski, M., Berry, S., Eichacker, L., and Nickelsen, J. (2004) PratA, a periplasmic tetratricopeptide repeat protein involved in biogenesis of photosystem II in Synechocystis sp. PCC 6803, *J Biol Chem 279*, 44639-44644.

APPENDICES

This section contains additional work related to my thesis work. These include the Q_A reoxidation kinetics of the single and dual D1 strains to analyze the decay in fluorescence (A1 and A2). The thylakoid membranes from the dual D1 strains were resolved by blue-native polyacrylamide gel electrophoresis to visualize the PSII assembly intermediates (A3). To study the rates of incorporation of mutant and wild type D1 proteins in the dual D1 strains, radioactive pulse-chase was performed on cells using ^{35}S [L-Cysteine]. Appendix 4 describes the brief procedure for in-vivo radiolabeling of cells and visualization of radioactive incorporation by autoradiography. A survey of the solvent exposed regions of various PSII proteins using LC-MSMS were performed. Appendix 5 describes the conditions used for obtaining maximal coverage of the core subunits of PSII.

A1. Q_A Reoxidation kinetics of D1-H337Y and nH337Y: eWT

As described in chapter four, the relative PSII activity of the single mutant D1-H337Y and the dual D1 strain nH337Y: eWT was measured using variable chlorophyll *a* fluorescence. The amplitude of variable fluorescence in the single mutant D1-H337Y was very low indicating that majority of reaction centers in this mutant is unable to undergo successful charge separation. In the presence of a wild type D1 in parallel the low

fluorescence phenotype of the mutant was restored (Figure A.1). The fluorescence decay resembled like that of the wild type as observed for the other two dual D1 strains used in this work. The amplitudes of variable fluorescence were comparable to the single wild type strain (eWT). This suggests that PSII complexes in the dual strain nH337Y: eWT are primarily consisting of wild type D1 protein incorporated.

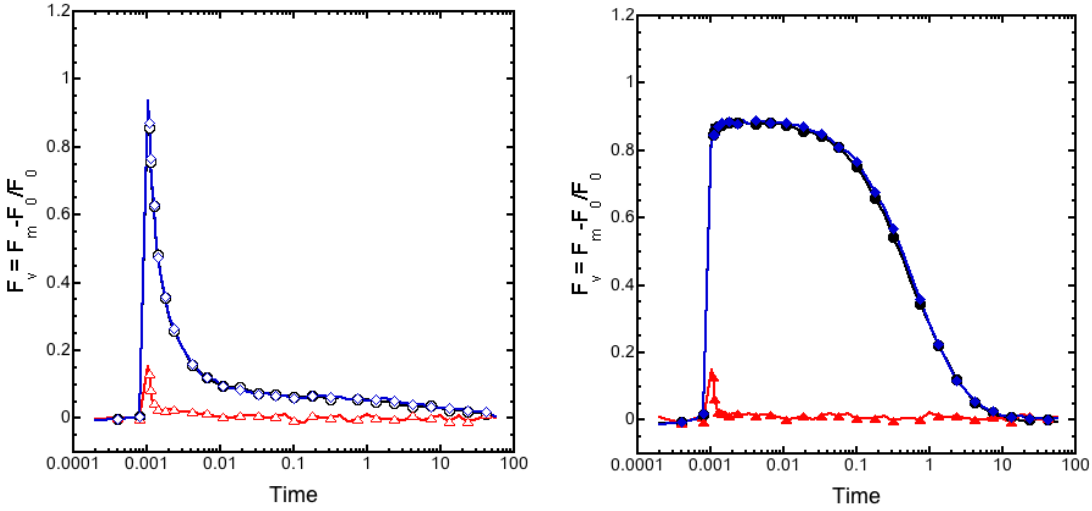

Figure A.1 Q_A reoxidation kinetics of WT (black), H337Y (red) and nH337Y: eWT (blue). Left (a) and right panel (b) indicate the decay kinetics of variable chlorophyll *a* fluorescence in the absence of DCMU (open symbols) and presence of 10 μM DCMU (closed symbols) respectively. Values plotted are calculated as $(Ft-F_0)/F_0$ wherein F_0 corresponds to the average fluorescence yield of first four weak measuring flashes given to each sample before exposure to actinic flash.

A.2 Fluorescence Decay Kinetics

The decay of chlorophyll *a* fluorescence in the presence of DCMU monitors the charge recombination between QA- and the donor side of PSII. The mutants used in this study were primarily affecting the donor side. Therefore, to analyze the decay of fluorescence yield, the amplitude of variable fluorescence was normalized for all the strains. As shown in Figure A.2, the decay in fluorescence of the dual D1 strains nS345P: eWT, nH337Y: eWT and nWT: eWT were all essentially similar to the eWT strain.

However, in nD170A: eWT strain there is a small fraction of PSII centers that decays faster (Figure. 4.6). The absence of any faster decay component in the other dual D1 strains suggest that the majority of reaction centers have wild type D1 protein incorporated.

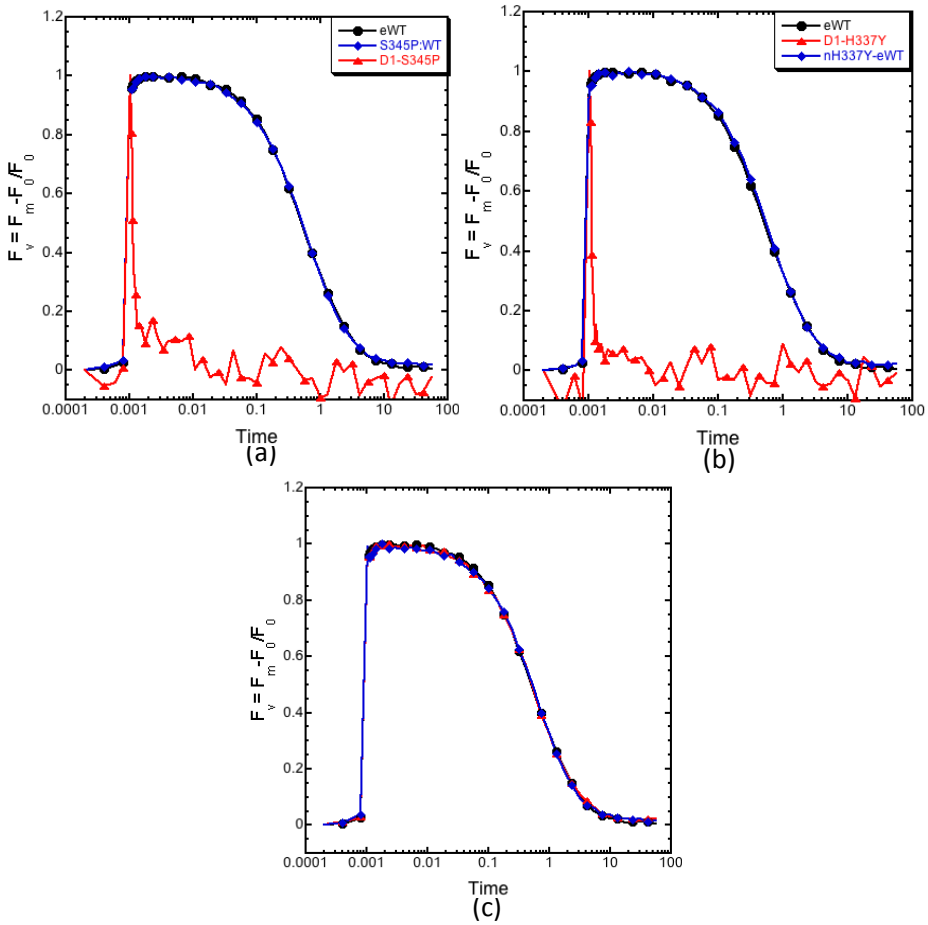

Figure A.2. Relaxation Kinetics of chlorophyll *a* fluorescence. (a) WT (black), S345P (red) and nS345P: eWT (blue); (b) WT (black), H337Y (red) and nH337Y: eWT (blue); (c) eWT (black), nWT (red) and nWT: eWT (blue); Decay of fluorescence during QA reoxidation was measured in the presence of DCMU for each sample. The values of variable fluorescence were normalized to 1 and plotted as F_t-F_0/ F_m-F_0 wherein F_0 and F_m are basal and maximal fluorescence before and after exposure of the sample to actinic light respectively. Data points represent an average of three different samples.

A.3. Resolving PSII assembly intermediates using two-dimensional BN-PAGE

Thylakoid membranes from nS345P:eWT and D1-S345P strain were analyzed on a two dimensional blue native polyacrylamide gel electrophoresis. This allows the visualization of PSII assembly intermediates like PSII dimer, monomer, RC47 and individual unassembled proteins. The procedure followed was adapted Aro et al., 2004 (*112*). Thylakoid membranes at 20 µg chlorophyll were resuspended in a resuspension buffer containing 20% Glycerol, 25 mM Bis-Tris (pH-7.0) and 10 mM $MgCl_2$. Equal volume of solubilization buffer (Same as resuspension buffer, additionally includes 4% dodecyl maltoside) was added to the membrane samples and incubated on for 20 minutes. Tubes were shaken in between and incubated for another 20 minutes at room temperature with shaking using a vortex at low speed. 0.1 volume of loading buffer consisting of 5% Coomassie Blue (G250), 100 mM Bis-Tris (pH-7.0), 30% Sucrose, 500 mM ε-amino caproic acid and 10 mM EDT was added to the samples. Samples were centrifuged at 14, 000 rpm for 15 minutes before loading on to a native 5% - 12.5% gradient gel. Samples were run at constant current 5 mA at 4 °C for 4-5 hrs. After one-third of the gel is run, the cathode buffer is exchanged to the cathode buffer without dye for the rest of the run. Strips for each lane was cut using a razor and incubated in a denaturation buffer containing 125 mM Tris-HCl, 2% SDS, 2% β-mercaptoethanol and 10% glycerol.

For the second dimension, a 12% denaturing SDS PAGE was used and the gel strips were incubated in the denaturation buffer for 30 minutes before loading the strip onto the gel. The edges of the gel were sealed using 1% Agarose (in water). The gel was

electrophoresed at a constant voltage of 100 V at 4 °C for 2 h. Gels were stained with Coomassie and imaged on the Typhoon Imager (Core facility).

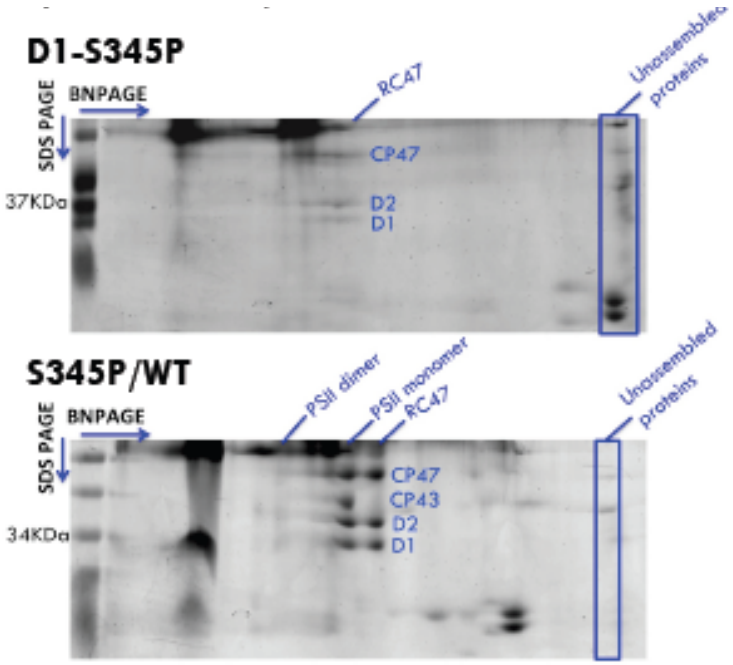

Figure A.3. Two dimensional Blue native PAGE of the mutant D1- S345P and nS345P:eWT strain. The dual D1 strain nS345P:eWT restores the mutant phenotype and undergoes complete PSII assembly.

A.4. *In vivo* radiolabelling using ^{35}S [L- Cysteine] and analysis by Autoradiography

The protocol devised was adapted from Nickelsen et al., 2004 (*113*) and Komenda et al., 2005 (*23*). Cultures from mid exponential phase were harvested and resuspended in BG-11 [NO sulfur] medium. The chlorophyll concentration is adjusted to 100 µg/ml and a total of 2 ml culture was aliquoted onto a six well plate. The cells were kept in constant shaking under 200 µmol m^{-1} s^{-1} for 20 minutes. 300µCi of ^{35}S[Cys] was added to the 2 ml culture (100 µg/ml). After pulse, the light intensity was immediately increased to 400 µmol m^{-1} s^{-1} and cells were kept under continuous shaking for 20 minutes. The plate was

rotated every 10 minutes to ensure equal light and heat transmission. Cold cysteine was added at a concentration of 2 mM and the light intensity was reduced back to 200 μmol m^{-1} s^{-1} for 2 minutes. Cells from the 6- well plate were transferred onto microfuge tube and were processed for micro scale thylakoid membrane isolation as described in the methods section. [CAUTION: care was taken to double glove while using isotope also gloves were frequently changed to prevent contamination].

Labeled thalakoid membranes were revolved on a 6 M Urea 12% - 20% SDS denaturing PAGE as described previously. A western transfer of the proteins was performed (refer to chapter two for methods). The transferred PVDF membrane was briefly dipped in methanol and dried in between filter papers (ensured that the blot is completely dried). The blot was carefully placed on top of the autoradiography film (Kodak Biomax) in the dark room and exposed for 12 hours. The film was developed in an X-ray developer (Core facility). Exposure times were changed for subsequent experiments to maximize exposure and resolution.

A.5. Solvent exposed regions in PSII proteins detected by LC-MSMS

The aim of this study was to monitor changes in the solvent exposed regions of PSII under different physiological conditions. In order to enable this, it was pertinent to analyze the solvent exposed regions of PSII proteins under native (non-treated) conditions. Core subunits of PSII, D1 and CP43 in particular were analyzed using LC-MSMS and in order to obtain maximal coverage of the proteins different proteases were surveyed.

For the analysis of proteins using LC-MSMS, PSII particles bound to the Ni^{2+} resin were directly used for proteolysis using different proteases. After proteolysis, the samples were purified using C18 columns before shooting them into the LC-MSMS (LTQ Orbitrap Mass Spectrometer, Core facility). Peptides detected by the mass spec are compared to a customized database for a match of the mass:charge (m/z) ratio. This information is utilized to generate a percent coverage map for the entire sequence of a protein.

D1 and CP43 are proteins consisting of many transmembrane helices that are extremely hydrophobic in nature. Therefore, a combination of different proteases was used to allow increased coverage. In my study I used Trypsin, Trypsin and Cyanogen bromide and Elastase. Maximal percent coverage was obtained using Trypsin and Cyanogen bromide with D1 showing 55% and CP43 showing 54% sequence coverage. A combination of all these three proteases was also tried and gave a higher coverage (D1-70% and CP43-60%) as well. Figure A.5 maps the regions that were recognized as solvent exposed regions under non- treated conditions.

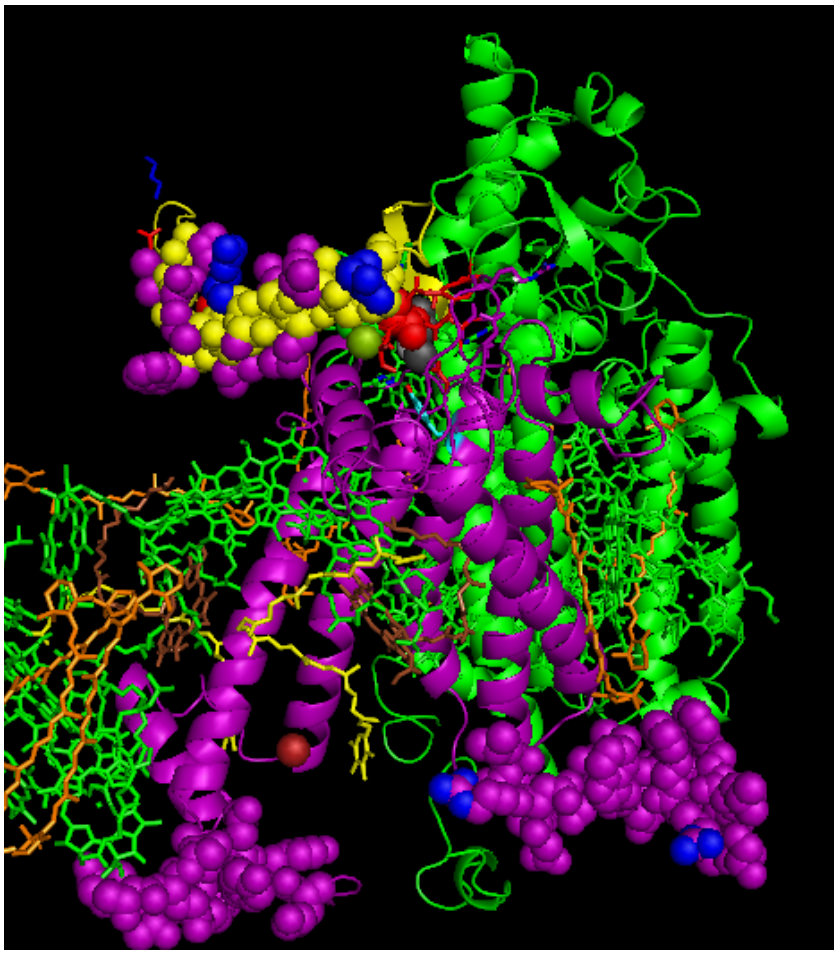

Figure A.5 (a) Solvent exposed regions in D1. Mapping the sequences that were covered in LC-MSMS under the above mentioned conditions show that C-terminus (yellow), N-terminus and DE loop of D1 protein are more accessible to proteases.

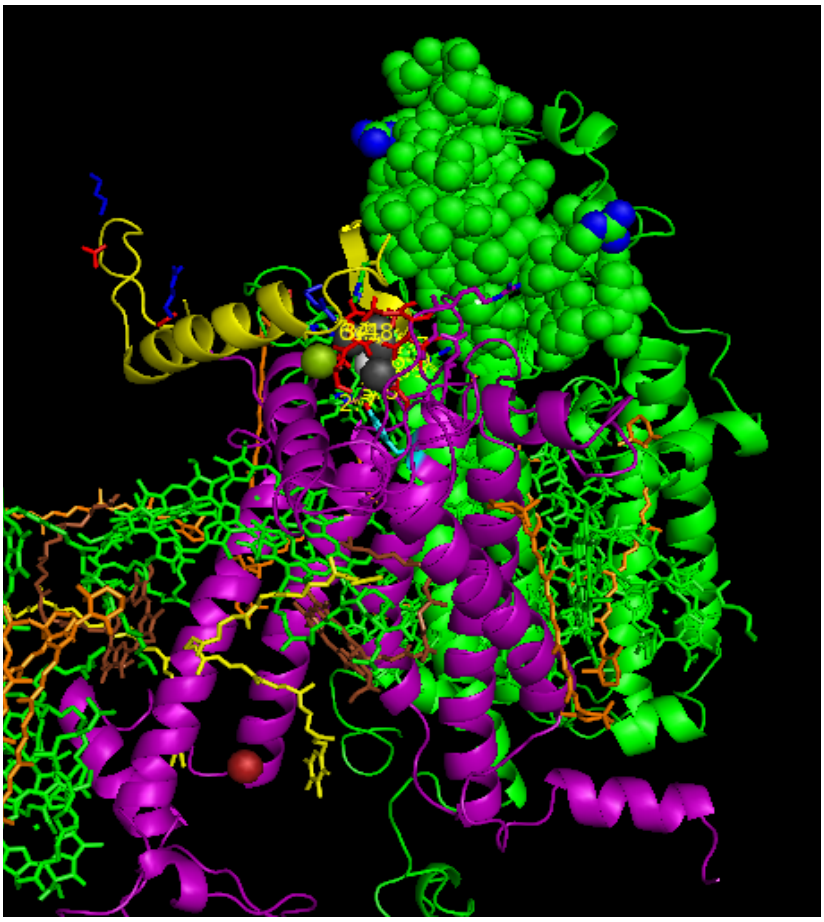

Figure A.5 (b) Solvent exposed regions in CP43. The E-loop of CP43 is represented as a solvent exposed region in the CP43 as seen by LC-MSMS as shown in green spheres.

VITA

APARNA NAGARAJAN

Candidate for the Degree of

Doctor of Philosophy

Thesis: INSIGHTS INTO THE MAINTENANCE AND REPAIR OF PHOTOSYSTEM II, A DYNAMIC MEMBRANE PROTEIN COMPLEX

Major Field: MICROBIOLOGY AND MOLECULAR GENETICS

Biographical:

Education:

Completed the requirements for the Doctor of Philosophy/Education in your major at Oklahoma State University, Stillwater, Oklahoma in December 2012.

Completed the requirements for the Master of Science in Biotechnology at University of Madras, Chennai, India in 2005.

Completed the requirements for the Bachelor of Science in Zoology at University of Delhi, New Delhi, India in 2003.

Publications:

Aparna Nagarajan and Robert L. Burnap, Patterns of conservation and divergence in Photosystem II complex, Chapter in Functional genomics and Evolution of photosynthetic systems, Springer, Dordrecht.

Aparna Nagarajan, Regan Winter, J. Eaton-Rye, Robert Burnap, A synthetic DNA and fusion PCR approach to the ectopic expression of high levels of the D1 protein of photosystem II in Synechocystis sp. PCC 6803, J Photochemistry and Photobiology B 2011 104, 212-219.

Hong Jin Hwang, Aparna Nagarajan, Aaron McLain and Robert L. Burnap, Assembly and disassembly of the Photosystem II manganese cluster reversibly alters the coupling of the reaction center with the lightharvesting phycobilisome, Biochemistry 2008 47 (37), 9747-9755.

Experience:

Project Assistant at National Institute of Immunology